의학박사 학위논문

Regulation of DNA damage responses by stimulatory G protein signaling in cancer cells

촉진성 G 단백질이 암세포주에서 DNA 손상반응을 조절하는 기전

2013 년 2 월

서울대학교 대학원

의학과 생화학전공

조 은 아

촉진성 G 단백질이 암세포주에서 DNA 손상반응을 조절하는 기전

지도교수 전 용 성

이 논문을 의학박사 학위논문으로 제출함

2013 년 2 월

서울대학교 대학원

의학과 생화학전공

조 은 아

조은아의 의학박사 학위논문을 인준함

2013 년 2 월

위 원 장 윤 홍 덕 (인)

부위원장 전 용 성 (인)

위 원 강 래 훈 (인)

위 원 예 상 규 (인)

위 원 김 인 혁 (인)

Regulation of DNA damage responses by stimulatory G protein signaling in cancer cells

by

Eun-Ah Cho

A thesis submitted to the Department of Biochemistry and Molecular Biology in partial fulfillment of the requirement of the Degree of Doctor of Philosophy in Medicine at Seoul National University College of Medicine

February, 2013

Approved by Thesis Committee:

Professor _____ Chairman

Professor _____ Vice Chairman

Professor _____

Professor _____

Professor _____

Abstract

Heterotrimeric stimulatory GTP-binding proteins (Gαs) activate cAMP signaling system and play important roles in the regulation of cell growth, proliferation, differentiation, and apoptosis. However, the role of Gαs protein in DNA damage response has not been studied extensively. Thus, the role of Gαs protein on DNA damage responses such as DNA repair and apoptosis was studied in this experiment.

In the first part of this study, in order to elucidate the molecular mechanism for Gαs system to regulate apoptosis, the effect of the Gαs system on cisplatin-induced apoptosis and the expression of IAP family proteins were examined in uterine cervical cancer cells. HeLa cells stably expression constitutively active GαsQL were established by transfection. Stable expression of constitutively active Gαs (GαsQL) decreased the release of cytochrome c from the mitochondria to the cytosol and cleavage of caspase-3 and poly (ADP-ribose) polymerases in HeLa cells treated with 30 μM cisplatin, indicating that Gαs inhibited cisplatin-induced apoptosis. Treatment with forskolin also inhibited apoptosis of C33A and CaSKi cervical cancer cells. Expression of GαsQL increased the expression of the X-linked inhibitor of apoptosis protein (XIAP) and partially maintained increased XIAP after cisplatin treatment. Knockdown of XIAP by siRNA augmented apoptosis.

Expression of GαsQL increased XIAP mRNA; this increase was inhibited by a protein kinase A inhibitor and cAMP response element (CRE) decoy. A cAMP response element (CRE)-like element at -1396 bp in the XIAP promoter was found to mediate the induction of XIAP by Gαs. In addition, expression of GαsQL protected against the ubiquitin/proteasome-dependent degradation of the XIAP protein. In conclusion, this study shows that Gαs inhibits cisplatin-induced apoptosis by increasing transcription of XIAP and by decreasing degradation of XIAP protein in HeLa cervical cancer cells.

In the second part of this study, to verify the hypothesis that the cAMP signaling may modulate DNA repair activity, the effects of the cAMP signaling system on γ-ray-induced DNA damage repair was investigated in lung cancer cells. Transient expression of a constitutively active mutant of stimulatory G protein (GαsQL) or treatment with forskolin, an adenylyl cyclase activator, augmented radiation-induced DNA damage and inhibited repair of the damage in H1299 lung cancer cells. Expression of GαsQL or treatment with forskolin or isoproterenol inhibited the radiation-induced expression of the XRCC1 protein, and exogenous expression of XRCC1 abolished the DNA repair-inhibiting effect of forskolin. Forskolin treatment promoted the ubiquitin and proteasome-dependent degradation of the XRCC1 protein, resulting in a significant decrease in the half-life of the protein after γ-ray irradiation. The effect of forskolin on XRCC1

expression was not inhibited by PKA inhibitor, but 8-pCPT-2'-O-Me-cAMP, an Epac-selective cAMP analog, increased ubiquitination of XRCC1 protein and decreased XRCC1 expression. Knockdown of Epac1 abolished the effect of 8-pCPT-2'-O-Me-cAMP and restored XRCC1 protein level following γ-ray irradiation. From these results, it was concluded that the cAMP signaling system inhibits the repair of γ-ray-induced DNA damage by promoting the ubiquitin-proteasome dependent degradation of XRCC1 in an Epac-dependent pathway in lung cancer cells.

In the third part of this study, the mechanism through which cAMP signaling regulates activation of ATM, which is the master regulator of DNA damage responses, and cellular responses to ionizing radiation was investigated. Transient expression of constitutively active stimulatory G protein (GαsQL) significantly inhibited the radiation-induced phosphorylation of ATM in H1299 human lung cancer cells. Treatment with okadaic acid abolished the inhibitory effect of Gαs on the radiation-induced ATM phosphorylation. Expression of GαsQL increased the phosphorylation of PP2A B56δ subunit and PP2A activity, and this PP2A-activating effect of Gαs was completely removed by H89. Expression of GαsQL increased radiation-induced cleavage of caspase-3 and PARP and the number of early apoptotic cells, and treatment with KU55933 also increased the apoptosis. Treatment of B16-F10 mouse cells with forskolin increased

the radiation-induced phosphorylation of B56δ but decreased the radiation-induced phosphorylation of ATM in the mouse lung. Expression of GαsQL increased the IκBα protein and decreased the levels of p50 and p65 subunits of NF-κB in nucleus after γ-ray irradiation, and PDTC increased the radiation-induced apoptosis. Pretreatment with prostaglandin E2 or isoproterenol increased the phosphorylation of B56δ and decreased the radiation-induced ATM phosphorylation and increased the apoptosis. In conclusion, cAMP signaling inhibits radiation-induced ATM activation by PKA-dependent activation of PP2A, and this signaling mechanism augments radiation-induced apoptosis by reducing ATM-dependent activation of NF-κB in lung cancer cells and mouse lung tissue.

From these studies, Gαs protein/cAMP signaling system regulates DNA damage responses such as DNA damage repair and apoptosis by various mechanisms. These findings suggest that Gαs protein/cAMP signaling system could be targeted to enhance the therapeutic efficiency of various cancers.

Key Words: Heterotrimeric stimulatory GTP-binding proteins (Gαs), cAMP signaling system, cisplatin, radiation, DNA repair, apoptosis, XIAP, XRCC1, Epac, ATM, cervical cancer, lung cancer

Student Number: 2006-30571

Contents

List of Figures

General Introduction

1. G protein

Heterotrimeric G proteins are the molecular switches that turn on intracellular signaling cascades in response to the activation of G-protein-coupled receptors (GPCRs) by extracellular stimuli. Therefore, G proteins have a crucial role in defining the specificity and temporal characteristics of the cellular response. The G proteins are composed of three subunits, α, β and γ, and their switching function depends on the ability of the G protein α-subunit ($G\alpha$) to cycle between an inactive GDP-bound conformation that is primed for interaction with an activated receptor, and an active GTP-bound conformation that can modulate the activity of downstream effector proteins A tremendous amount of structural information about G proteins is known from X-ray crystallographic studies, which have provided insight into GTP-mediated conformational changes in $G\alpha$, subunit interactions with effector proteins, and the mechanism of GTP hydrolysis. In humans, there are 21 $G\alpha$ subunits encoded by 16 genes, 6 $G\beta$ subunits encoded by 5 genes, and 12 $G\gamma$ subunits. Heterotrimers are typically divided into four main classes based on the primary sequence similarity of the $G\alpha$ subunit: $G\alpha_s$, $G\alpha_i$, $G\alpha_q$ and $G\alpha_{12}$ (1).

1-1. Heterotrimeric G protein structure

The Gα subunit structures reveal a conserved protein fold that is composed of a GTPase domain and a helical domain. The GTPase domain is conserved in all members of the G protein superfamily, including monomeric G proteins and elongation factors. This domain hydrolyses GTP and provides the binding surfaces for the Gβγ dimer, GPCRs and effector proteins. The helical domain is unique to Gα proteins and is composed of a sixα-helix bundle that forms a lid over the nucleotide-binding pocket, burying bound nucleotides in the core of the protein. All Gα subunits, except $G\alpha_t$, are post-translationally modified with the fatty acid palmitate at the N terminus. Members of the $G\alpha_i$ family are also myristoylated at the N terminus. These modifications regulate membrane localization and protein–protein interactions. The Gβ subunit has a seven-bladed b-propeller structure that is composed of seven WD40 sequence repeats. The N terminus of Gβ adopts an α-helical conformation that forms a coiled-coil with the N terminus of Gγ, and the C terminus of Gγ binds to blades five and six. All of the Gγ subunits undergo post-translational isoprenylation of their C termini with either a farnesyl ($G\gamma_1$, $G\gamma_8$ and $G\gamma_{11}$) or geranylgeranyl (all others) moiety. The G protein β- and γ-subunits form a functional unit that can only be dissociated under denaturing conditions (2).

2. cAMP signaling system

Cyclic adenosine 3′,5′-monophosphate (cAMP) is a universal second messenger that plays a crucial role in the intracellular signal transduction of various stimuli controlling a wide variety of cellular events including secretion, cell proliferation, differentiation, migration, and apoptosis. Cyclic AMP is produced from ATP by adenylyl cyclase isoforms, the majority of which are embedded in the cell surface membrane. These are activated by G protein-coupled receptors (GPCRs). GPCR activates adenylyl cyclase in their proximity and generates pools of cAMP. The local concentration and distribution of the cAMP gradient are limited by phosphodiesterases (PDEs). Particular GPCRs are confined to specific domains of the cell membrane in association with intracellular organelles or cytoskeletal constituents.

The subcellular structures may harbor specific isozymes of PKA that, through anchoring via AKAPs, are localized in the vicinity of the receptor and the cyclase. PDEs are also anchored and serve to limit the extension and duration of cAMP gradients. These mechanisms serve to localize and limit the assembly and triggering of specific pathways to a defined area of the cell close to the substrate. Cyclic AMP has effects on a range of effector molecules encompassing PKA, PDEs, guanine nucleotide exchange factors (GEFs) known as exchange proteins activated by cAMP (Epacs), and 4) cyclic nucleotide-gated ion channels (Figure. 1) (3).

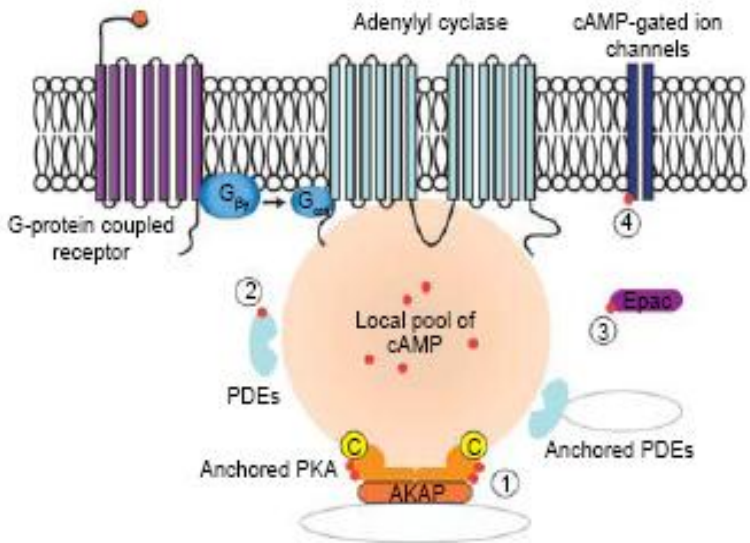

Figure 1. cAMP signaling pathway. Adapted from Pidoux G and Tasken K. (3).

2-1. Cyclic AMP-dependent Protein Kinase (PKA)

The PKA holoenzyme is 170 kDa and a heterotetramer composed of two catalytic subunits held in an inactive statement by association with a regulatory subunit dimer (Figure. 2). Cyclic AMP binds with two sites termed A and B on each R subunit. In the inactive form, only the B site is exposed and available for cAMP binding. When occupied, this enhances the cAMP binding to the A site by an intramolecular steric change. Binding of four cAMP molecules, two to each R subunit, leads to a conformational change and dissociation into R subunit dimer with four cAMP molecules bound and two C mononers. The C subunits become active catalytically and phosphorylate nearby target substrates on serine/threonine residues presented in a sequence context of Arg-Arg-X-Ser/Thr, Arg-Lys-X-Ser/Thr, Lys-Arg-X-Ser/Thr, or Lys-Lys-XSer/Thr (3).

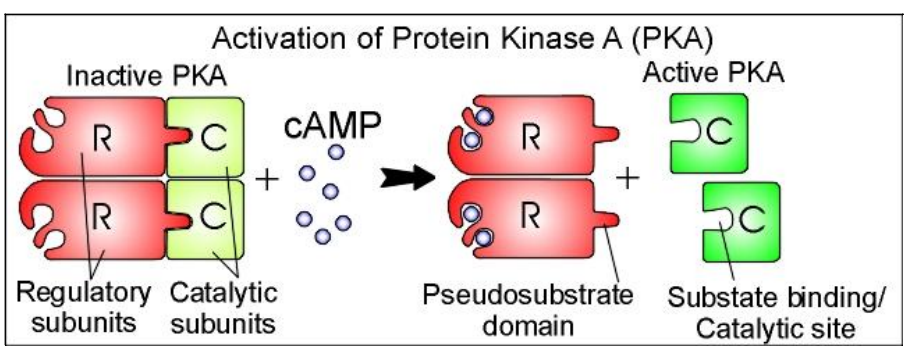

Figure 2. Subunits of PKA and PKA structural change. Adapted from O'Day DH. (4).

2-2. Exchange Proteins directly Activated by cAMP (Epac)

Epac responds to the second messenger cyclic AMP (cAMP) and are activated by Gs coupled receptors (Figure. 3). They act as specific guanine nucleotide exchange factors (GEFs) for the small G proteins, Rap1 and Rap2 of the Ras family. Epac and protein kinase A (PKA) may act independently but are often associated with the same biological process, in which they fulfill either synergistic or opposite effects. In addition, compelling evidence is now accumulating about the formation of molecular complexes in distinct cellular compartments that influence Epac signaling and cellular function (5).

There are two isoforms of Epac, Epac1 and Epac2, which are coded by two distinct genes, RAPGEF3 and RAPGEF4 in mammals. While Epac1 is ubiquitously expressed in all tissues with high levels of expression in the kidney, Epac2 is detectable most notably in the brain, pituitary, adrenal gland and pancreas (6). A shorter N-terminal splice variant of Epac2 named Epac2B has been recently identified in the adrenal gland suggesting that alternative splicing events may further add to the complexity of the functional characterization of Epac isoforms. Following this discovery, the long isoform Epac2 was renamed Epac2A. Epac1 and Epac2 are multi-domain proteins that share high homology sequence. Both isoforms contain an N-terminal regulatory region and a C-terminal catalytic region (Figure. 4) (7).

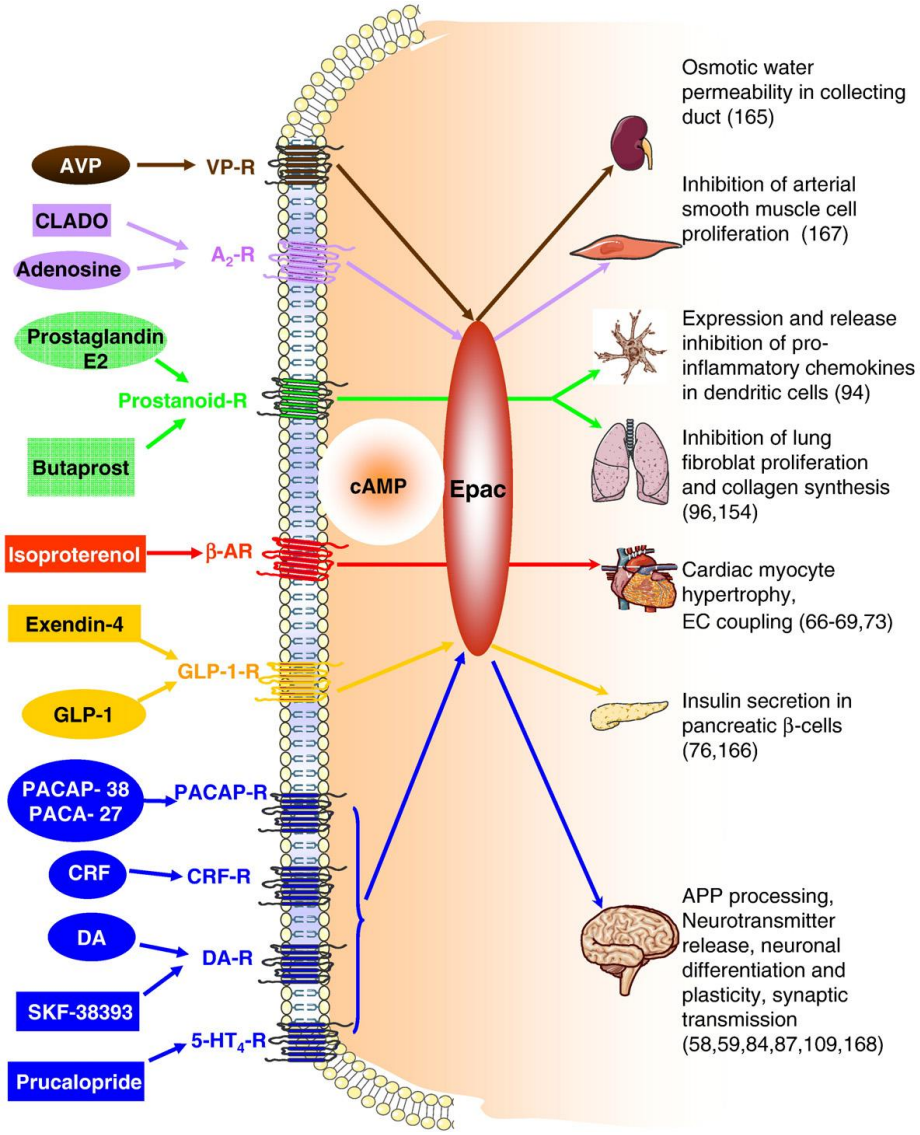

Figure 3. Epac-mediated actions of Gs-protein coupled receptors.

Adapted from Breckler M, et al (5).

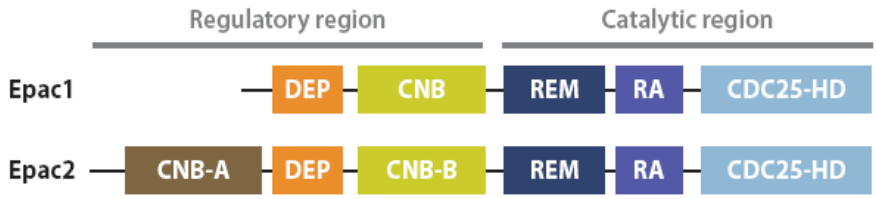

Figure 4. Domain architecture of the Epac proteins. Adapted from Gloerich M and Bos JL. (7).

3. DNA damage

3-1. DNA damage and response

DNA double-strand breaks (DSBs) bring about a serious threat to cell viability and genome stability. DSBs are generated naturally when replication forks encounter blocking lesions such as those produced by metabolic byproducts of cellular respiration (reactive oxygen species (ROS)) leading to fork collapse; during programmed genome rearrangements induced by nucleases, including yeast mating-type switching, V(D)J recombination, class-switch recombination, and meiosis. DSBs are also produced when cells are exposed to DNA damaging agents including ionizing radiation (IR), which creates DSBs directly and indirectly via production of ROS; chemical agents and UV light that create replication blocking lesions (alkyl adducts, pyrimidine dimers, and crosslinks); and cancer chemotherapeutics that poison

topoisomerase I, which produces replication-blocking lesions, or topoisomerase II, which traps the enzyme-DNA complex after DSB induction and can potentially produce DSBs during any phase of the cell cycle. The failure to repair DSBs, or misrepair, can result in cell death or large-scale chromosome changes including deletions, translocations, and chromosome fusions that enhance genome instability and are hallmarks of cancer cells. Cells have evolved groups of proteins that function in signaling networks that sense DSBs or other DNA damage, arrest the cell cycle, and activate DNA repair pathways. These cellular responses can occur at various stages of the cell cycle and are collectively called DNA damage checkpoints, but when cells suffer too much damage overlapping signaling pathways can trigger apoptosis to prevent propagation of cells highly unstable genomes with (8).

Eukaryotic cells repair DSBs primarily by two mechanisms: nonhomologous end-joining (NHEJ) and homologous recombination (HR). Frank DSBs, such as those produced by nucleases and IR, can be repaired by either pathway. DNA repair is dependent on the family of phosphatidylinositol-3-OH-kinase-like kinases (PIKKs), like ATM (ataxia-telangiectasia mutated) and ATR (ataxiatelangiectasia and Rad-3-related) kinases, and DNA PKcs (DNA protein kinase catalytic subunit). The kinases phosphorylate a variety of proteins that transduce the DNA damage signal (leading to cell cycle arrest), alternate transcription, start DNA repair or, if the damage cannot be

repaired, activate apoptosis (Figure. 5). One of the targets of ATM and ATR kinases is the MRN complex (MRE11/ RAD50/ NBN), a highly conserved protein complex involved in DNA replication, DNA repair, telomere maintenance, and signaling to the cell cycle checkpoints. The MRN complex plays a critical role in the DNA damage sensing, signaling and repair mechanism, as well as maintenance of chromosomal integrity in the cell (9).

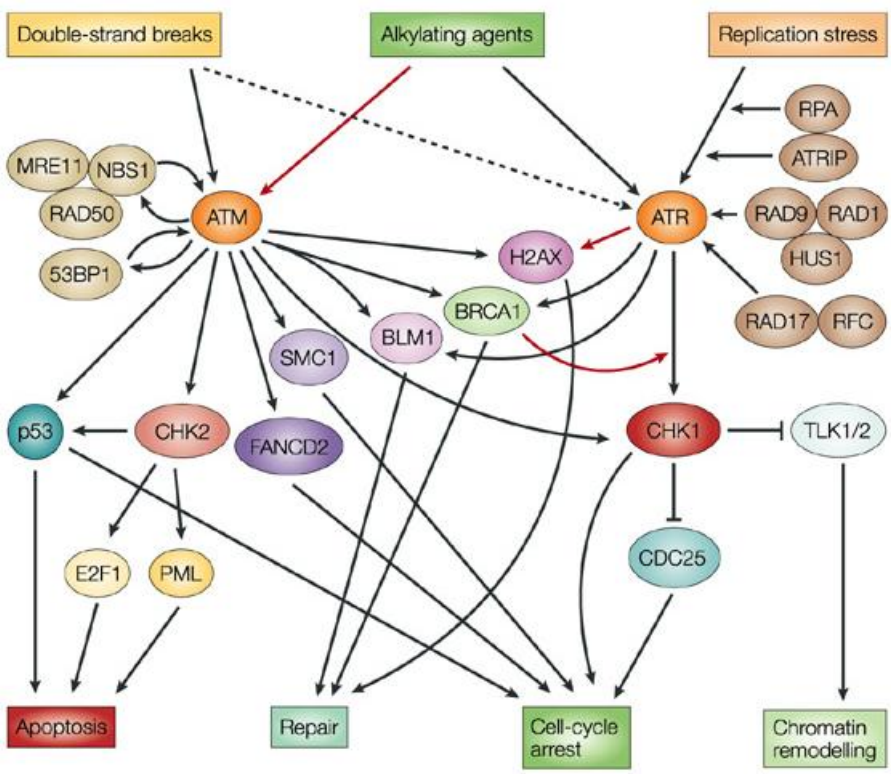

Figure 5. DNA damage response signal-transduction network. Adapted from Zhou BB and Bartek J. (10).

3-1-1. XRCC1

DNA repair plays a critical role in protecting the genome of the cell from ionizing radiation. Reduced DNA repair activity could increase the susceptibility to environmental- or occupational-induced cancers and apoptosis. Three coding polymorphisms at codon 194, codon 280 and codon 399 in the x-ray cross complementing group 1 (XRCC1) DNA repair gene have been identified, and it is possible that these polymorphisms might affect DNA repair activity and thus modulate cancer susceptibility. Also, XRCC1 polymorphisms have a relationship with lung cancer risk. It increased significantly for the variant XRCC1-77 genotypes (TC and CC) compared with the TT genotype (11).

Recently, it has been proposed that several factors are involved in alternative/backup pathways for NHEJ. These pathways are independent of Ku 70/80 and suppressed by DNA-PK. Although Polβ, XRCC1, PARP-1, and DNA ligase III (Lig3) contribute predominantly to BER and SSB repair, these three proteins are also considered to be candidate components for backup pathways for NHEJ. Lig3 provides a major ligation activity for these NHEJ pathways. However, very low residual ligation activity is still observed even without Lig4 and Lig3, indicating that yet other factors may act in the ligation step. In addition, these backup NHEJ pathways are markedly dependent on the cell's growth state, and enhanced repair activity was observed in the G2-phase. It is expected that other factors also participate to support not only NHEJ but also HR to protect DNA from potentially lethal DSBs.

3-1-2. ATM

ATM is a Ser/Thr protein kinase and is a member of the phosphoinositide 3-kinase (PI3K)-related protein kinase (PIKK) family, which also includes Rad3-related protein (ATR), the catalytic subunit of DNA-dependent protein kinase (DNA-PKcs) and SMG1, a protein kinase that is involved in the DNA-damage response but is also required for nonsense-mediated decay of mRNA that contains premature terminator codons. The kinase domain is located close to the C terminus in all of these proteins except SMG1, in which the kinase domain is more central. This domain has protein kinase activity, and p53 was the first substrate of ATM to be identified *in vitro* and *in vivo*. The stabilization and activation of p53 was defective in A-T cells, and these cells were also characterized by a defective G1–S checkpoint, in which p53 has a central role. ATM has multiple substrates. Indeed, recent proteomic analysis results of phosphorylated proteins induced by DNA damage suggest that the ATM and ATR network might have as many as 700 substrates. ATM also has a number of other domains, including a FAT domain which is common to ATM, mammalian target of rapamycin (mTOR) and transformation/transcription domain-associated protein (TRRAP) and an extreme C-terminal FATC domain that is found in combination with FAT in this subfamily of proteins. Other domains include an N-terminal substrate-binding domain, a Leu zipper, a Pro-rich region that enables

it to bind to ABL kinase and a peroxisomal targeting signal sequence (PTSI) (Figure. 6).

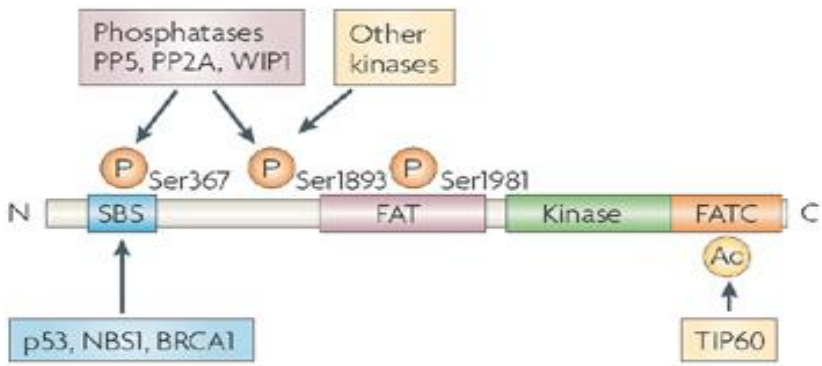

Figure 6. Schematic representation of ATM. Adapted from Lavin MF. (12).

Dephosphorylation by protein phosphatase (PP2A) also participates in the regulation of these phosphorylation signals. In the absence of DNA damage, dimers of ATM (inactive ATM) undergo a basal level of auto-phosphorylation at serine 1981 that is removed by bound PP2A (Figure. 7). The addition of OA to cells inhibits PP2A protein phosphatase activity, allowing auto-phosphorylated ATM to accumulate in the absence of DSBs and without an increase in protein kinase activity. IR causes dissociation of PP2A from ATM in a mechanism that requires the protein kinase activity of ATM, leading to accumulation of auto-phosphorylated ATM. Independently, IR causes the recruitment of the MRN complex to sites of DNA damage (13). Auto-phosphorylated ATM is then recruited to the DSB, possibly resulting in full activation of ATM protein kinase activity, followed by phosphorylation of histone H2AX at serine 139 (γ-H2AX) across several megabases of DNA and localized phosphorylation of ATM substrates at IR-induced foci.

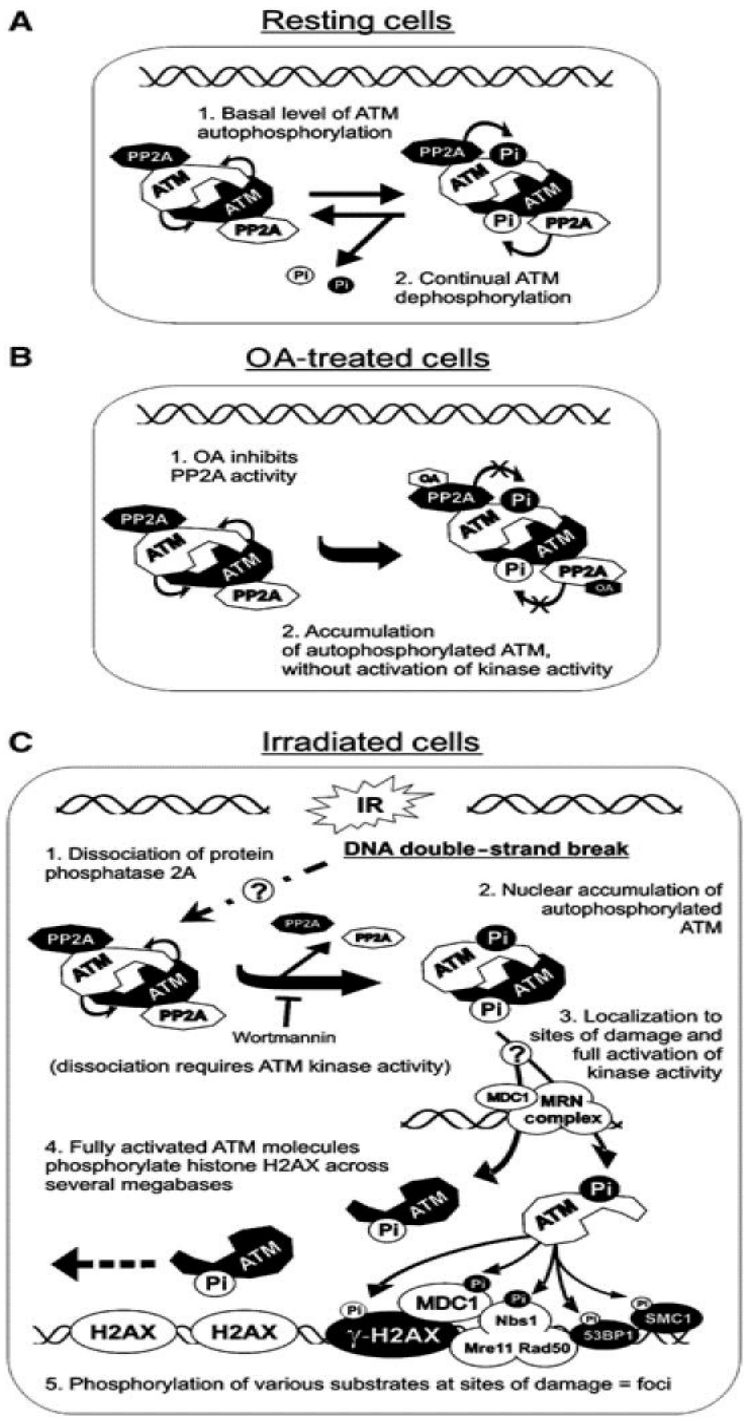

Figure 7. A model for the regulation of ATM by PP2A. Adapted from Goodarzi AA, et al (13).

4. Apoptosis

4-1. Apoptosis

Apoptosis was first observed in 1842 by a German scientist Carl Vogt in Jent und Gassman, Solothurn 1842; 130 and in 1951, Glucksmann, A (in Cambridge Philosophical Society of biological review 26; 59) reviewed and rediscovered developmental cell deaths in embryological tissues. In 1964, Lockshin, RA and Williams, CM first used the term of “programmed cell death” to describe the breakdown of the intersegmental muscles of silkworms. In 1972, three British scientists Kerr, Wyllie and Currie proposed the term of “apoptosis” for morphology of naturally occurring or physiological cell deaths. They recognized the importance of apoptosis and suggested that it is a basic biological phenomenon with wide-ranging implications in tissue kinetics.

Apoptosis is a naturally occurring process by which a cell is directed to programmed-cell death. It is based on a genetic program that is an indispensable part of the development and function of an organism. In this process, cells that are no longer needed or that will be detrimental to an organism or tissue are disposed of in a neat and orderly manner; this prevents the development of an inflammatory response, which is often associated with Necrotic cell death. There are at least two broad pathways that lead to Apoptosis, an "Extrinsic" and an "Intrinsic" Pathway (Figure. 8). In both pathways, signaling results in the

activation of a family of Cys (Cysteine) proteases, named caspases that act in a proteolytic cascade to dismantle and remove the dying cell. Extensive plasma membrane blebbing occurs followed by karyorrhexis and separation of cell fragments into apoptotic bodies during a process called “budding.” Apoptotic bodies consist of cytoplasm with tightly packed organelles with or without a nuclear fragment. These bodies are subsequently phagocytosed by macrophages, parenchymal cells, or neoplastic cells and degraded within phagolysosomes. Macrophages that engulf and digest apoptotic cells are called “tingible body macrophages” and are frequently found within the reactive germinal centers of lymphoid follicles or occasionally within the thymic cortex. The tingible bodies are the bits of nuclear debris from the apoptotic cells. There is essentially no inflammatory reaction associated with the process of apoptosis or with the removal of apoptotic cells. This is because; apoptotic cells do not release their cellular constituents into the surrounding interstitial tissue. Also, they are quickly phagocytosed by surrounding cells thus likely preventing secondary necrosis and the engulfing cells do not produce anti-inflammatory cytokines.

It is important to understand the molecular events that contribute to drug-induced apoptosis, and how tumors evade apoptotic death. Defects in apoptosis are implicated in both tumorigenesis and drug resistance, and these defects are cause of chemotherapy failures. Especially, the role of apoptosis regulation in lung cancer shows the

differential sensitivities in the major subtypes of lung cancer. Small cell lung carcinoma (SCLC) and non-small cell lung carcinoma (NSCLC) represent the two major categories of lung cancer that differ in their sensitivity to undergo apoptosis.

4-1-1. Extrinsic pathway

This pathway involves responses to death inducing ligands including TNF, FasL, or TRAIL. Binding of death ligands to their receptors, including FAS (for FasL), TNFR1 (for TNF), or DR4 and DR5 (for TRAIL) trigger apoptosis via the recruitment of adaptor protein FADD, which subsequently helps in the recruitment of procaspase-8. Conforming of ligand receptor complex, FADD and caspase-8 results the formation of a Death Inducing Signaling Complex (DISC). Upon its recruitment to the DISC, caspase-8 is activated by cross-proteolysis which leads to activation of downstream effector caspases either directly (Type I cells) or via an amplification loop involving truncated Bid (tBid) mediated release of cytochrome c from the mitochondria (Type II cells) (14).

4-1-2. Intrinsic pathway

The other major apoptotic initiator pathway involves release of cytochrome *c* from mitochondria in response to several internal and some external stimuli, such as growth factor withdrawal, osmotic stress, and hypoxia. Cytochrome c forms a multi-protein complex with the

adaptor molecule Apaf-1 and procaspase-9 in the presence of dATP to form a multi-protein complex, called an. Procaspase-9 is activated upon recruitment to this complex and in turn activates the effector caspases. However, cytochrome c-mediated caspase activation may not be sufficient to lead to cell death. This is due to the presence of a family of proteins, called the IAPs (inhibitor of apoptosis protein), which can bind and inhibit the active caspases in the apoptosome. This inhibition is relieved by the release of another mitochondrial protein, called Smac/Diablo, which binds to the IAPs and releases active caspases from their inhibitory influence.

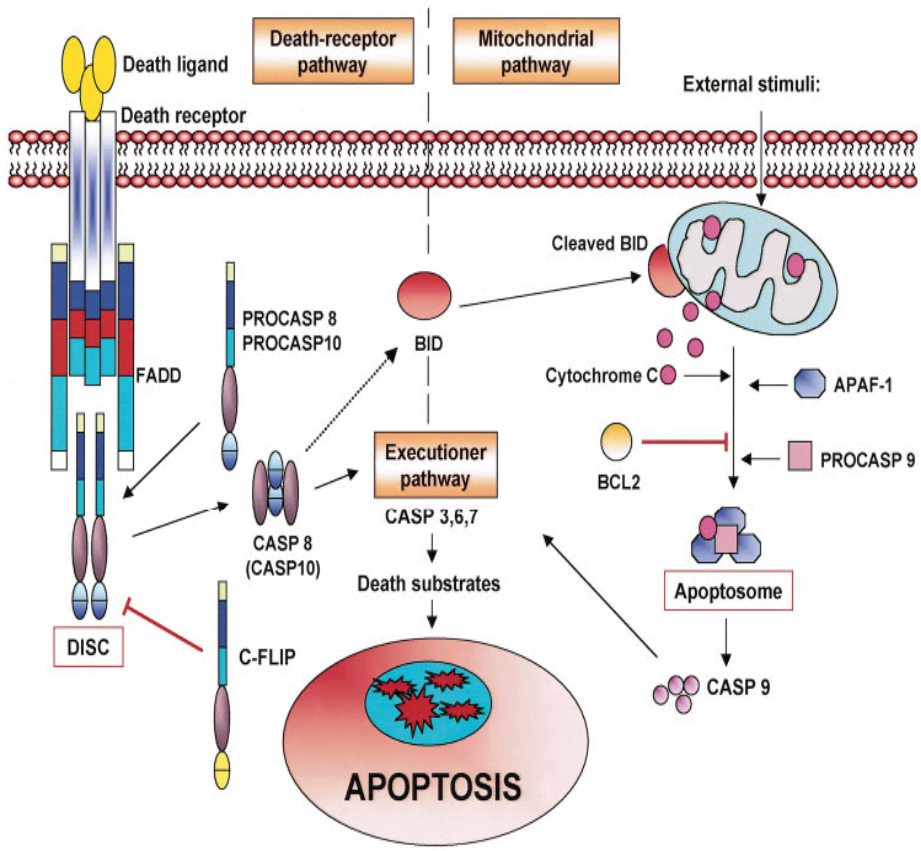

Figure 8. Apoptosis pathway. Adapted from Shivapurkar N, et al (14).

4-2. Bcl-2 family proteins

Bcl-2 is the mammalian homologue of the *C. elegans* protein Ced-9 (Figure. 9). The Bcl-2 gene was discovered when it was found to be linked to an immunoglobulin locus by translocation in follicular lymphomas. The finding that Bcl-2 inactivation prevented apoptosis instead of promoting cell proliferation was a crucial discovery, eventually leading to the concept that inhibition of apoptosis was one of the hallmarks of cancer. Bcl-2 has four conserved Bcl-2 homology (BH) domains. In mammals, the Bcl-2 family consists of at least 20 members, all of which share at least one BH domain. Bcl-2 and at least four other family members are anti-apoptotic proteins (Bcl-2, Bcl-XL, Mcl-1, Bcl-w and so on), and share BH1, 2, and 3 regions. The Bax subfamily contains BH1, 2, and 3 domains, but is pro-apoptotic in function. Most pro-apoptotic family members (Bax, Bak, Bad, Bid, Bik, Noxa, Puma and so on) share only a short BH3 domain (BH3 only subfamily; Bad, Bid, Bik, Bim, Noxa, Puma and so on) (Figure. 10). Normally they are sequestered on the cytoskeleton, but pro-apoptotic signals cause them to insert their BH3 domain into a groove in pro-survival family members. The Bax proteins, Bax and Bak are widely distributed; act further downstream, probably on the mitochondrial membrane. Inactivation of both genes is needed for impaired apoptosis.

Bcl-2 and related proteins are among the best studied of the apoptotic molecules in lung cancer, with over 50 references. Bcl-2 is expressed

relatively early during bronchial preneoplasia and is related to smoke exposure. Bcl-2 expression in SCLC is greater than in NSCLC, and the levels in squamous cell carcinomas are higher than in adenocarcinomas. Since Bax is a pro-apoptotic member of the Bcl-2 family, the Bcl-2: Bax ratio has been proposed as a measure of tumor resistance to apoptosis. In neuroendocrine lung tumors, there was an inverse correlation between the ratios in low-grade (typical and atypical carcinoids) and high-grade tumors with a predominant Bax expression in the first group and predominant Bcl-2 expression in the second. The highest levels of Bcl-2 expression and Bcl-2: Bax ratios were associated with a p53 mutant immunophenotype. Aggressiveness, response to therapy, and prognosis in lung tumors could be linked to Bcl-2 family proteins.

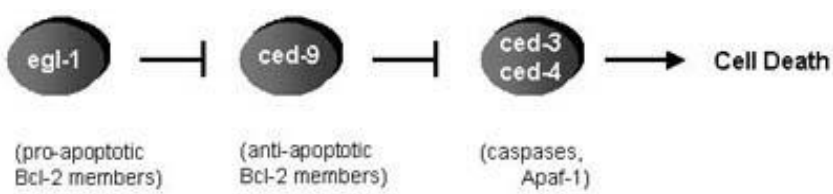

Figure 9. C.elegans as a model system contains basic components of the cell death machinery. Adapted from Gewies A. (15).

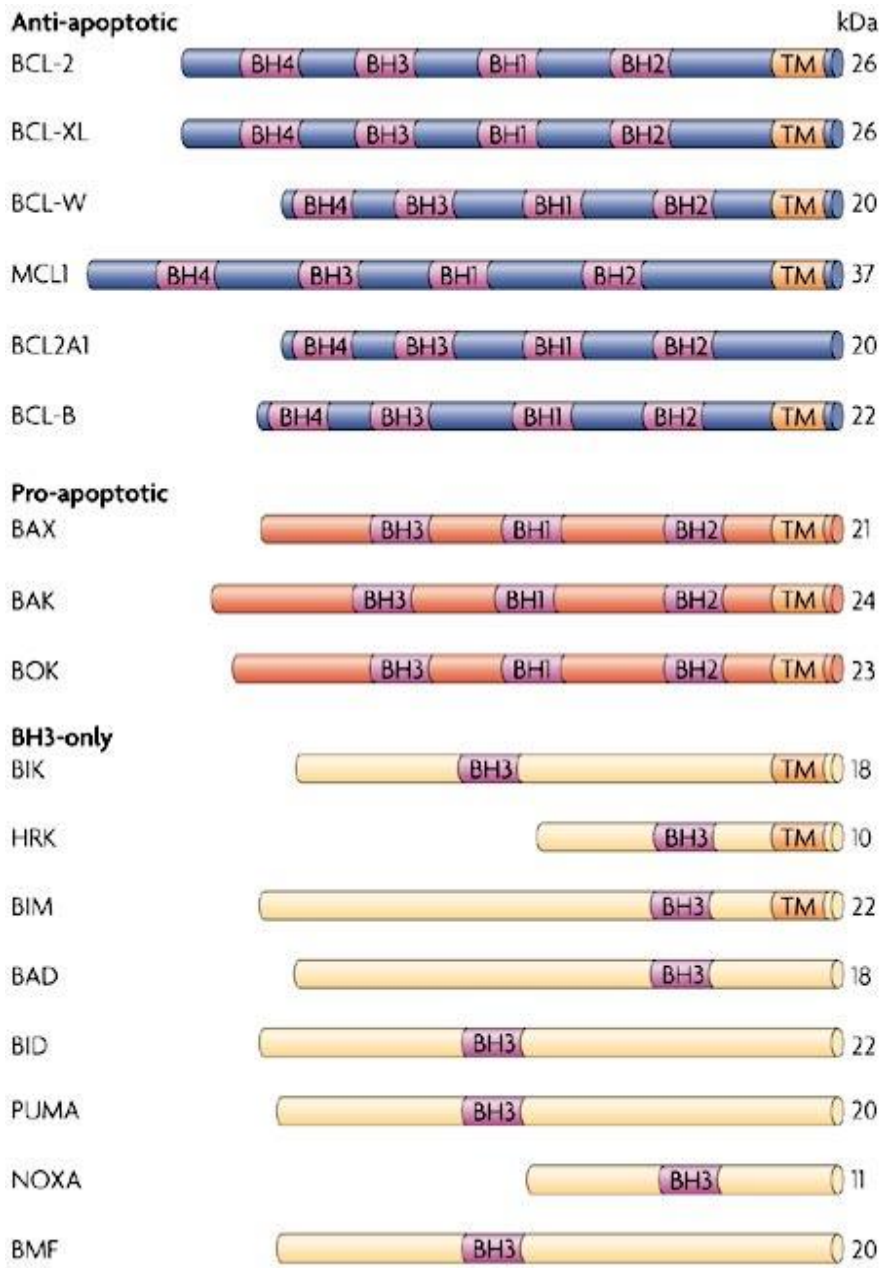

Figure 10. Summary of anti- and pro-apoptotic Bcl-2 family proteins. Adapted from Taylor RC, et al (16).

4-3. Inhibitors of apoptosis proteins (IAPs) family proteins

The IAP class of proteins was originally identified in baculovirus and later in metazoans. While the anti-apoptotic members of the Bcl-2 family inhibit the mitochondrial pathway, IAP molecules are found in the genomes of all metazoans, and are characterized by the presence of 1–3copies of a ~ 70 amino acid zinc-finger fold, designated the BIR. IAP family include XIAP (X-linked IAP), c-IAP1, c-IAP2, ILP2 (IAP-like protein-2), ML-IAP (melanoma IAP)/Livin, NAIP (neuronal apoptosis-inhibitory protein) and survivin, and are also known as MIHA/ILP1, MIHB/HIAP2, MIHC/HIAP1, Ts-IAP, KIAP, BIRC1 and TIAP, respectively. A conserved linker peptide that precedes the BIR2 (baculoviral IAP repeat-2) domain of XIAP, c-IAP1 or c-IAP2 is responsible for inhibiting caspases-3 and -7 in mammals. On the basis of structural information, residues 126–143 of NAIP are predicted to carry out this function. Only the BIR3 domain of XIAP can potently inhibit caspase-9. Most IAPs contain other structural motifs including a caspase-recruitment domain (CARD), and a RING finger. IAPs also inhibit apoptosis by modulation of the transcription factor NF-κB. Because their action is downstream of the anti-apoptotic Bcl-2 proteins (which acts at the mitochondrial pathway), the IAPs, by inhibiting the executioner pathway, inhibit all of the apoptotic pathways. The mitochondrial protein Smac antagonizes the IAPs by releasing the IAP-bound caspases (Figure. 11) (17).

Relatively little has been published on the role of IAPs in lung cancer.

Survivin is unique among the IAPs. Survivin has a single BIR and its expression is cell cycle related. It is localized to components of the mitotic spindle. It appears to be an oncofetal protein, with strong expression in embryonic and fetal tissues but is absent in most differentiated adult tissues. Considerable over expression has been documented in several tumor types including lung. Although survivin is expressed in the vast majority of NSCLC tumors, its absence may be associated with improved prognosis (18).

X-linked inhibitor of apoptosis protein (XIAP), also known as inhibitor of apoptosis protein 3 (IAP3), is a protein that stops apoptotic cell death. In human, this protein (XIAP) is produced by a gene named XIAP gene located on the X chromosome. XIAP is inhibited by Smac/DIABLO and HTRA1 (Omi), two death-signaling proteins released into the cytoplasm by the mitochondria. Smac/DIABLO, a mitochondrial protein and negative regulator of XIAP can enhance apoptosis by binding to XIAP and preventing it from binding to caspases. This allows normal caspase activity to proceed. The binding process of Smac/DIABLO to XIAP and caspase release requires a conserved tetrapeptide motif.

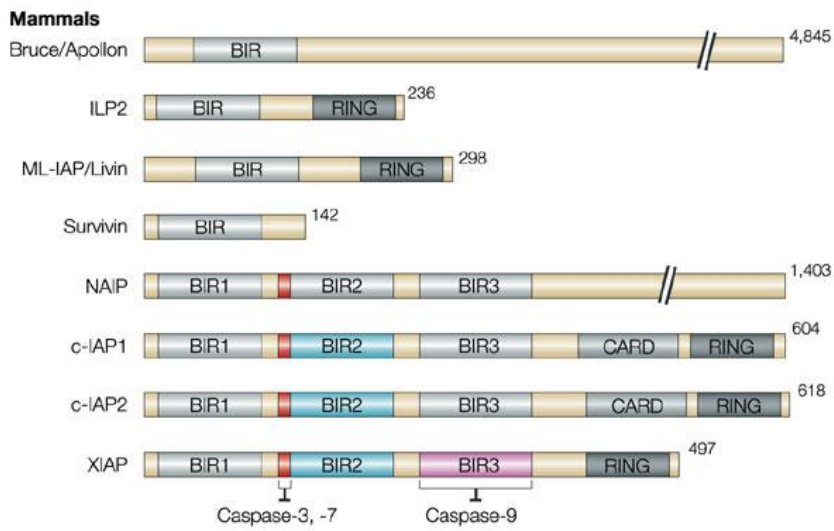

Figure 11. IAPs in mammals. Adapted from Riedl SJ and Shi Y. (19).

Purpose

This study aimed to investigate whether Gαs-cAMP signaling system regulates the DNA damage responses and if so, the underlying molecular mechanism in cancer cells.

The aim of this study was:

1. To investigate the effect of Gαs onto cisplatin-induced apoptosis and its underlying molecular mechanism in cervical cancer cells.

2. To analyze the effects of the cAMP signaling system on radiation-induced DNA damage repair in non-small cell lung cancer cells.

3. To examine the effect of Gαs on radiation-induced apoptosis and its regulating mechanism in non-small cell lung cancer cells.

Part I.

Effect of Gαs protein on cisplatin-induced apoptosis

Introduction

Cisplatin is widely used for the treatment of human malignant tumors, and it is known to form intrastrand cross-links between neighboring purines in genomic DNA to induce apoptosis in various tumor cells (20). Cisplatin-induced DNA damage activates both the intrinsic and extrinsic apoptotic pathways; the former is mitochondria-dependent (21) and the latter is the Fas/Fas ligand-dependent apoptotic cascade (22).

Apoptosis is a type of programmed cell death and is known to play important roles in the maintenance of homeostasis of multicellular organisms and in the pathogenesis of various human diseases, such as cancer (23). Improving the specificity and efficiency of cancer treatments-induced apoptosis is a potential strategy for developing better cancer treatment methods. The activation of caspase is regulated by death receptors, Bcl-2 family proteins, cytochrome c, and inhibitors of apoptosis (IAPs) (19, 24).

Heterotrimeric GTP-binding proteins (G proteins) transduce extracellular signals into intracellular signals by coupling with receptors and effectors. G proteins are composed of α-, β-, and γ-subunits (25) and are classified into four main families based on the α subunits of the G protein (Gα): Gαs, Gαi/o, Gαq11, and Gα12/13 (26). When a signaling molecule binds to a G protein-coupled receptor (GPCR), the

receptor stimulates replacement of GDP with GTP on Gα on the inner surface of the cell membrane. Once GTP is bound, the Gα is activated and dissociates both from the receptor and from the βγ subunits (27). Both the activated α and βγ subunits regulate cell growth, proliferation, differentiation, and apoptosis (28).

Materials and Methods

Cell culture and reagents

Human cervical cancer cells: HeLa cells (Korea Cell Line Bank, Seoul, Korea), C33A and CaSKi cells (ATCC, Manassas, VA, USA) were cultured in Dulbecco's modified Eagle's medium (DMEM) containing 10% fetal bovine serum (JBI, Korea) and 100 units/ml penicillin/streptomycin. Cells were maintained in a 5% CO_2 incubator at 37ºC. Cisplatin, H89, cycloheximide (CHX), and dimethyl sulfoxide (DMSO) were purchased from Sigma (St. Louis, MO, USA); forskolin, isobutylmethylxanthine (IBMX), and MG132 were purchased from Calbiochem (La Jolla, CA, USA).

Expression constructs and transient transfection

HeLa cells that stably express the constitutively active mutant of a long form Gαs (GαsQ227L, GαsQL) were established by transfecting the mutant construct in a pcDNA3 vector (Invitrogen, Paisley, UK). The GαsQL mutant has a mutation of a residue that is essential for the intrinsic GTPase activity (29). Luciferase reporter plasmids containing the XIAP promoter were kindly provided by Dr. Taeg Kyu Kwon (Keimyung University, Korea) (30). Decoy oligonucleotides for the cAMP response element (decoy CRE) were prepared as described previously (31). XIAP siRNA oligonucleotides were purchased from

Cell Signaling (Danvers, MA, USA) and control siRNA were from Bioneer (Korea), with the following sequences: sense, 5'-CCUACGCCACCAAUUUCGU-3', antisense, 5'-AGCAAAUUGGUGGCGUAGG-3'. Cells were transfected by the calcium phosphate method (32).

Western blot analysis

Western blotting was performed as previously described (31). Antibodies against Gαs, XIAP and c-IAP2 were from Santa Cruz Biotechnology (CA, USA), and antibodies against PARP, cleaved caspase-3 (Asp175), phosphorylated CREB (Ser133), and CREB were from Cell Signaling Technology (Beverly, MA, USA). An antibody against β-Actin was purchased from Sigma (St. Louis, MO, USA) and the hemagglutinin (HA) antibody was from Covance Research Products (Berkeley, CA, USA). Cytochrome c release from the mitochondria into the cytoplasm was analyzed by subcellular fractionation (33) followed by immunoblotting using an antibody from BD Biosciences (San Diego, CA, USA). Proteins were visualized by the Enhanced Chemiluminescence (ECL) reagent (Thermo scientific, Waltham, MA). The densities of the bands were quantified using the Multi Gauge v2.3 software (Fuji, Tokyo, Japan), and relative band densities were expressed as percentages of corresponding control densities.

Real-time quantitative reverse transcription polymerase chain reaction (RT-PCR)

Real-time RT-PCR was performed using a PRISM 7700 ABI thermal cycler (31). PCR was performed with specific primers: XIAP, forward primer 5'-ACACCATATACCCGAGGAAC-3' and reverse primer 5'-CTTGCATACTGTCTTTCTGAGC-3'; GAPDH, forward primer 5'-ACCACAGTCCATGCCATCAC-3' and reverse primer 5'-TCCACCACCCTGTTGCTGTA-3'. After 32 cycles of PCR, average threshold cycle (Ct) values for XIAP from triplicate PCR reactions were normalized against the average Ct values for GAPDH from the same cDNA sample.

Generation of CRE-like element reporter constructs with truncation mutations

The forward primer for cloning the XIAP promoter containing the CRE-like element region had a SacI site at the 5' terminus, 5'-CGAGCTCTGAGGTCA-GGAGTTCA-3', and the forward primer for constructing mutations in the CRE-like element also had a SacI site at the 5' terminus, 5'-CGAGCTCTGTTGTCA-GGAGTTCA-3'. The reverse primer had a HindIII site at the 5' terminus, 5'-CCCAAGCTTCTTCTCTTGAAAAT-3'. PCR was performed using LA *Taq* polymerase (Takara Shuzo Co., Japan), and the PCR products were ligated into a T-vector and digested with XcmI (TA cloning). The cloned promoter regions were then subcloned into a pGL2-basic vector

(Promega Corp., Madison, WI, USA) for analysis of XIAP promoter activity.

Dual-luciferase reporter assay

HeLa cells (vector- or GαsQL-transfected) were transfected with plasmids containing luciferase reporter genes (XIAP-pLuc and Renilla-pLuc) by the calcium phosphate method. Luciferase activities were assayed using the Dual-Luciferase Reporter Assay System (Promega Corp., Madison, WI) according to the manufacturer's instructions. At least four independent experiments in duplicate were performed, and promoter activities were normalized versus Renilla luciferase activity.

Data analysis

At least three or more independent experiments were conducted for all the analyses, and data were presented as means ± standard errors (SE). The nonparametric Mann-Whitney U test was used to analyze mean values, and a *p* value of less than 0.05 was considered statistically significant.

Results

Gαs inhibited cisplatin-induced apoptosis of HeLa cervical cancer cells

To examine the effect of Gαs into cisplatin-induced apoptosis, GαsQL was stably expressed in HeLa cells by transfection. The expression of GαsQL was confirmed by western blotting using a Gαs-specific antibody. There are 4 alternatively spliced variants of Gαs, and they are usually visualized as 2 bands in western blots. The GαsQL protein appeared as a slow moving upper band in western blots. The expression of GαsQL increased the expression and phosphorylation at Ser-133 of cAMP response element binding protein (CREB) in western blotting (Figure. 12), indicating that the expressed GαsQL was functionally active because Gαs stimulates adenylate cyclases to increase cAMP levels, which activate the cAMP-dependent protein kinase (PKA) that phosphorylates CREB (34). Flow cytometric analysis of Annexin V-FITC- and propidium iodide-stained cells showed that GαsQL effectively decreased the number of cells that was stained with Annexin V-FITC but not stained with propidium iodide-stained following cisplatin treatment (Figure. 13). The expression of GαsQL significantly decreased cleavage of caspase-3 and PARP compared with vector-expressing control cells. GαsQL also reduced cytochrome c release from mitochondria into the cytosol (Figure. 14). Moreover, when the

expression of Gαs was knocked down by transfection of a Gαs small hairpin RNA (shRNA) construct, an increase in cleavage of caspase-3 and PARP, compared with LacZ shRNA-transfected control cells, was observed (Figure. 15). These results indicate that Gαs inhibits cisplatin-induced apoptosis of HeLa cells.

Gαs inhibited cisplatin-induced apoptosis by increasing XIAP protein levels in HeLa cells

Next, in order to determine the mechanism by which Gαs inhibited cisplatin-induced apoptosis, the effect of Gαs on the expression of IAPs was analyzed. Expression of GαsQL significantly increased the basal XIAP by 1.7 ± 0.2-fold (p = 0.036) in clone #5, and 1.6 ± 0.3-fold (p = 0.014) in clone #11 in comparison with the vector-expressing cells (Figure. 16). Treatment with cisplatin decreased XIAP to 37.1 ± 0.1% in vector-transfected cells, and expression of GαsQL reduced XIAP to 15.8 ± 0.1% in clone #5 and 17.1 ± 0.3% in clone #11. However, the expression of cellular IAP (cIAP) was not changed by GαsQL expression or cisplatin treatment. To confirm that XIAP can mediate the anti-apoptotic effect of GαsQL, the effect of XIAP knock down was examined. Knock down of XIAP by siRNA increased the cleavage of caspase-3 (1.4 ± 0.0-fold, p = 0.037) and PARP (2.0 ± 0.9-fold, p = 0.052) compared with the control siRNA (Figure. 17). These results indicated that XIAP mediates the protective effect of Gαs against

cisplatin-induced apoptosis of HeLa cells. In addition, we analyzed the effect of Gαs on apoptosis induced by other chemotherapeutic drugs. Expression of GαsQL also inhibited doxorubicin-induced apoptosis with an increased level of XIAP in HeLa cells from the vector transfected cells. However, expression of GαsQL failed to show any inhibitory effect against paclitaxel-induced apoptosis (Figure. 18).

To examine whether XIAP mediates the anti-apoptotic effect of the Gαs-cAMP signaling system in other cervical cancer cells, we assessed the effect of increased cAMP levels on cisplatin-induced apoptosis. Treatment with forskolin and IBMX, which increase cAMP levels as Gαs does, decreased the cleavage of caspase-3 and PARP, and increased XIAP in C33A cells (Figure. 19) and CaSKi cells (Figure. 20). These results indicate that XIAP also mediates the anti-apoptotic effect of the Gαs-cAMP signaling system in several cervical cancer cells. Because the anti-apoptotic effect was observed both in HPV-positive HeLa cells and CaSKi cells and in HPV-negative C33A cells, the effect does not seems to be related with HPV infection.

Gαs up-regulated XIAP expression by stimulating transcription through a cAMP, PKA, CREB, and novel CRE-like element-dependent pathway

To investigate how Gαs increased XIAP expression, the effect of Gαs on the XIAP mRNA levels was examined by real-time RT-PCR. Stable

expression of GαsQL increased the basal XIAP mRNA by 4.7 ± 3.2-fold (p = 0.037) and maintained the increased XIAP mRNA even after cisplatin treatment (2.3 ± 1.5-fold, p = 0.046) from 0.4 ± 0.1-fold in cisplatin-treated vector-expressing cells (Figure. 21). To confirm that Gαs induces XIAP by activation of the cAMP signaling pathway, we analyzed the effects of forskolin, IBMX, H89, and CRE-decoy oligonucleotides. Treatment with forskolin and IBMX increased basal XIAP mRNA to 4.5 ± 2.5-fold (p =0.013) of the untreated HeLa cells, and cisplatin-induced XIAP mRNA to 1.75 ± 0.5 from 0.44 ± 0.0 of the untreated control (p = 0.015) (Figure. 22). Treatment with H89, a PKA inhibitor, decreased XIAP mRNA to 3.3 ± 0.1-fold (p = 0.034) and 1.43 ± 0.4-fold (p = 0.043) in vector- and Gαs-expressing cells, respectively, which resulted in increased expression of XIAP protein (Figure. 23). The effect of forskolin, IBMX, and H89 on cAMP signaling pathway was confirmed by analyzing the effect on phosphorylation of CREB (Figure. 24). In addition, transfection of CRE-decoy oligonucleotides also decreased XIAP mRNA to 5.0 ± 0.1-fold (p = 0.034) and 1.00 ± 0.5-fold (p = 0.043) in vector- and Gαs-expressing cells, respectively, compared with transfection of the control oligonucleotides (Figure. 25), which resulted in decreased expression XIAP protein (Figure. 26). CRE-decoy successfully decreased CRE-luciferase activity (Figure. 27). These results indicate that Gαs increases XIAP mRNA levels in a cAMP-, PKA- and CREB-dependent pathway.

Next, to investigate the mechanism of Gαs-increased XIAP mRNA levels, we analyzed the effect of Gαs onto XIAP transcriptional activity using a dual-luciferase reporter system containing the 5' untranslated region of the XIAP promoter from -1510 bp (WT). Expression of GαsQL significantly increased the basal XIAP luciferase activity to 7.2 ± 1.6-fold, and cisplatin-treated activity to 5.5 ± 1.0-fold compared with vector-expressing cells (Figure. 28). Because CREB was found to be involved in XIAP expression, we analyzed the nucleotide sequences of the XIAP promoter to find the CRE, and identified a novel CRE-like element (TGAGGTCA) at -1396 bp of the XIAP promoter. Thus, we examined the involvement of this CRE-like element in the Gαs-induced transcription of XIAP. Expression of GαsQL increased luciferase activity to 3.4 ± 0.3-fold under the control of the XIAP promoter construct that had a truncation upstream of the CRE-like element (TWT), and to 1.4 ± 0.2-fold (p = 0.049) under the control of the XIAP promoter construct that had the same truncation and replacement of AG to TT in the CRE-like element (TM). The mutation of the CRE-like element (TM) augmented cisplatin-induced decreases in XIAP luciferase activity (0.9 ± 0.3-fold, p = 0.046), compared with TWT (Figure. 28), indicating that Gαs induces XIAP transcription partly via the CRE-like element in the XIAP promoter.

Gαs up-regulated XIAP expression by inhibiting the degradation of XIAP protein

To examine the effect of Gαs on the XIAP protein stability, the degradation rate of XIAP was analyzed in the presence of cycloheximide. XIAP protein was degraded rapidly in vector-expressing cells with a half-life of 42 minutes. In contrast, XIAP protein in Gαs-expressing cells was degraded slowly, and more than 70% of XIAP protein remained intact after 60 min (Figure. 29). Moreover treatment with MG-132, a proteasome inhibitor, completely blocked the degradation of XIAP in vector-expressing cells, demonstrated by recovery of the XIAP protein to 1.09 ± 0.1 from the value of 0.5 ± 0.0 (p = 0.021), showing that XIAP was degraded via the proteasomal degradation pathway (Figure. 30). Expression of GαsQL decreased the levels of ubiquitinated XIAP without regard to cisplatin treatment and compared with expression of control vector (Figure. 31). This result indicates that Gαs upregulates XIAP expression partly by inhibiting ubiquitination and proteasomal degradation of XIAP.

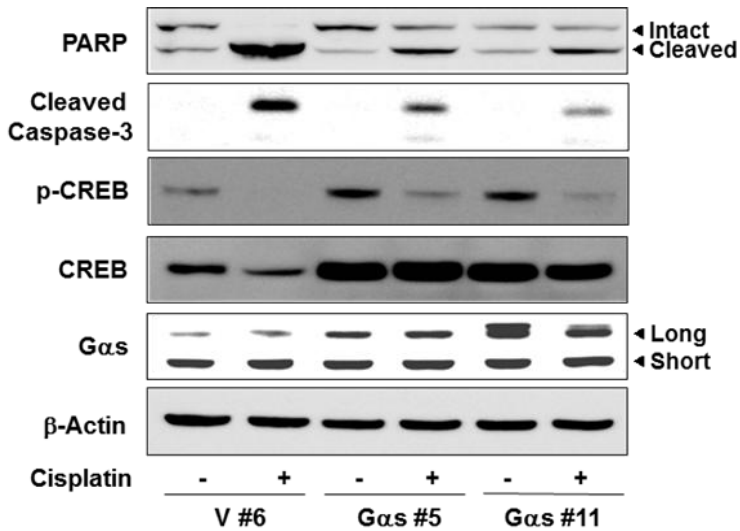

Figure 12. Cisplatin-induced apoptosis decrease by Gαs

Expression of GαsQL inhibited cisplatin-induced cleavage of caspase-3 and PARP. GαsQL was stably expressed by transfection the construct in a pcDNA3 vector in HeLa cells. Expression of GαsQL and phosphorylation of CREB were analyzed by western blot analysis using an antibody against Gαs and phosphorylated CREB (Ser-133). The cells were treated with 30 μM cisplatin for 24 h, and then the resulting cell lysates (80 μg) were immunoblotted using an antibody against PARP and cleaved caspase-3.

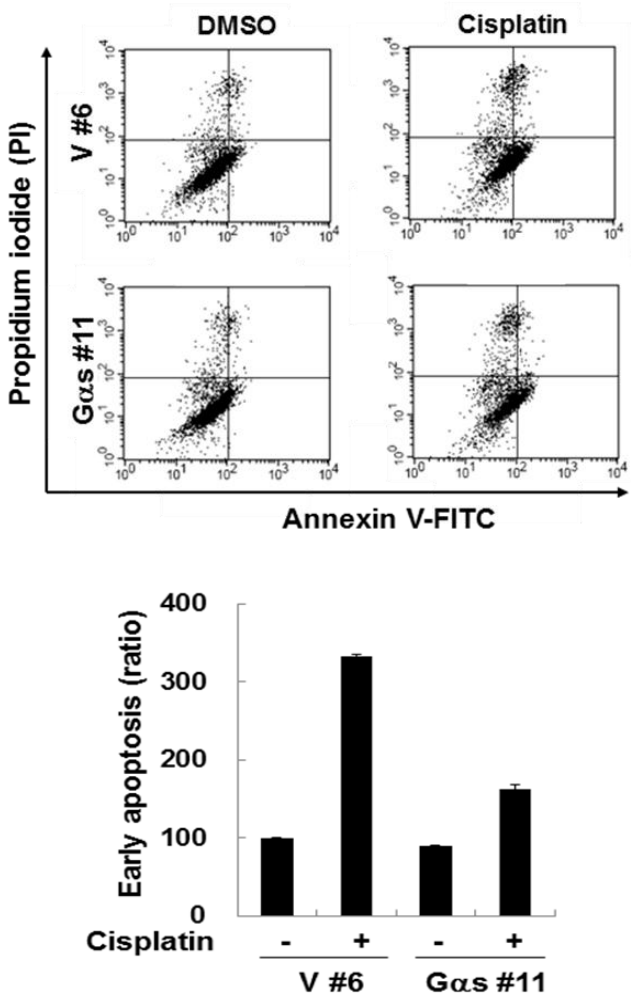

Figure 13. Decrease in cisplatin-induced Annexin V stained cells by Gαs

Gαs decreased Annexin V-positive and PI-negative cells following cisplatin treatment. Flow cytometric analysis of apoptosis was performed using detection Kit I and FACSCalibur (BD Biosciences). HeLa cells were incubated 24 h with or without cisplatin. Data are presented from three independent experiments.

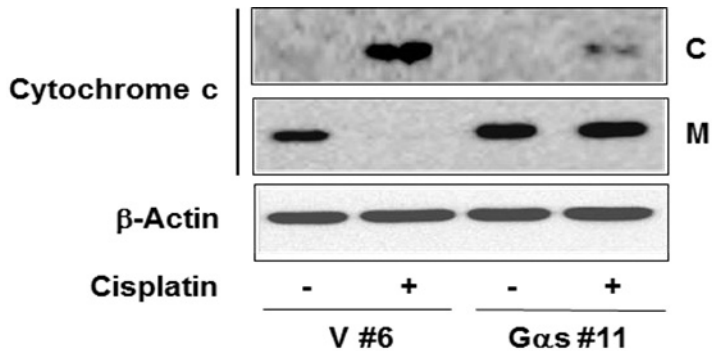

Figure 14. Decrease in cisplatin-induced cytochrome c release by Gαs

Gαs inhibited chytochrome c release into cytosol following cisplatin treatment. After treatment with 30 μM cisplatin for 24 h, cells were homogenized and fractionated into mitochondria (M) and cytosol (C) by centrifugation. The distribution of cytochrome c in each fraction was analyzed by western blotting.

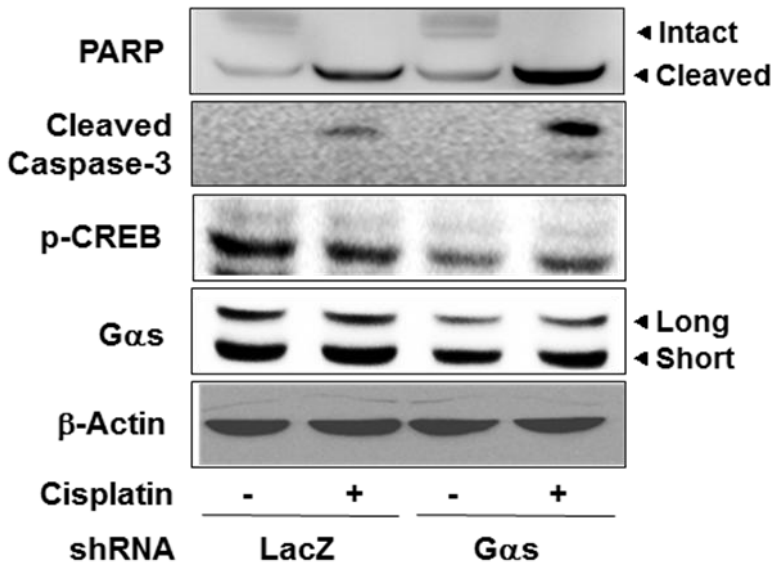

Figure 15. Increase in cisplatin-induced cleavage of PARP and cleaved caspase-3 by Gαs-shRNA

Knock down of Gαs partially abolished the inhibitory effect against cisplatin-induced cleavage of caspase 3 and PARP. The expression of Gαs in HeLa cells was knocked down by transfecting a shRNA construct or LacZ shRNA as a control. After 24 h of transfection, cells were treated with cisplatin (30 μM) for 24 h, and expression of Gαs and cleavage of caspase-3 and PARP were analyzed. Expression of β-actin was analyzed as a loading control. V and Gαs refer to vector-transfected cells and GαsQL-transfected cells, respectively, and the numbers refer to the cell clones.

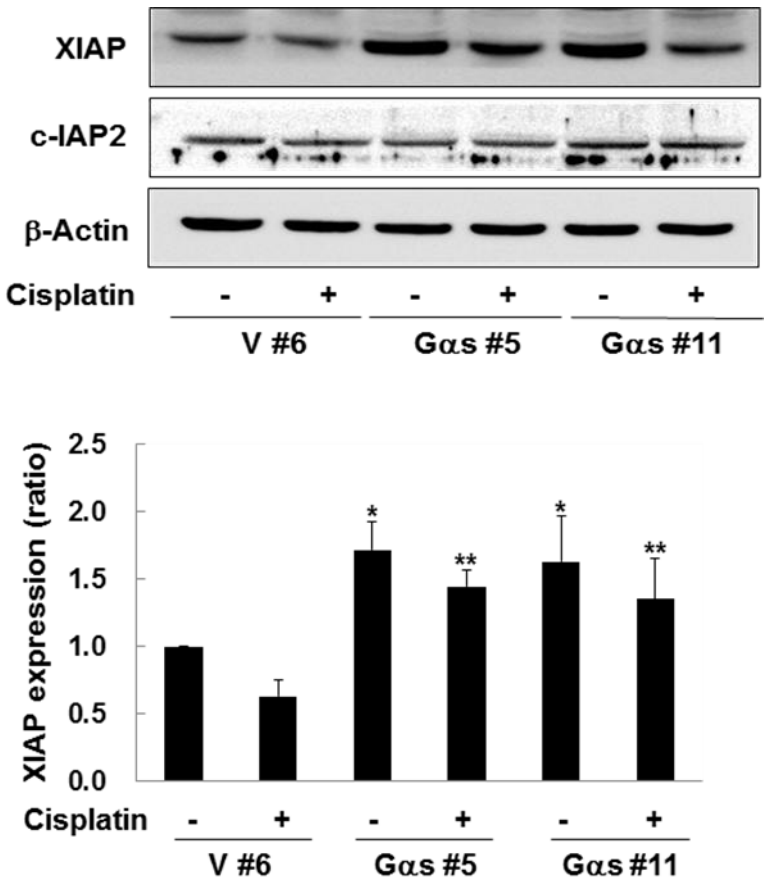

Figure 16. XIAP protein increases by Gαs

Expression of GαsQL increased the expression of XIAP protein. HeLa cells were treated with 30 μM cisplatin for 24 h and then the expression of IAP proteins was assessed by western blotting. The densitometric results of blots were presented as ratios to the vector-transfected control. Asterisks indicate significant differences from vector-transfected control (*) or cisplatin-treated vector control (**) ($p < 0.05$, Mann-Whitney U test).

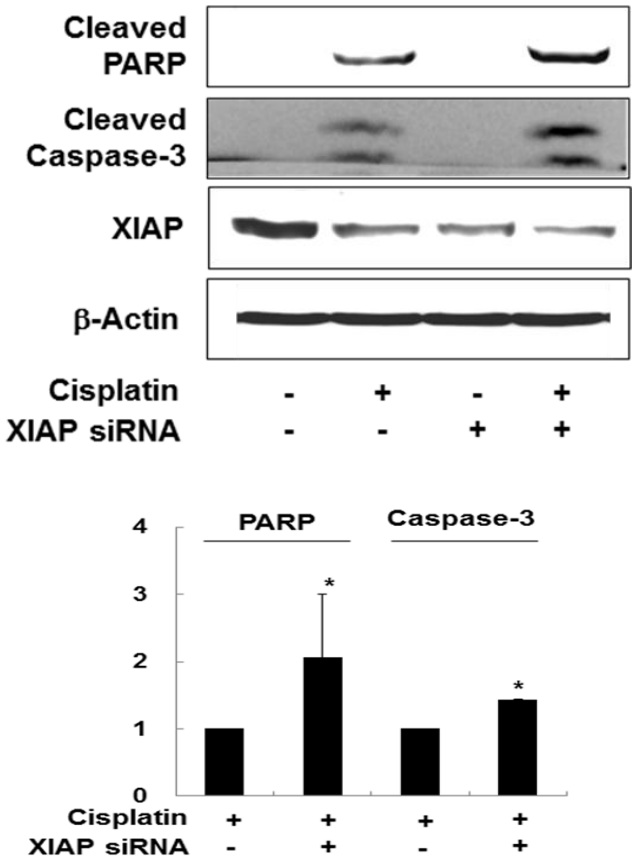

Figure 17. Increase in cisplatin-induced PARP and cleavage of caspase-3 by XIAP siRNA

Knock down of XIAP increased cisplatin-induced cleavage of casapase-3 and PARP. HeLa cells stably expressing GαsQL was transfected with XIAP siRNA and incubated for 24 h. The transfected cells were treated with 30 μM cisplatin for 24 h, and then the expression of XIAP and cleavage of caspase-3 and PARP were assessed. An asterisk (*) indicates a significant difference from control siRNA-transfected controls ($p < 0.05$, Mann-Whitney U test).

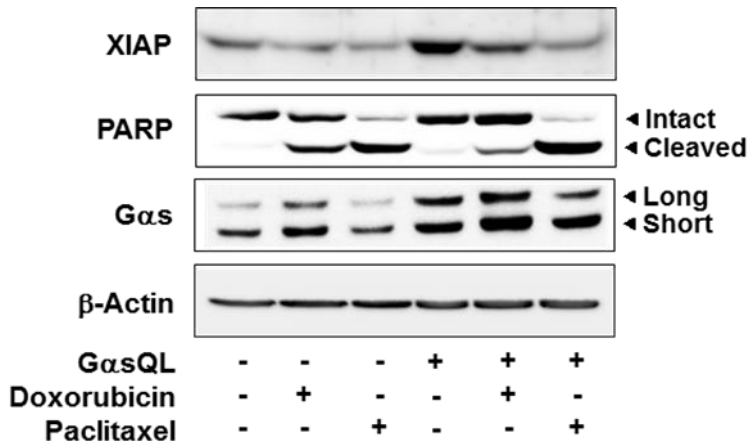

Figure 18. Gαs decreases doxorubicin-triggered apoptosis, but paclitaxel is not

Gαs inhibited doxorubicin-induced apoptosis but not paclitaxel-induced apoptosis. HeLa cells were transiently transfected with vector or GαsQL constructs. The transected cells were treated with doxorubicin (1 μM) or paclitaxel (125 nM) for 24 h, and then the expression of XIAP and PARP cleavage were analyzed.

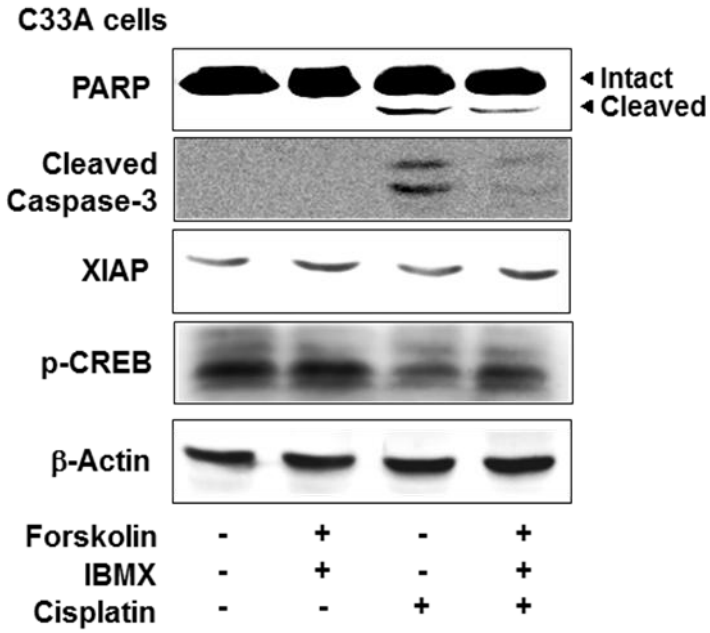

Figure 19. Effects of Forskolin on apoptosis in C33A cells

Activation of the cAMP signaling pathway inhibited cisplatin-induced apoptosis of other cervical cancer cells. Cervical cancer cells, C33A cells, were pre-treated with 40 μM forskolin and 100 μM IBMX for 30 min before treatment with 30 μM cisplatin for 24 h. Then, the expression of X-linked inhibitor of apoptosis protein (XIAP), p-cAMP response clement binding (CREB), and cleavage of caspase-3 and poly (ADP-ribose) polymerases (PARP) were assessed by western blotting.

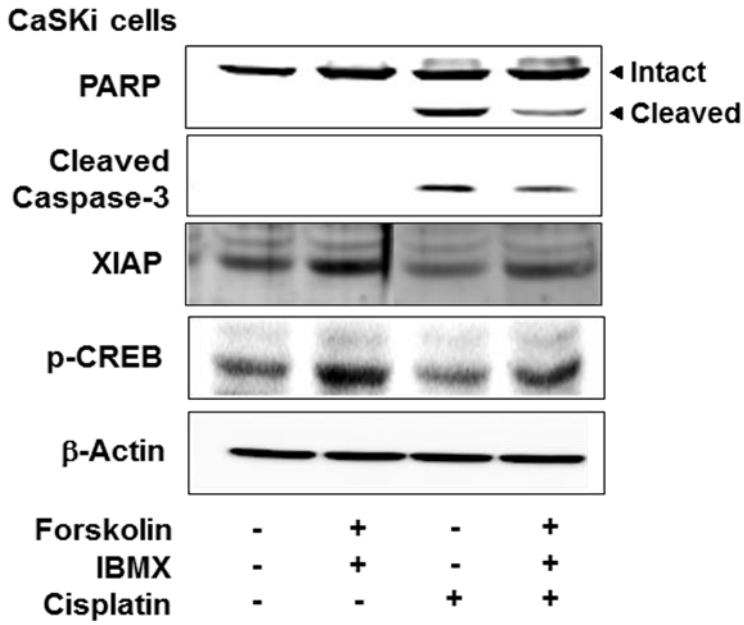

Figure 20. Effects of Forskolin on apoptosis in CaSKi cells

Activation of the cAMP signaling pathway inhibited cisplatin-induced apoptosis of other cervical cancer cells. Cervical cancer cells, CaSKi cells, were pre-treated with 40 μM forskolin and 100 μM IBMX for 30 min before treatment with 30 μM cisplatin for 24 h. Then, the expression of XIAP, p-CREB, and cleavage of caspase-3 and PARP were assessed by western blotting.

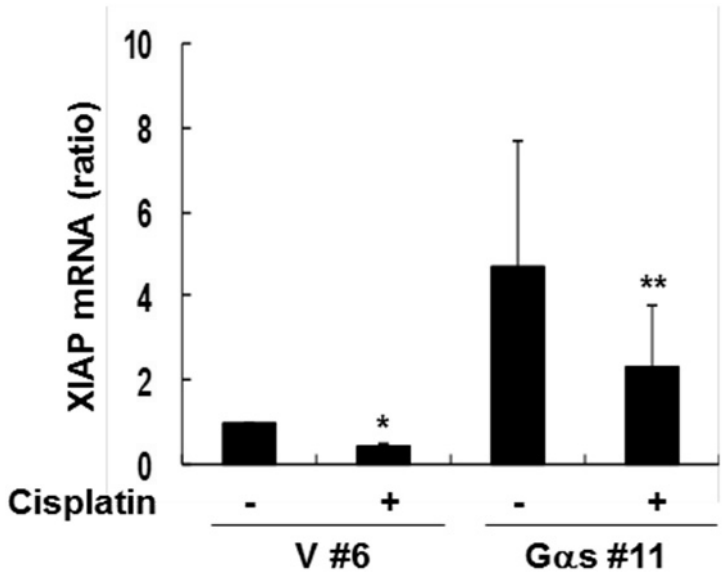

Figure 21. Increase of basal XIAP mRNA by Gαs

Gαs increased mRNA level of XIAP mRNA levels after treatment with 30 μM cisplatin for 24 h in HeLa cells.

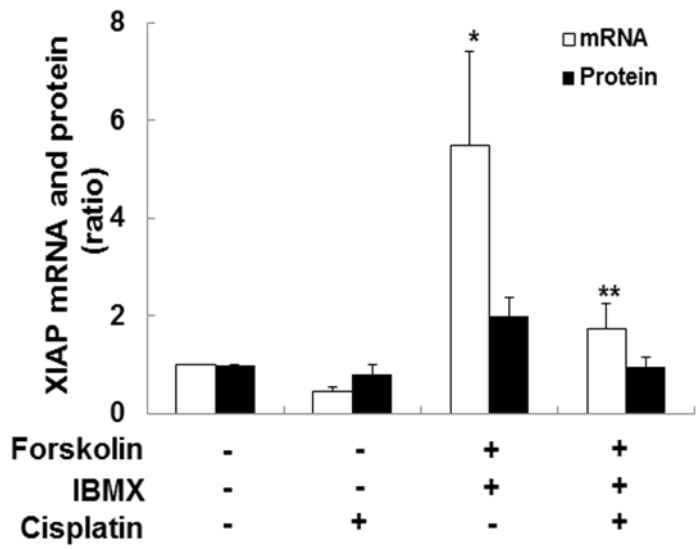

Figure 22. Increase of basal XIAP protein and mRNA by Forskolin

Treatment with forskolin and IBMX increased mRNA and protein level of XIAP. HeLa cells were pre-treated with forskolin (40 μM) and IBMX (100 μM) for 30 min before treatment with 30 μM cisplatin for 24 h.

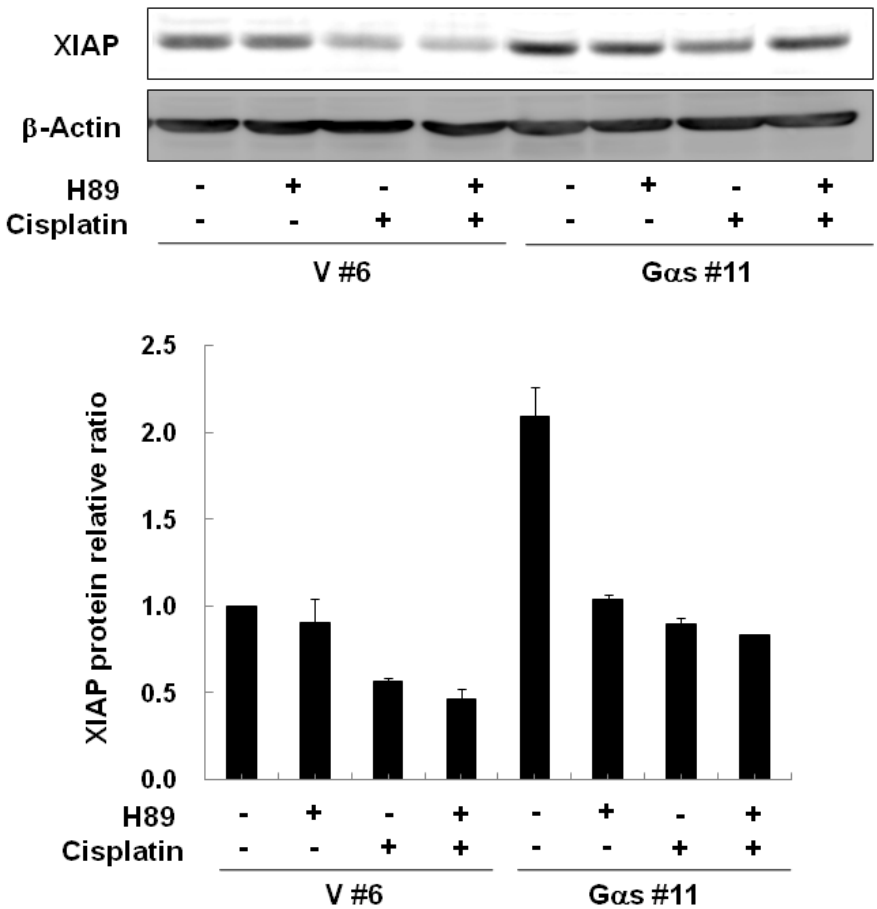

Figure 23. Effect of H89 on XIAP protein

HeLa cells were treated forskolin (40 μM)/IBMX (100 μM) and H89 (10 μM) for 24 h. The expression of p-CREB and CREB were assessed by western.

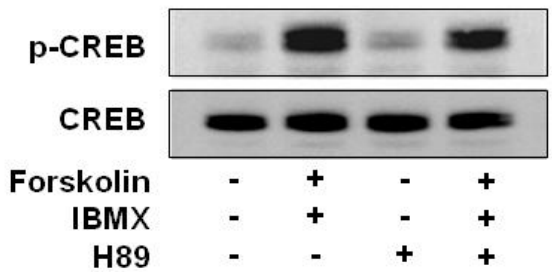

Figure 24. Effect of Forskolin and H89 on p-CREB

Treatment with H89 decreased the expression of XIAP protein induced by GαsQL. The expression of assessed by western blotting, and the densitometric results of blots were presented as ratios to the control.

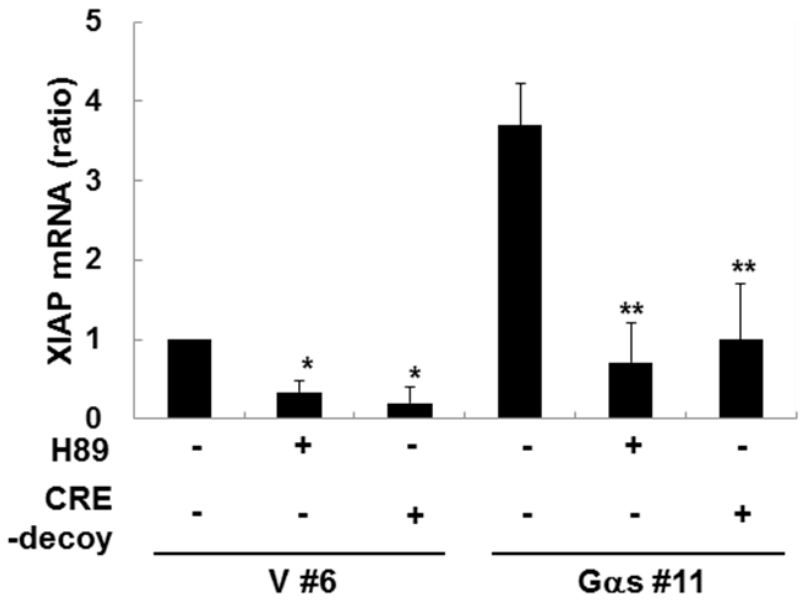

Figure 25. H89 and CRE-decoy decreases XIAP mRNA of basal XIAP protein and mRNA by Forskolin

Treatment with H89 and CRE-decoy decreased mRNA level of XIAP. HeLa cells were pre-treated with H89 (10 μM) for 30 min or transfected with CRE-decoy oligonucleotides (150 nM) for 24 h, and then XIAP mRNA expression was analyzed. XIAP mRNA expression levels were analyzed by real-time quantitative RT-PCR and XIAP protein levels were assessed by western blotting. Asterisks indicate a significant difference from vector-transfected control (*), cisplatin-treated vector control (**) (a, b), or Gαs-transfected control (**) (c) ($p < 0.05$, Mann-Whitney U test).

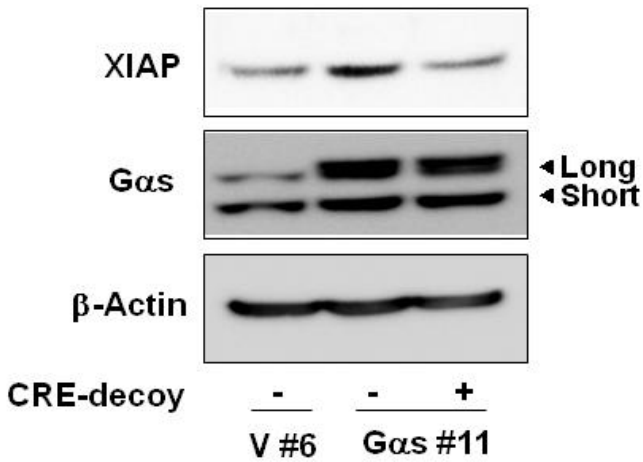

Figure 26. Effect of CRE-decoy on XIAP protein

CRE-decoy decreased the expression of XIAP protein in HeLa cells.

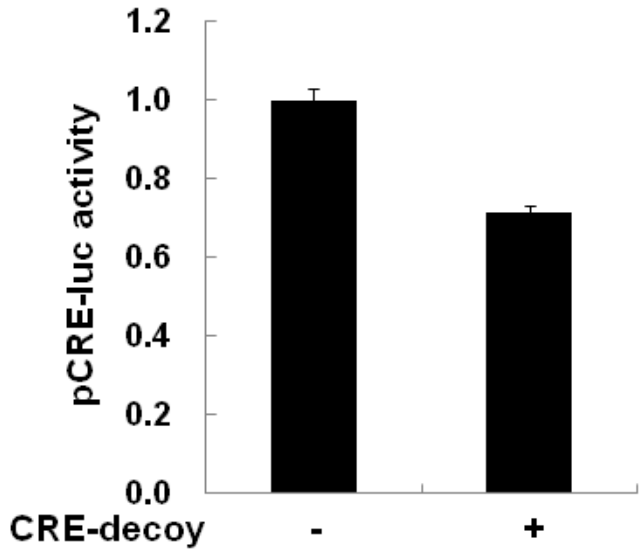

Figure 27. Effect of CRE-decoy on pCRE-luciferase activity

CRE-luciferase activity was analyzed after transfection in HeLa cells. The luciferase activities were measured using the dual-luciferase system (Promega Corp).

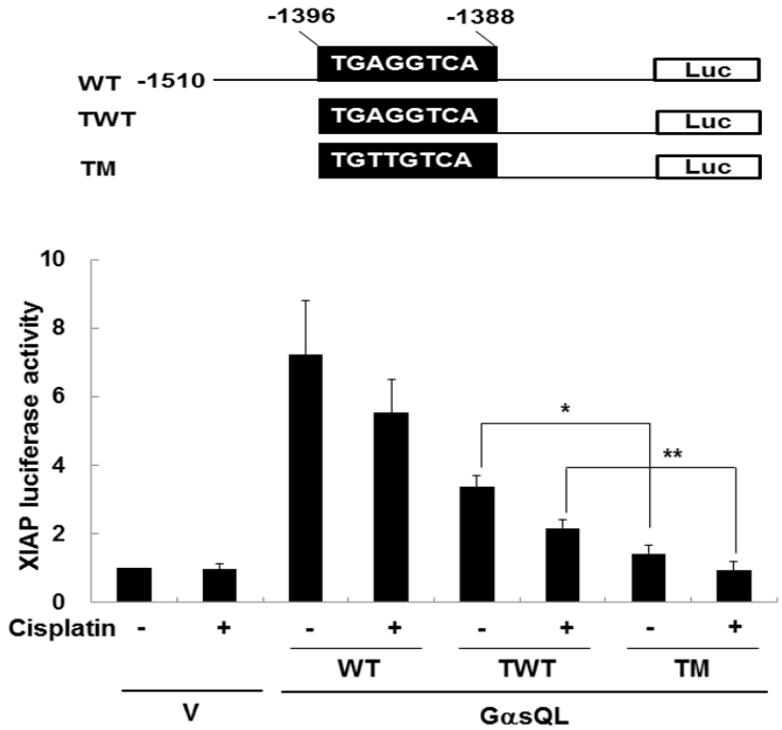

Figure 28. Effect of CRE-like element on XIAP-luciferase activity

A CRE-like element in the XIAP promoter mediated Gαs-induced expression of XIAP in HeLa cells. HeLa cells stably expressing GαsQL or pcDNA3 (V) were co-transfected with XIAP-luciferase plasmids containing the WT, TWT, and TM sequences, respectively. Twenty-four hours after transfection, cells were treated with cisplatin (30 μM) for 24 h. The luciferase activities were measured using the dual-luciferase system and presented as the ratio of activity of each promoter construct versus vector-transfected controls. Asterisks indicate a significant difference from the controls ($p < 0.05$, Mann-Whitney U test).

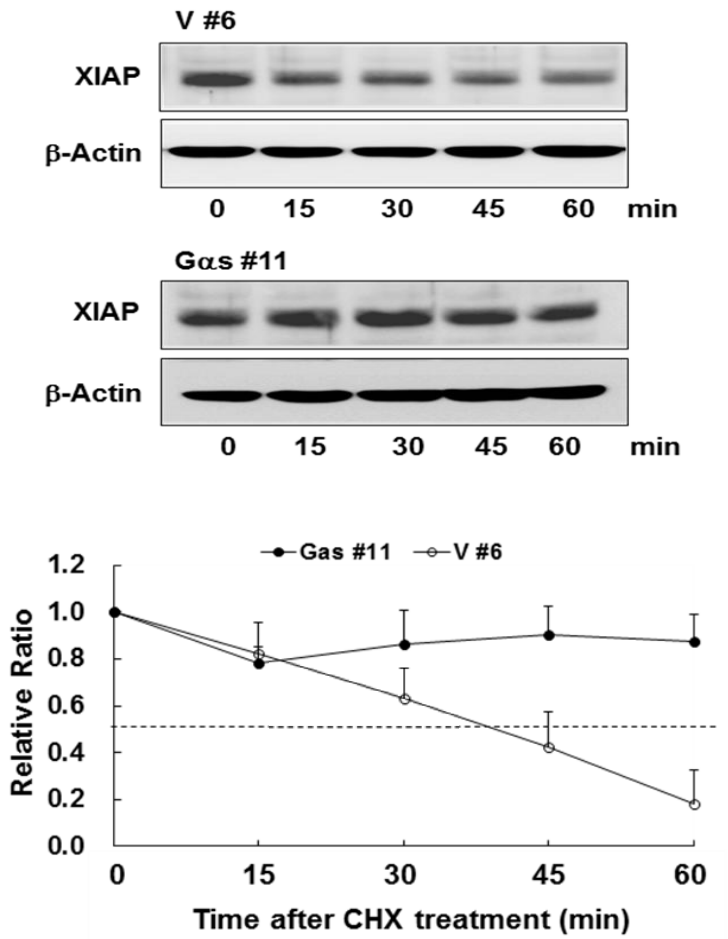

Figure 29. Effect of Gαs on degradation rate of XIAP protein

Gαs delayed degradation of XIAP protein. HeLa cells were treated with 10 μg/ml cycloheximide (CHX) time-dependently, and then the remaining XIAP protein was quantified by western blotting. The graph shows the average densities of XIAP protein from three independent analyses.

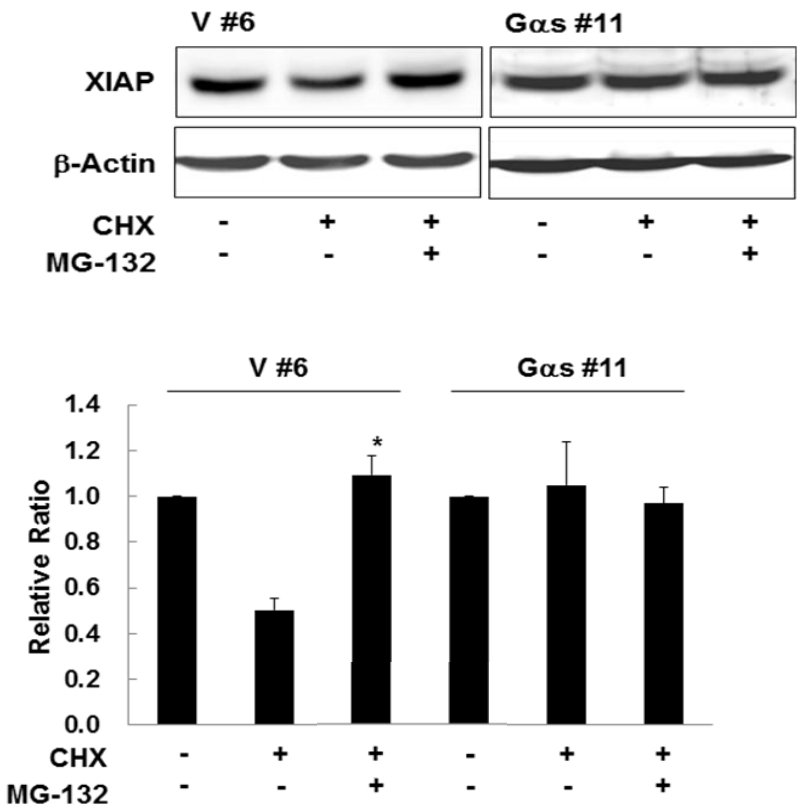

Figure 30. Proteosomal degradation regulates XIAP protein

Treatment with MG-132 blocked degradation of XIAP protein. HeLa cells were treated with 10 μg/ml cycloheximide and 10 μM MG-132 for 1 h, and then the remaining XIAP protein levels were quantified by western blotting.

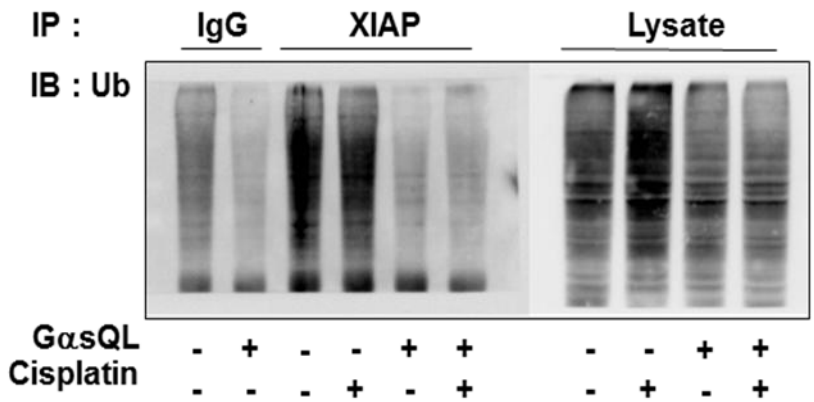

Figure 31. Effects of Gαs on the XIAP ubiquitination

Gαs decreased ubiquitination of XIAP protein. HeLa cells were treated with 30 μM cisplatin for 24 h, and XIAP was immunoprecipitated using an XIAP antibody. The ubiquitinated proteins in the immunoprecipitate were analyzed by western blotting using an antibody specific to ubiquitin. Rat immunoglobulin G (IgG) was used as a control for immunoprecipitation, and total cell lysate (Lysate) was also analyzed as a control for ubiquitination. Asterisks indicate a significant difference from the controls ($p < 0.05$, Mann-Whitney U test).

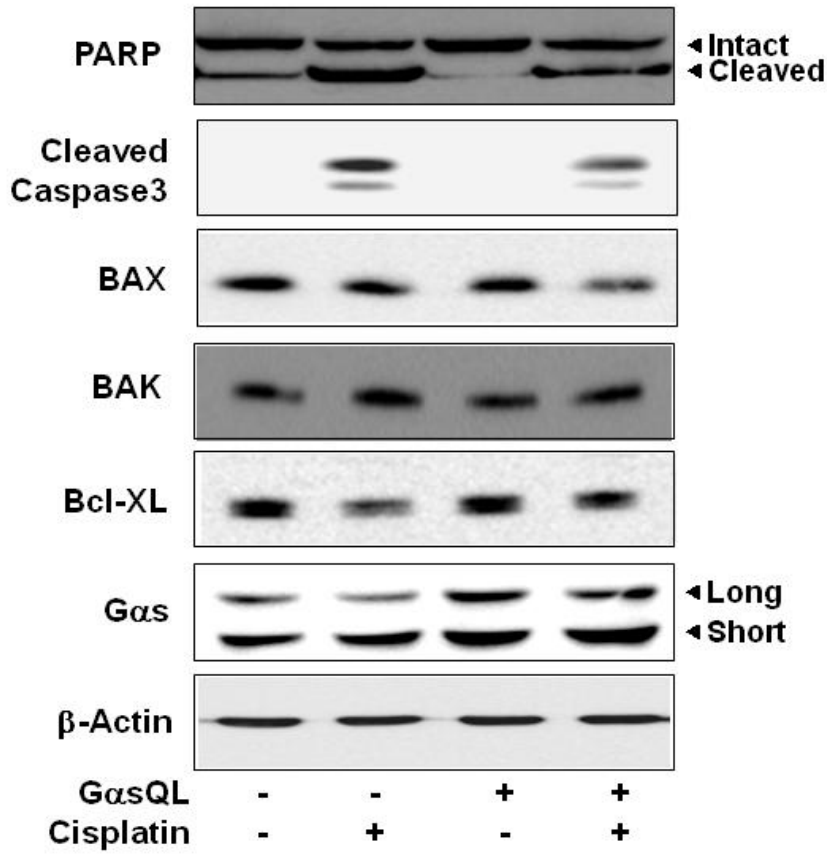

Figure 32. Effect of Gαs on the Bcl-2 family

HeLa cells were transfected with GαsQL and then treated cisplatin 30 μM for 24 h. Then, the expression of cleaved caspase-3 and PARP, Bax, Bak, and Bcl-XL were analyzed by western blotting.

Discussion

This study investigated the effect of Gαs onto cisplatin-induced apoptosis and its underlying molecular mechanism in cervical cancer cells. We found that GαsQL inhibits cisplatin-induced apoptosis by increasing the expression of XIAP, and that occurs by its transcription through a novel CRE-like element dependent pathway, and by decreasing proteasomal degradation of the XIAP protein.

This finding is supported by the results that expression of GαsQL inhibited apoptosis of HeLa cells with a concomitant increase XIAP, and knock down of Gαs or XIAP abolished the inhibitory effect on apoptosis. Activation of the cAMP signaling system also inhibited apoptosis in other cervical cells, such as C33A and CaSKi cells, with a concomitant increase of XIAP.

XIAP is the IAP family member that protects cells from apoptosis by inhibiting caspase-3, -7, and -9. It is considered to be the only mammalian IAP protein that can function as a direct competitive inhibitor of caspases activity through binding to their catalytically active site (35). Overexpression of XIAP has been shown to protect tumor cells from anticancer drug-induced apoptosis in vitro (36), and siRNA against XIAP induced apoptosis of cancer cells(37). Moreover, XIAP was reported to inhibit caspase activation in lung cancer cells (38). In this study, the expression of Gαs was found to increase the expression

of XIAP, but not the expression of cIAP-1 and cIAP-2 in HeLa cells (data not shown), suggesting that the effect of Gαs is specific to XIAP.

We found a novel CRE-like element (TGAGGTCA) at -1396/-1388 of the XIAP promoter, which differs by one base from that of the canonical palindromic CRE (TGACGTCA), and mutation of the sequences decreased XIAP transcription. Activation of Gαs-cAMP signaling results in the phosphorylation of CREB at serine-133, which binds to CRE to facilitate transcription of the target genes by promoting assembly of the transcriptional apparatus. Activated CREB is known to bind to not only canonical palindromic CRE and half CRE (TGACG or CGTCA) (34) but also CRE-like elements that differ by one or two base pairs from the canonical CRE. The same CRE-like element as that in XIAP was also found in the promoter of the surfactant protein B gene and the thyrotropin receptor gene, where the CRE-like element acts as the target of CREB (39, 40). The involvement of other CRE-like elements in the regulation of gene expression by cAMP was also reported in several genes, including mitochondrial matrix enzyme 5-aminolevulinate synthase (41). In addition, expression of XIAP mRNA was significantly decreased by cisplatin treatment, and similar finding was reported in previous papers from several groups (42, 43). However, it needs to be clarified how cisplatin inhibits expression of XIAP mRNA.

In addition to an increase in XIAP transcription, this study shows that Gαs delays ubiquitination and degradation of XIAP protein

to increase XIAP levels, which was inhibited by treatment with MG-132. XIAP has been reported to be degraded through the ubiquitin–proteasome pathway (44). Prostacyclin (PGI_2) binds to a specific IP receptor, which activates cAMP signaling pathways, but PGI_2 was reported to inhibit XIAP ubiquitination and degradation via the Ras/MEK-1/ERK-1/ERK signaling pathway in human umbilical vein endothelial cells (44). This report supports our finding that Gαs, which activates cAMP signaling, delays degradation of XIAP by inhibiting ubiquitination of XIAP in cervical cancer cells.

We previously reported that the Gαs protein inhibits apoptosis by increasing Bcl-xL or decreasing Bak in SH-SY5Y human neuroblastoma cells (31, 45), and similar effects on Bcl-2 family protein were observed in HeLa cervical cancer cells in this study (Figure. 32). This study presents a novel mechanism for Gαs to inhibit apoptosis by increasing XIAP in uterine cervical cancer cells, which indicates that Gαs modulates apoptosis by regulating the expression of not only Bcl-2 family proteins, but also IAP proteins. This is the first report that the Gαs-cAMP pathway regulates the expression of XIAP to modulate apoptosis. On the other hand, the Gαs-cAMP pathway has been reported to augment apoptosis by up-regulating Bak expression in human lung cancer cells (46), and activation of the cAMP pathway by prostaglandin E1 induced apoptosis in IPC-81 leukemia cells (47). Thus, the effect of Gαs on apoptosis seems to be

different depending on the cell types.

These results suggest that the activity of the Gαs-cAMP signaling pathway may contribute to carcinogenesis and progression of cervical cancer cells and may affect the efficiency of chemotherapy of cervical cancer with cisplatin. Ionizing radiation induces DNA damage and triggers apoptosis of cervical cancer cells in a similar way to that of cisplatin (48), so the Gαs-cAMP signaling system might also affect the efficiency of radiotherapy for cervical cancer.

From this study, we conclude that Gαs inhibits cisplatin-induced apoptosis partly by increasing XIAP in cervical cancer cells. That is happened through stimulating transcription of the XIAP gene via a CRE-like element and through inhibition of degradation of the XIAP protein. These findings provide a novel mechanism for the Gαs-cAMP signaling pathway to modulate apoptosis of cervical cancer cells and suggest that the Gαs-cAMP signaling pathway can be utilized to enhance the therapeutic efficiency of cisplatin treatment of cervical cancers.

Part II.

Effect of cyclic AMP on radiation-induced apoptosis

Introduction

Mammalian cells are constantly subjected to their DNA damage from exogenous DNA-damaging agents, such as ionizing radiation and chemical agents, and endogenous processes, such as replication and programmed genome rearrangements (49). The resulting DNA damage may induce mutations that cause the loss or incorrect transmission of genetic information, which in turn can cause developmental abnormalities, cell death and tumorigenesis. Thus, eukaryotic cells have evolved several mechanisms to monitor the integrity of their genome and to repair the damaged DNA (50). The X-ray repair cross-complementing protein 1 (XRCC1) gene was the first mammalian gene isolated that affects cellular sensitivity to ionizing radiation (51). Human XRCC1 is a 70-kDa protein that contains 633 amino acid residues. XRCC1 does not have any enzyme activity, but it has at least three discrete domains that can interact specifically with enzymes involved in DNA repair (52). Thus, XRCC1 plays an essential role in base excision repair and single strand break repair (53). Epidemiological association of XRCC1 polymorphisms and carcinogenesis have been studied extensively in incidences of breast cancer and lung cancer (54), and XRCC1 was reported to have potential as a predictive marker in lung, head and neck cancer patients treated with radiation and chemotherapy (55). The cyclic AMP (cAMP)

signaling system is activated by cAMP, a second messenger molecule formed from ATP by adenylyl cyclase. The activity of adenylyl cyclase is stimulated by stimulatory heterotrimeric GTP-binding proteins (G proteins), which are activated by various external signals bound to G protein-coupled receptors (56). Cyclic AMP activates cAMP-dependent protein kinase (PKA), exchange proteins directly activated by cAMP (Epac), and cyclic nucleotide-gated ion channels, and thereby regulates a variety of cellular responses. The cAMP signaling system is involved in sensory perception, metabolic control, and the regulation of gene expression, cellular growth, differentiation and proliferation (57, 58). In previous studies, we found that the cAMP signaling system modulates DNA-damaging agent-induced apoptosis by regulating the expression of Bcl-2 family proteins and inhibitors of apoptosis (IAPs) (31, 46, 59).

Materials and Methods

Cell culture and reagents

Human non-small cell lung cancer cells, H1299 and A549 cells (Korea Cell Line Bank, Seoul, Korea), were cultured in Dulbecco's modified Eagle's medium (DMEM) containing 10% fetal bovine serum (JBI, Korea) and 100 units/ml penicillin/streptomycin. Cells were maintained in a 5% CO_2 incubator at 37 °C. H89, cycloheximide (CHX), dimethyl sulfoxide (DMSO), 4,6-diamidino-2-phenylindole dihydrochloride (DAPI), 8-pCPT-2′-O-Me-cAMP, and avidin-labeled 8-oxo-7,8-dihydro-2′-deoxyguanosine fluorescein isothiocyanate isomer I (avidin-8-oxo-dG-FITC) were purchased from Sigma (St. Louis, MO, USA); forskolin, isobutylmethylxanthine (IBMX), and MG-132 were purchased from Calbiochem (La Jolla, CA, USA).

Expression constructs and transient transfection

H1299 cells were transfected with a constitutively active mutant of a long form of Gαs (GαsQ227L) in a pcDNA3 vector (Invitrogen, Paisley, UK) using the calcium phosphate method. The GαsQL mutant contains a mutation of a glutamine residue that is essential for the intrinsic GTPase activity (60). Plasmid for expression of deca-histidine tagged wild-type XRCC1 (PCD2E-XH) was a gift from Dr. Keith W. Caldecott (University of Sussex, UK), and plasmid for expression of dominant

negative PKA in MT-REVab was a gift from Dr. G. Stanley McKnight (University of Washington, WA, USA). The sequence of small hairpin RNA for Epac1 was 5′-CCGGGCAGGACTTCAACCGTATCATCTCGAGATGATACGGTTGAAGTCCTGCTTTTTG-3′.

Irradiation with γ-rays

Cells were plated in 10-cm dishes and incubated until they became 60% confluent. Cells were then exposed to γ-rays from a ^{137}Cs source at a delivering dose rate of 170.93 cGy/min.

Immunoblot analysis

Western blotting was performed as previously described (31). Antibodies against Gαs, XRCC1, and p-CREB (S133) were purchased from Santa Cruz Biotechnology (CA, USA), an antibody against β-Actin was from Sigma (St. Louis, MO, USA), and the EE-tag antibody was from Covance (Princeton, NJ, USA). The proteins on the blots were visualized by the Enhanced Chemiluminescence (ECL) reagent (Thermo scientific, Waltham, MA), and the densities of the bands were quantified using Multi Gauge v2.3 software (Fuji, Tokyo, Japan).

Real-time PCR

Real-time quantitative RT-PCR was performed as described previously (59). The primers used were as follows: XRCC1, 5′-

CGCTGGGGAGCAAGACTATG-3′ and 5′-CAAATCCAACTTCCTCTTCC-3′; GAPDH, 5′-ACCACAGTCCATGCCATCAC-3′ and 5′-TCCACCACCCTGTTGCTGTA-3′.

Analysis of DNA damage

Confocal analysis of 8-oxo-dG: cells were fixed in 4% paraformaldehyde for 20 min, permeated with 0.5% TritonX-100 for 10 min, and blocked in 2% bovine serum albumin for 1 h. The cells were incubated with avidin-8-oxo-dG-FITC (1:100) or DAPI (0.5 μl/ml) for 1 h at room temperature. The stained cells were observed using a confocal microscope (LSM 501 META, Carl Zeiss, Inc. USA). Comet assay: a comet assay was performed using a Comet Assay kit (Trevigen, Inc. MD, USA) (60). DNA was visualized by staining with 1 μg/ml ethidium bromide for 5 min in a refrigerator. The comet tail was captured and scored according to labeled DNA intensity using Komet software (Andor Technology, Belfast, UK).

Data analysis

At least three independent experiments were conducted for all of the analyses, and data are presented as the mean ± standard errors (SE). The nonparametric Mann–Whitney U test was used to analyze mean values, and a *p* value of less than 0.05 was considered as statistically significant.

Results

The cAMP signaling system inhibited the repair of radiation-induced DNA damage in H1299 lung cancer cells

We assessed the effect of cAMP signaling system on DNA damage repair by expression of constitutively active Gαs or treatment with forskolin, which activates cAMP signaling system by stimulating adenylyl cyclase. Transient expression of constitutively active GαsQL augmented radiation-induced DNA damage and inhibited repair of the damage in H1299 lung cancer cells. Expression of GαsQL increased the green fluorescence of 8-oxo-deoxyguanosine (8-oxo-dG) by 3.27-fold over vector-transfected cells following γ-ray irradiation (Figure. 33). Augmentation of γ-ray-induced DNA damage by GαsQL expression was confirmed by a comet assay, which also showed 1.9 ±0.3-fold increases in tail intensity over vector control (Figure. 34). The fluorescence of 8-oxo-dG in GαsQL-expressing cells did not return to the basal level until 3 h after irradiation, in contrast to the fluorescence in vector-transfected cells that returned to the basal level by 1 h after irradiation (Figure. 35). Similar to the expression of GαsQL, treatment with forskolin also inhibited the repair of radiation-induced 8-oxo-dG DNA damage (Figure. 36). This result shows that cAMP signaling system inhibits repair of radiation-induced DNA damage in H1299 cells.

The cAMP signaling system inhibited the repair of radiation-induced DNA damage by decreasing expression of XRCC1 in lung cancer cells

To probe the mechanism how the cAMP signaling system inhibits the repair of radiation-induced DNA damage, the effect of Gαs on the expression of XRCC1 was analyzed. Expression of GαsQL increased the basal XRCC1 protein level, but decreased the expression of XRCC1 following γ-ray irradiation. In the vector-transfected control cells, the basal XRCC1 protein level was low, but the expression of XRCC1 protein increased by 4.78 ± 0.45-fold following γ-ray irradiation (Figure. 37). The expression of XRCC1 mRNA was not changed significantly in Gαs-transfected cells, γ-ray-irradiated cells, and in irradiated Gαs-transfected cells ($p > 0.05$).

Pretreatment with forskolin decreased the expression of XRCC1 when cells were exposed to γ-ray irradiation, but did not significantly change the basal expression level of the XRCC1 protein (Figure. 38). Pretreatment with isoproterenol, a Gαs-coupled receptor agonist also decreased the γ-ray-induced expression of XRCC1 without altering the basal expression level (Figure. 39). Similar to H1299 lung cancer cells, treatment of A549 lung cancer cells with forskolin also inhibited the γ-ray-induced expression of XRCC1 (Figure. 40). Exogenous expression of XRCC1 abolished the inhibitory effect of forskolin and reduced 8-oxo-dG fluorescence to the basal level by 30 min (Figure. 41). This

result indicates that cAMP signaling system inhibits repair of γ-ray-induced DNA damage by decreasing expression of XRCC1 in lung cancer cells.

The cAMP signaling system decreased XRCC1 expression by promoting the degradation of XRCC1 protein

To investigate the mechanism for decrease in the radiation-induced expression of XRCC1 by cAMP system, the effect of forskolin on the degradation of XRCC1 was analyzed, because the level of XRCC1 mRNA did not changed significantly. Treatment with forskolin promoted the degradation of XRCC1 following γ-ray irradiation. The half-life of the XRCC1 protein in forskolin-treated H1299 cells decreased to 13 ± 3.0 min from 31 ± 3.6 min in DMSO-treated control cells ($p < 0.05$, Figure. 42). Because XRCC1 was reported to be degraded by proteasomal system (61), the effect of proteasomal inhibitor on the forskolin-promoted degradation of XRCC1 was analyzed. Treatment with a proteasomal inhibitor, MG132, completely blocked the forskolin-promoted degradation of XRCC1 protein, resulting in an increase in the protein amount to more than basal level (Figure. 43). Then the effect of forskolin on ubiquitination of XRCC1 was analyzed. Forskolin pretreatment increased the ubiquitination of XRCC1 following γ-ray irradiation (Figure. 44). This result indicates that cAMP signaling system decreases XRCC1 expression by promoting the ubiquitin proteasome-dependent degradation of XRCC1 protein.

EPAC1 mediated the promotion of XRCC1 degradation by cAMP signaling system

To determine which effector molecule mediates cAMP-promoted degradation of XRCC1, we analyzed the role of PKA and EPAC. Treatment with H89, a PKA inhibitor, had no effect on the forskolin-promoted degradation of XRCC1 (Figure. 45), and pretreatment with 8-pCPT-2′-O-Me-cAMP, an EPAC-selective cAMP analog, decreased expression of XRCC1 following γ-ray irradiation, which was not blocked by treatment with H-89 nor by expression of dominant negative PKA (Figure. 46). Knockdown of EPAC1 by shRNA abolished the effect of 8-pCPT-2′-O-Me-cAMP and restored the radiation-induced expression of XRCC1 (Figure. 47), and pretreatment with 8-pCPT-2′-O-Me-cAMP increased ubiquitination of XRCC1 protein (Figure. 48). This result indicates that Epac mediates the promotion of XRCC1 degradation induced by cAMP signaling system.

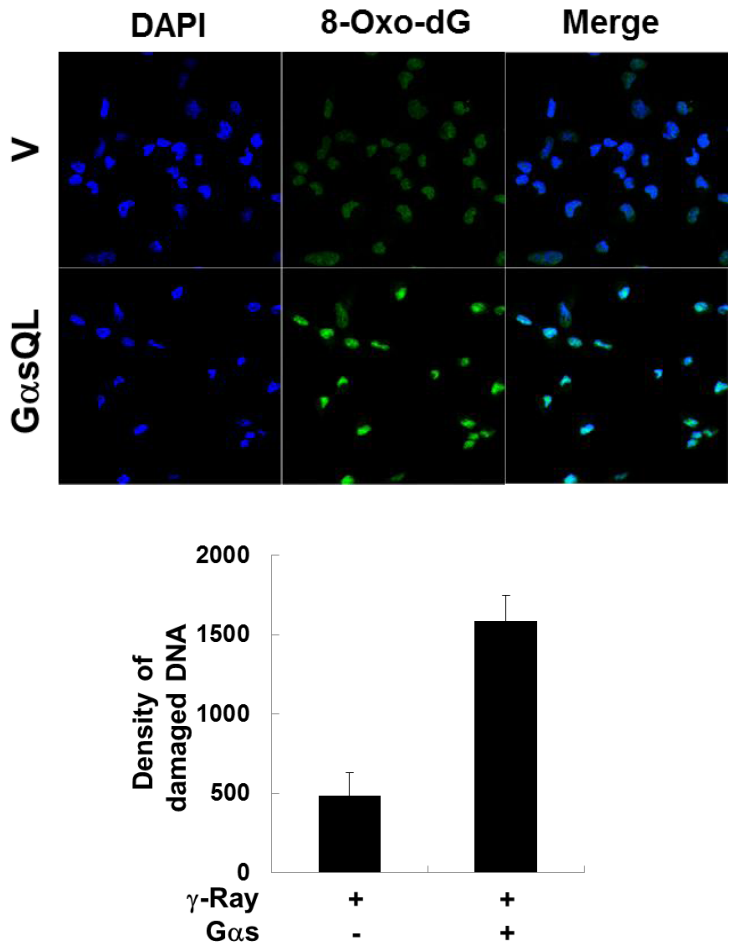

Figure 33. Effect of GαsQL expression on the formation of 8-oxo-dG following γ-ray irradiation

Effects of GαsQL expression on the formation of 8-oxo-dG following γ-ray irradiation. H1299 cells were transfected with GαsQL or a pcDNA3 vector (V), incubated for 24 h, and irradiated with γ-rays (5 Gy). Then the resulting DNA-damage was assessed at 30 min by staining with DAPI or an avidin-8-oxo-dG-FITC and confocal microscopy.

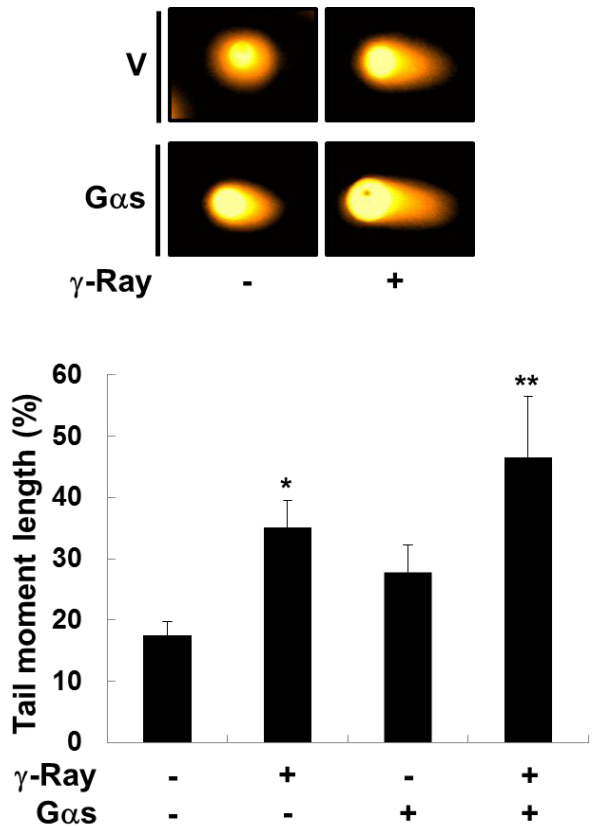

Figure 34. Effects of GαsQL on radiation-induced DNA damage

H1299 cells were transfected with GαsQL or pcDNA3 vector (V), incubated for 24 h, and irradiation with γ-rays (5 Gy). Then the resulting DNA-damage was assessed at 30 min by a comet assay. The histograms present means and standard errors of at least three independent experiments, and the asterisk (*) indicates a statistically significant difference from the vector-transfected control cells; the double asterisks (**) represent a statistically significant difference from the Gas-transfected control cells (p <0.05, Mann-Whitney U test).

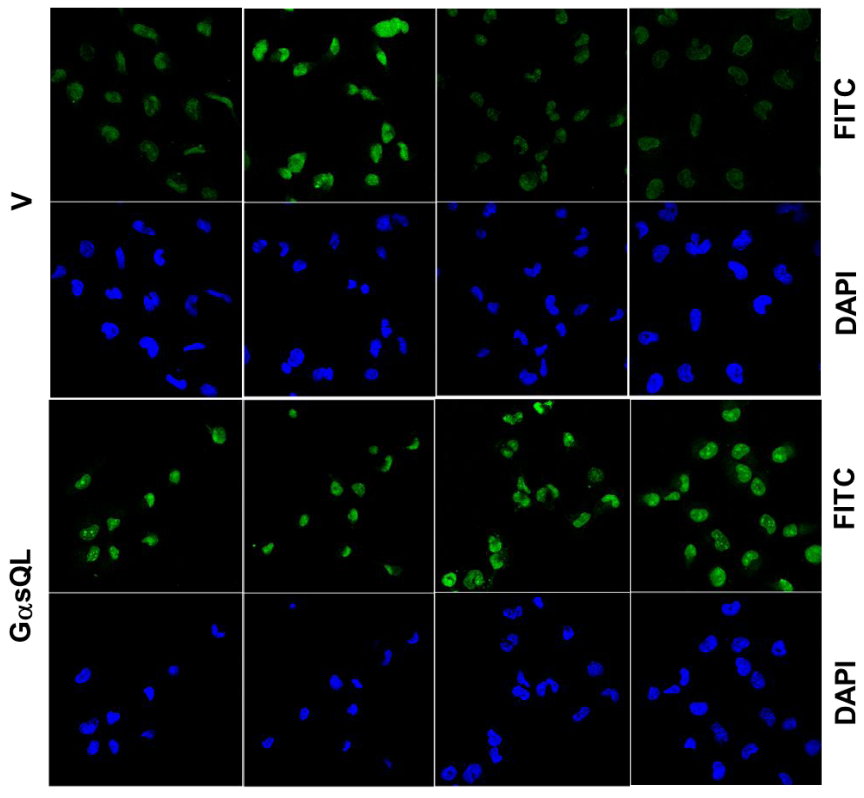

Figure 35. Effects of GαsQL on the removal of 8-oxo-dG

H1299 cells were transfected with vector or GαsQL and irradiated. H1299 cells were transfected with GαsQL or a pcDNA3 vector (V), incubated for 24 h, and irradiated with γ-rays (5 Gy). Then the resulting DNA-damage was assessed at the indicated times by staining with DAPI or avidin-8-oxo-dG-FITC and confocal microscopy.

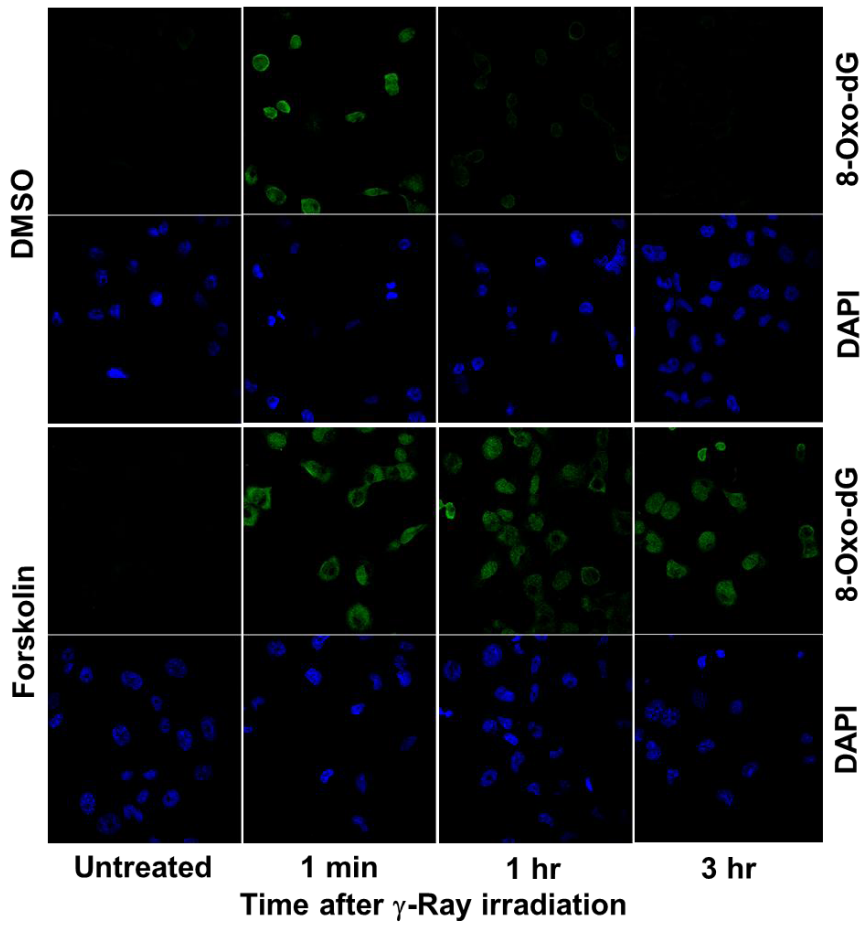

Figure 36. Effects of forskolin on the removal of γ-ray-induced 8-oxo-dG

The H1299 cells were pre-treated with forskolin (40 μM) or DMSO for 30 min and then exposed to γ-rays (5 Gy). The resulting DNA damage was assessed at the indicated times by staining with DAPI or avidin-8-oxo-dG-FITC.

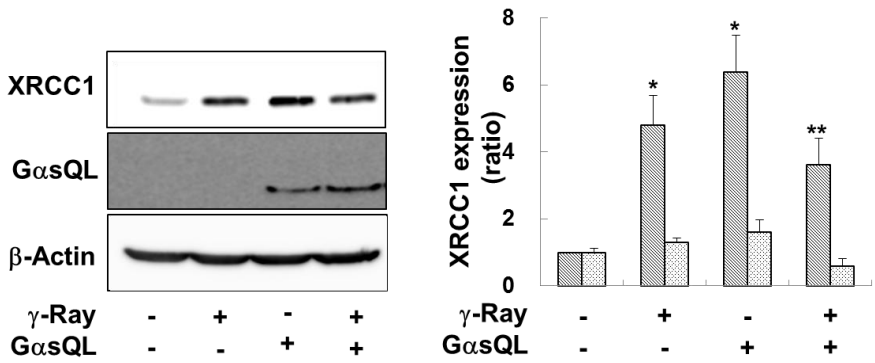

Figure 37. Effects of GαsQL on radiation-induced XRCC1 expression

Twenty-four hours after transfection with GαsQL or the vector (V), the H1299 cells were irradiated with γ-rays (5 Gy) and incubated for 30 min further before harvesting for analysis. The expression of XRCC1 and GαsQL was analyzed by western blotting. β-Actin was used as a loading control. The expression of XRCC1 mRNA was assessed by real-time PCR, and the β2-microgloblin was used as a control. The striped bar represent the XRCC1 protein, and the dot bars represent XRCC1 mRNA.

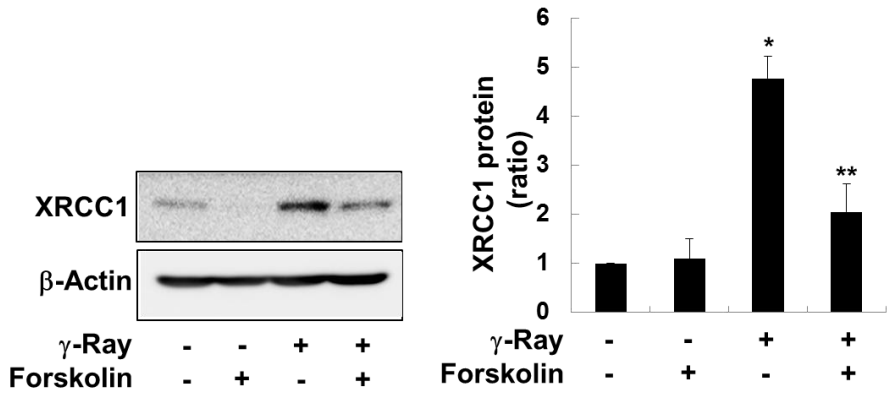

Figure 38. Effects of forskolin on radiation-induced XRCC1 expression

The H1299 cells were treated with 40 μM forskolin for 30 min and then irradiated with γ-rays (5 Gy). After incubation for 30 min, the expression of XRCC1 and β-Actin was assessed by western blotting.

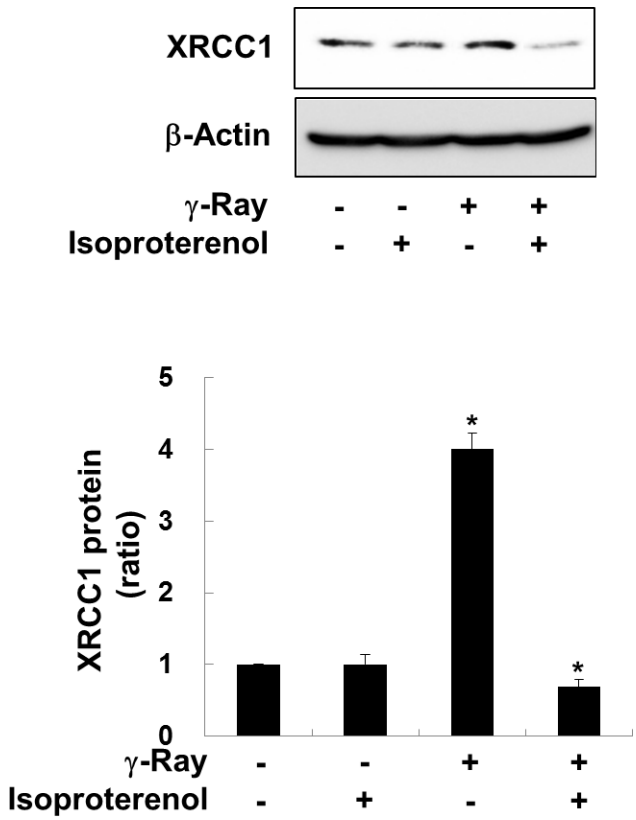

Figure 39. Effects of Isoproterenol on XRCC1 expression

The H1299 cells pre-treated with 1 μM isoproterenol for 30 min and then irradiated with γ-rays (5 Gy). After incubation for 30 min, the expression of XRCC1 and β-Actin was assessed by western blotting.

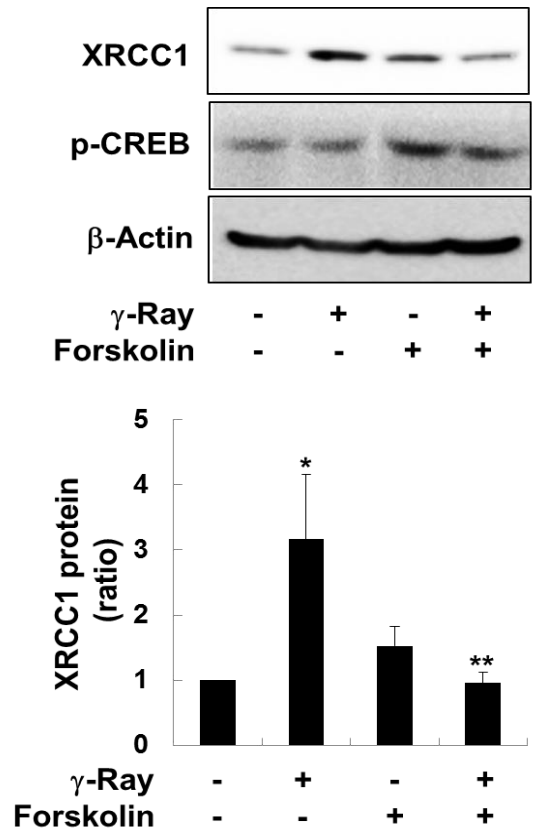

Figure 40. Effects of forskolin on the XRCC1 expression in A549 cells

The A549 lung cancer cells were pre-treated with 40 μM forskolin for 30 min and exposed to γ-ray (5 Gy). After 30 min, XRCC1 and p-CREB were analyzed by western blotting, and the densitometric results of blots were presented as ratios to the control. The histograms present means and standard errors of at least three independent experiments, and the asterisk (*) indicates a statistically significant difference from the untreated control cells; the double asterisks (**) represent a statistically significant difference from the γ-ray irradiated cells (p <0.05, Mann-Whitney U test).

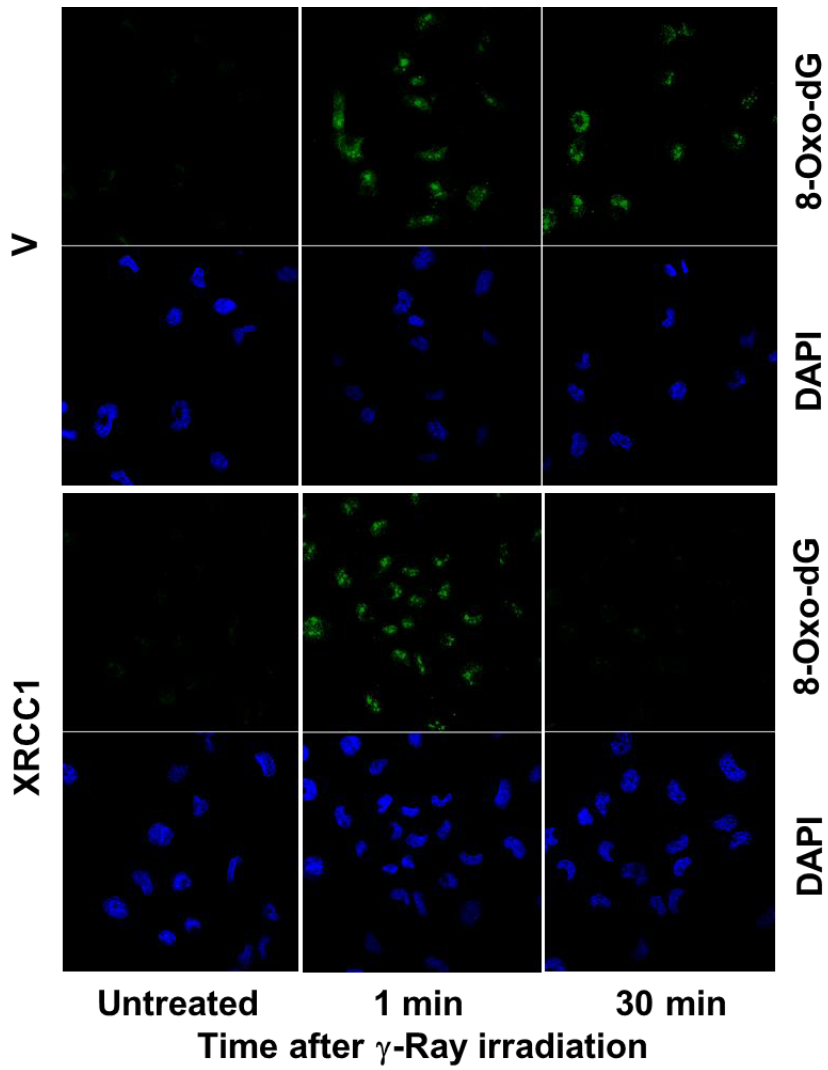

Figure 41. Effects of exogenous expression of XRCC1 on the removal of 8-oxo-dG in forskolin-pretreated cells

XRCC1 expression construct or a vector (V) was transfected to H1299 cells, and after 24 h incubation, the cells were with 40 μM forskolin for 30 min and then irradiated with γ-rays (5 Gy). The resulting DNA-

damage was assessed at 30 min by staining with DAPI or a FITC-8-oxo-dG antibody and confocal microscopy. The histograms present the means and standard errors of at least three independent experiments, and the asterisk (∗) indicates a statistically significant difference from the vector-transfected control cells or untreated cells; the double asterisks (∗∗) represent a statistically significant difference ($p < 0.05$) from the irradiated vector-transfected control cells ($p < 0.05$, Mann–Whitney U test).

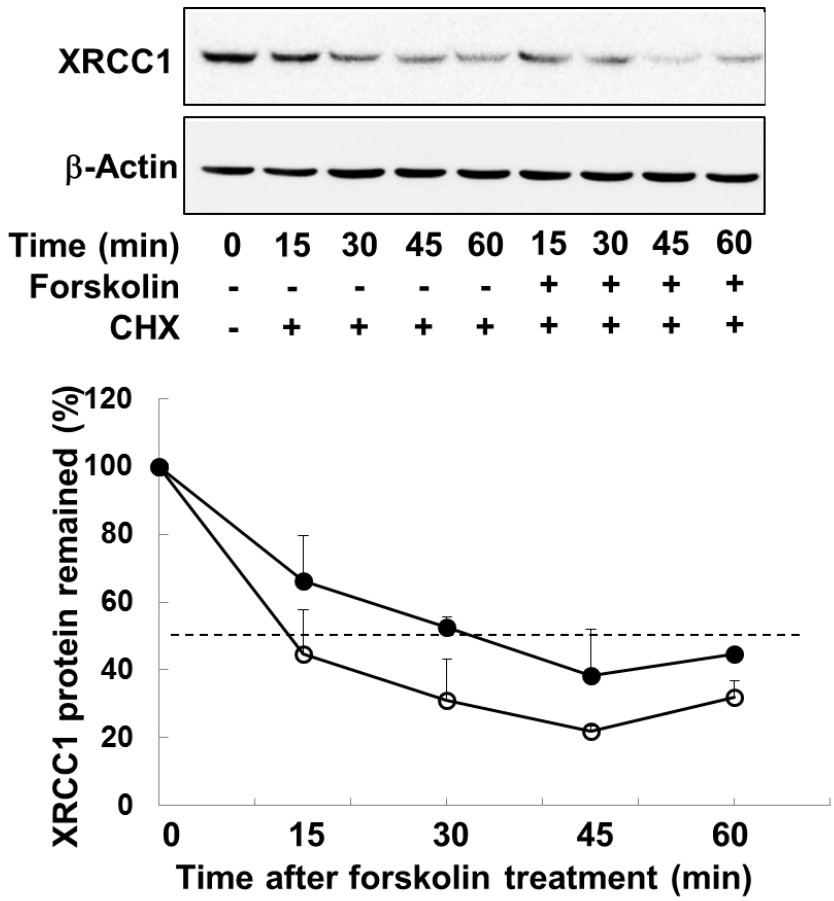

Figure 42. Effects of forskolin on the degradation of XRCC1 proteins

H1299 cells were pre-treated with 10 μg/ml cycloheximide (CHX) and 40 μM forskolin or DMSO for 30 min, and then cells were irradiated with γ-rays (5 Gy). The cells were harvested at the indicated times, and XRCC1 protein was analyzed by western blotting. The graph shows the average densities of XRCC1 from three independent analyses.

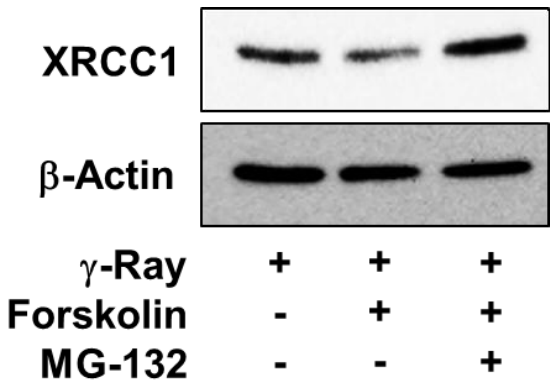

Figure 43. Effects of MG-132 on the forskolin-promoted degradation of XRCC1

The cells were pretreated with 40 μM MG-132, and the remaining XRCC1 protein levels were quantified 30 min after irradiation by Western blotting.

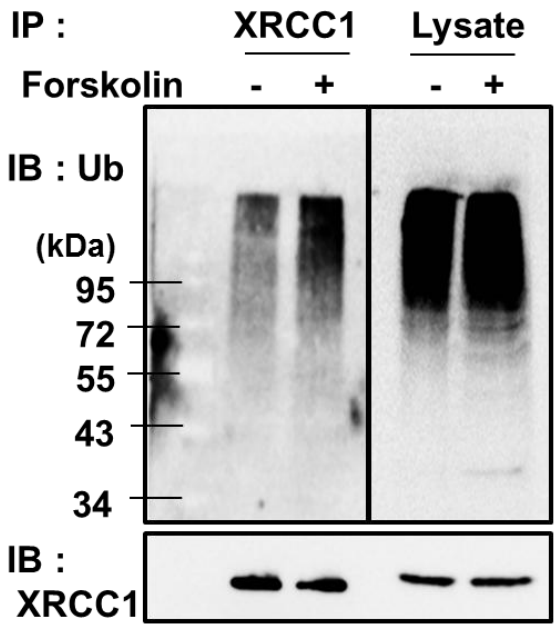

Figure 44. Effects of forskolin on the ubiquitination of XRCC1 following γ-ray irradiation

The cells were treated with 40 μM forskolin or DMSO for 30 min in the presence of 40 μM MG-132 before the γ-ray exposure. Ubiquitinated XRCC1 was immunoprecipitated with an antibody against either ubiquitin or XRCC1, and then analyzed by western blotting.

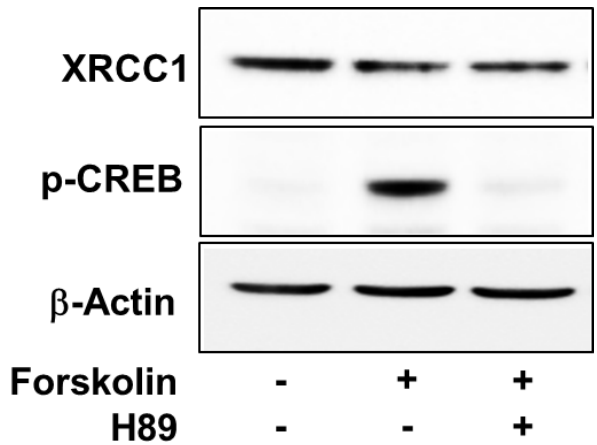

Figure 45. Effects of H89 on XRCC1 expression in forskolin-pretreated cells

The cells were treated with 20 μM for 30 min, and irradiated with γ-ray (5 Gy).

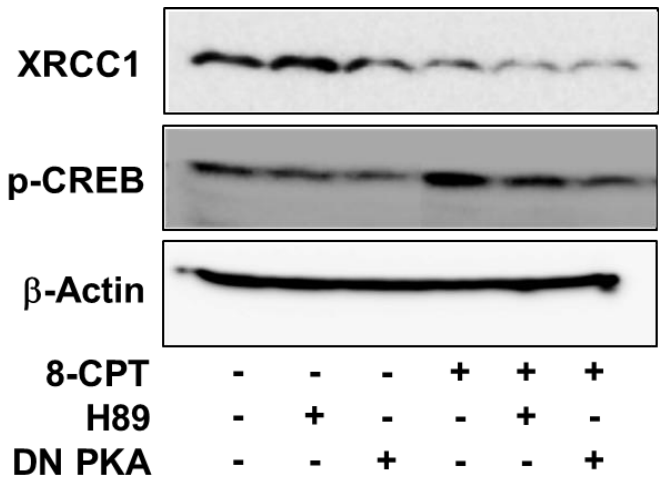

Figure 46. Effects of 8-pCPT-2′-O-Me-cAMP on radiation-induced XRCC1 expression

The cells were treated with 20 μM 8-pCPT-2′-O-Me-cAMP (8-CTP) in the presence of 20 μM H89 or dominant negative PKA (DN-PKA).

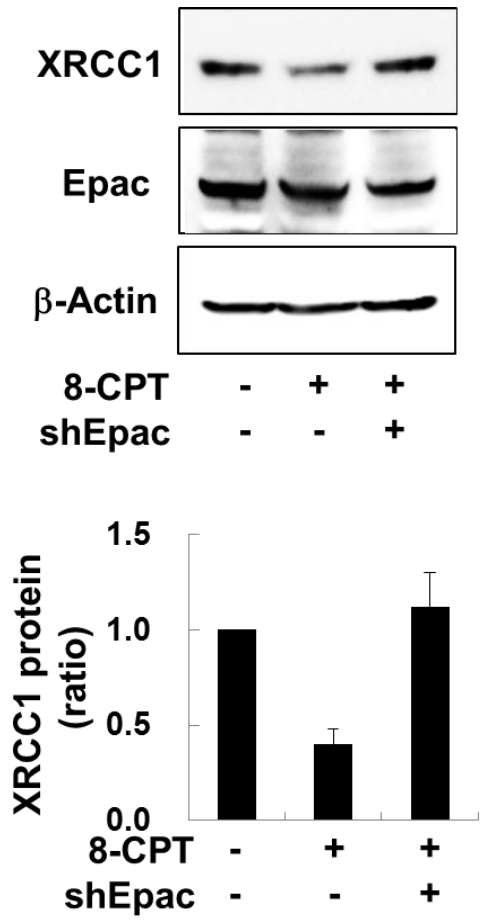

Figure 47. Effects of Epac1 knockdown on the radiation-induced XRCC1 expression

H1299 cells were transfected with shEpac1, and after 24 h, they were treated with 20 μM 8-pCPT-2′-O-Me-cAMP for 30 min. Then the cells were irradiated with γ-rays (5 Gy), and after 30 min, the expression of XRCC1 was assessed by western blotting. The histograms present the means and standard errors of at least three independent experiments, and the asterisk (*) indicates a statistically significant difference from the vector-transfected control cells ($p < 0.05$, Mann–Whitney U test).

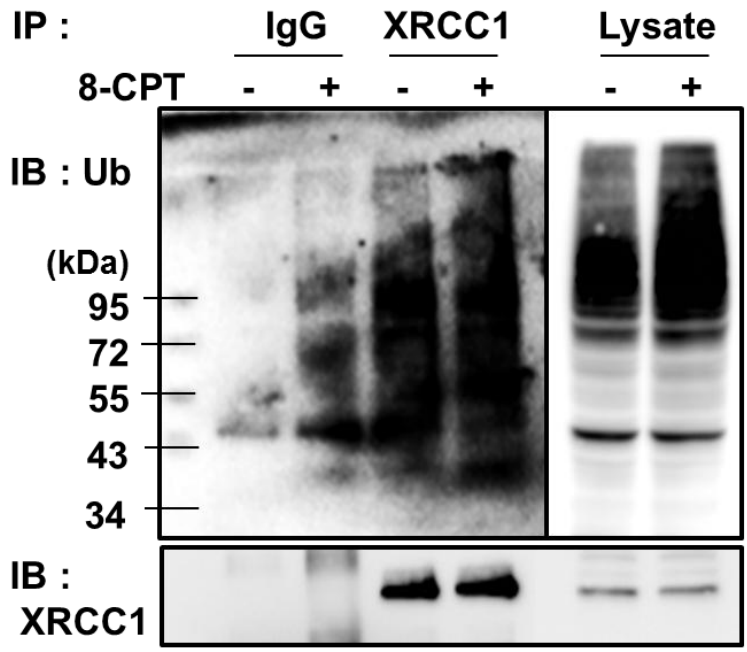

Figure 48. Effects of 8-pCPT-2′-O-Me-cAMP on radiation-induced XRCC1 ubiquitination

The cells were treated with 20 μM 8-pCPT-2′-O-Me-cAMP or DMSO for 30 min in the presence of 40 μM MG-132 before the γ-ray exposure. Ubiquitinated XRCC1 was immunoprecipitated with an antibody against either ubiquitin or XRCC1, and then analyzed by western blotting.

Discussion

This study was performed to determine whether the cAMP signaling system can modulate the repair of γ-ray-induced DNA damage in lung cancer cells and, if so, to elucidate the underlying molecular mechanism. This study shows that the cAMP signaling system inhibits the repair of γ-ray-induced DNA damage by decreasing expression of XRCC1 protein in lung cancer cells, and that it decreases XRCC1 expression by promoting EPAC-mediated ubiquitin-proteasome dependent degradation of XRCC1.

The finding that the cAMP signaling system inhibits radiation-induced DNA damage in lung cancer cells is evidenced by the result that the expression of constitutively active Gαs or pretreatment with forskolin, an adenylyl cyclase activator that results in the formation of cAMP and the activation of the cAMP signaling system, augmented radiation-induced DNA damage, and that such activation of the cAMP signaling system inhibited the repair of γ-ray-induced DNA damage. This finding corresponds with previous reports that the cAMP signaling system is involved in the DNA damage response and cellular resistance to DNA damaging agents. For instance, the activity of PKA is involved in resistance to cisplatin and its associated DNA repair capacity (62), and high cAMP levels reduce the double-strand break (DSB)-rejoining fidelity (63).

Then, we found that the cAMP signaling system inhibits radiation-induced DNA damage by decreasing expression of a DNA repair protein, XRCC1. This finding is supported by the fact that expression of constitutively active Gαs or pretreatment with either forskolin or isoproterenol decreased the radiation-induced expression of XRCC1 and inhibited DNA repair, and that exogenous expression of XRCC1 abolished the DNA repair-inhibiting effect of forskolin. Isoproterenol is an agonist for the β-adrenergic receptor, which is coupled with the Gαs protein to stimulate adenylyl cyclase. Furthermore, a similar decrease in XRCC1 expression following γ-ray irradiation was observed in another lung cancer cell line, A549 cells pretreated with forskolin, suggesting that the cAMP signaling system may have the similar effect on XRCC1 expression in other lung cancer cells.

To our knowledge, this study is the first report that the cAMP signaling system regulates the expression of XRCC1, except for one paper that described the promoter region of baboon XRCC1 as having a putative cAMP response element, the mutation of which did not significantly change the promoter activity(64). XRCC1 is a scaffold protein that interacts with several DNA repair proteins and thereby coordinates and facilitates DNA base excision repair and repair of DNA single strand breaks (52, 53). Therefore, this study presents a novel mechanism, which involves the regulation of XRCC1 expression, for modulation of DNA repair by cAMP signaling system, and this

mechanism is considered to mediate the potential DNA repair modulating effect of various molecules acting on cAMP signaling system. Furthermore, XRCC1 is assumed to involve in carcinogenesis and cancer cell death, because it facilitates DNA repair. The expression level of XRCC1 was reported to predict cancer-specific survival after various cancer treatments (55). The polymorphisms of XRCC1 gene has been intensively studied on the association with the variability in toxicological response to environmental agents (54), the risk of developing cancer of lung, breast, stomach and liver (65), and the clinical response of various cancers to chemotherapy and radiotherapy (66, 67). Therefore, the regulation of XRCC1 expression by cAMP signaling system might influence on carcinogenesis and responses to cancer treatments, so the cAMP signaling system can be used as a potential target for prevention of carcinogenesis or improvement of the efficiency of various cancer treatments.

From the study on how the cAMP signaling system decreases γ-ray-induced expression of XRCC1, we found the cAMP signaling system to decreases γ-ray-induced expression of XRCC1 by promoting the proteasomal degradation of XRCC1, which is mediated by Epac. This conclusion is corroborated by the result that forskolin pretreatment promoted the ubiquitination and degradation of XRCC1 protein following γ-ray irradiation, which was completely inhibited by a proteasome inhibitor, MG132. Furthermore, the effect of forskolin on XRCC1 expression was not inhibited by PKA inhibitor, and 8-pCPT-2′-

O-Me-cAMP, an Epac-selective cAMP analog (68), increased ubiquitination of XRCC1 protein and decreased XRCC1 expression. Knockdown of Epac1 abolished the effect of 8-pCPT-2′-O-Me-cAMP and restored XRCC1 protein level following γ-ray irradiation. XRCC1 acts as a scaffold for the formation of DNA-repair complexes on damaged DNA to stabilize the BER proteins, and therefore, when XRCC1 is no longer needed for the repair complex, it is ubiquitinated by the E3 ubiquitin ligase CHIP and degraded by the proteasome (61). The cytoplasmic form of the casein kinase 2 phosphorylates XRCC1 to prevent its ubiquitination and proteasomal degradation (69, 70). In addition, XRCC1 is ubiquitinated by a poly (ADP-ribose)-dependent E3 ligase, iduna that regulates cell survival and DNA repair (71). Our study shows that the ubiquitin-proteasome dependent degradation of XRCC1 is promoted by cAMP signaling system, suggesting the ubiquitination of XRCC1 and possibly other proteins may be modulated by various signals acting on cAMP signaling system.

Epac proteins are one family of cAMP effectors, and plays a role as cAMP-dependent guanine nucleotide exchange factors (GEFs) for both Rap1 and Rap2, which belong to the Ras family of small G proteins. Epac proteins have been shown to be involved in a large number of cellular functions such as cell division, differentiation, secretion and growth (7, 72) This study shows a novel role of Epac1, the mediation of cAMP-induced degradation of XRCC1, which leads to inhibition of DNA damage repair. Thus, Epac proteins are suggested to

involve in carcinogenesis, cancer progression, and cell death induced by anticancer drugs and radiation, in which DNA damage repair plays an important role. However, the mechanism how Epac proteins regulate ubiquitination of XRCC1 and the responsible signaling pathway need to be investigated in the future study.

From these results, we conclude that the cAMP signaling system inhibits the repair of DNA damage induced by γ-ray by promoting the Epac-mediated ubiquitin-proteasome dependent degradation of XRCC1 in lung cancer cells. This finding suggests that the cAMP signaling system may play important roles in modulation of DNA damage repair pathways.

Part III.

Effect of Gαs protein on radiation-induced apoptosis

Introduction

Radiotherapy is one of the major modality of treatment for benign and malignant diseases throughout the body, and is used to treat about 50% of all cancer patients with a wide inter-patient variability in tumour response. The strategy to improve radiotherapy seeks to increase the radiation effect on the tumour or to decrease the effects on normal tissues. An improved understanding of the molecular response of cells and tissues to ionizing radiation has contributed to the improvement (73). Ionizing radiation can induce single-strand breaks (SSBs) and double-strand breaks (DSBs) in the DNA double helix backbone, which triggers the DNA damage responses. The DNA damage response machinery delays cell cycle cell-cycle progression and activate the cell cycle checkpoints to provide more time for repair of the lesions and to prevent the transfer of DNA damage to progeny. It facilitates a complex DNA damage repair machinery to detect and repair various forms of DNA damages. When repair fails, the damaged cells are commonly eliminated from the proliferative pool through cellular senescence and the several forms of cell death including apoptosis (74).

The ataxia–telangiectasia mutated (ATM) protein kinase plays a central role in coordinating the cellular response to DNA damages, together with ataxia–telangiectasia and RAD3-related (ATR) and DNA-

dependent protein kinase catalytic subunit (DNA-PKcs) (75-77). The deficiency ATM kinase causes ataxia-telangiectasia, a rare autosomal recessive disorder characterized by hypersensitivity to radiation and predisposition to cancer development. ATM belongs to the phosphatidylinositol 3 kinase-like kinase (PIKK) family of Ser/Thr-protein kinases, which contains ATR, DNA-PKcs and mTOR (mammalian target of rapamycin) (78). Following DNA damage, an intermolecular autophosphorylation occurs on Ser1981 of ATM, which disrupted the inactive homodimer to enables the kinase domain to phosphorylate several target substrates triggering downstream signaling pathways (77). Many ATM substrates are the regulators for gene expression, cell-cycle checkpoint, DNA repair and apoptosis (79). Thus, ATM is a potential target molecule for development of novel radiosensitizers (80) (81).

Cyclic adenosine 3', 5'-monophosphate (cAMP) is a second messenger, which is produced from ATP by adenylate cyclases and degraded into 5'-AMP by cyclic nucleotide phosphodiesterases. Adenylate cyclase is activated by stimulatory heterotrimeric GTP-binding proteins (G proteins), which is activated by G protein coupled receptor-agonist complexes (26). cAMP binds to and activates the cAMP-dependent protein kinase (PKA), cyclic nucleotide gated channels functioning in transduction of sensory signals and the cAMP-activated guanine exchange factors (Epacs), the guanine nucleotide exchange factors (GEFs) for monomeric G protein Raps (82). The

cAMP signaling system regulates numerous cellular responses including gene expression, cell growth, differentiation, proliferation, and apoptosis

We have reported that cAMP signaling system modulates apoptosis of cancer cells induced by various DNA damaging agents including ionizing radiation by regulating the expression of Bcl-2 family proteins (46) (83) and an inhibitors of apoptosis protein (IAP) (59). Recently, the cAMP signaling system was found to inhibit the repair of gamma-ray-induced DNA damage by promoting degradation of XRCC1 protein in human lung cancer cells (84). Thus, we made a hypothesis that the cAMP signaling system might be involved in the regulation of ATM activation, the key event triggering signaling pathways to various DNA damage responses. This study aimed to investigate the mechanism how cAMP signaling system regulates the activation of ATM and cellular responses following γ-ray irradiation. We found that Gαs inhibits ATM activation via the Gαs-cAMP-PKA-PP2A pathway and augments radiation-induced apoptosis following γ-ray irradiation in non-small cell lung cancer cells.

Materials and Methods

Cell culture and reagents

Human non-small cell lung cancer cells: H1299 and A549 cells (Korea Cell Line Bank, Seoul, Korea) and B16-F10 mouse melanoma cells (ATCC, Manassas, VA, USA) were cultured in Dulbecco's modified Eagle's medium (DMEM) containing 10% fetal bovine serum (JBI, Korea) and 100 units/ml penicillin/streptomycin. Cells were incubated in a 5% CO_2 incubator at 37ºC. H89, isoproterenol, dimethyl sulfoxide (DMSO), and 4′,6-diamidino-2-phenylindole, dihydrochloride (DAPI) were purchased from Sigma (St. Louis, MO, USA); forskolin, pyrrolidine dithiocarbamate (PDTC), and isobutylmethylxanthine (IBMX) from Calbiochem (La Jolla, CA, USA); FITC Annexin V apoptosis detection kit from BD Biosciences (San Diego, CA, USA); Prostaglandin E2 (PGE2) and okadaic acid (OA) from Cayman Chemical (Ann Arbor, MI, USA); KU-55933 from Selleck Chemicals (Houston, TX, USA); Bovine serum albumin (BSA) and goat anti-rabbit IgG-FITC from Santa Cruz Biotechnoloty (CA USA; Phenylmethanesulfonylfluoride (PMSF), sodium orthovanadate, sodium fluoride, and a protease inhibitor mixture from Roche Molecular Biochemicals, Indianapolis, IN).

Expression constructs and transient transfection

H1299 cells were transfected with a constitutively active mutant of a long form Gαs (GαsQ227L, GαsQL) in a pcDNA3 vector (Invitrogen, Paisley, UK) using the calcium phosphate method (32). The GαsQL has a mutation of a residue that is essential for the intrinsic GTPase activity (29). Dominant negative mutant of PKA (dnPKA) was a gift from Dr. G. Stanley McKnight (University of Washington, WA, USA).

Preparation of cytosolic and nuclear fraction

The cultured cells were harvested and then disrupted in lysis buffer A (0.33 M sucrose, 10 mM Hepes (pH 7.4), 1 mM $MgCl_2$, 0.1% TritonX-100, protease inhibitor cocktail (PIC), and PMSF. The cell lysate were centrifuged for 5 min at 800 *g*, and the supernatant was collected to use as the cytosolic portion. The resulting pellets were resuspended in lysis buffer B (0.45 M NaCl, 10 mM Hepes (pH 7.4), PIC, and PMSF) and centrifuged for 5 min at 20,000 *g*. The supernatant was collected to use as the nuclear portion.

Western blot analysis

Western blotting was performed as previously described (31). Antibodies against Gαs, Ku70, ATM, COX-1, phosphorylated cAMP response element binding protein (p-CREB, Ser133), PP2A B56δ, IκBα, p50 and p65 of NF-κB were from Santa Cruz Biotechnology (CA,

USA), and antibodies against Rad 50, p-ATM (Ser 1981), γ-H2AX, Ku80, CREB, DNA-PKcs, poly (ADP-ribose) polymerase (PARP), cleaved caspase-3 (Asp175), p-AKT (Ser473), AKT, p-IκBα, and Myc-tag were from Cell Signaling Technology (Beverly, MA, USA). An antibody against β-Actin was purchased from Sigma (St. Louis, MO, USA) and antibody against EE-tag was from Covance (Princeton, NJ, USA). Antibody against p-PP2B56δ (Ser 566) was kindly provided by Dr. Paul Greengard (The Rockefeller University, New York) (85). Proteins were visualized by the Enhanced Chemiluminescence (ECL) reagent (Thermo scientific, Waltham, MA) and detected by LAS-3000 (R&D Systems, Inc. Minneapoli, MN, USA. The densities of the protein bands were quantified using the Multi Gauge v2.3 software (Fuji, Tokyo, Japan), and relative band densities were expressed as ratios of the corresponding control densities.

Immunofluorescence microscopy

H1299 cells were plated in 60 mm dishes and incubated until they became 60% confluent. Cells were transfected with plasmids containing vector or GαsQL and then after 24 h irradiated with γ-ray (5 Gy) from Cs irradiator (84). After 30 min, the cells were fixed with 4% paraformaldehyde for 20 min and permeated with 0.5% TritonX-100 for 10 min. After blocking with 2% BSA for 1 h, the cells were incubated overnight with an antibody against p-ATM (1:200) in 2% BSA and goat

anti-rabbit IgG-FITC (1:100) with DAPI (0.5 μl/ ml) was incubated for 1 h. The stained cells were observed with a confocal microscope (LSM 501 META, Carl Zeiss, Inc. USA).

TUNEL assay

Extracted lung tissues from BALB/c mice were deparaffinized and hydrated. After pretreatment, apoptosis was detected using an ApopTag fluorescein *in situ* apoptosis detection kit (Chemicon International, Temecula, CA, USA). The tissues were observed using confocal laser scanning microscopy (TCS SP2, Leica, Wetzler, Germany). To determine TUNEL expression, the number of apoptotic events was counted in ten random fields and divided that number by the total number of cells per field.

PP2A activity assay

Cells were prepared and lysed following the manual of the PP2A activity assay kit (R&D Systems, Inc. Minneapoli, MN, USA). In brief, cell lysate were incubated with Serine/Threonine Phosphatase substrate I for 30 min, and then 10 μl of Malachite Green Reagent A was added and incubated for 10 min. Then, 10 μl of Malachite Green Reagent B was added and incubated for 20 min, and the absorbance at 620 nm was measured with the Benchmark plus^{TM} microplate reader (Bio-Rad, PA, USA).

Flow cytometry

The cells were exposed to γ-radiation (10 Gy) and incubated for 24 h. Then the cells were washed twice with phosphate-buffered saline, harvested, and spun at 3,500 *g* for 5 min at 4ºC. The cells were incubated in the 1X Annexin V buffer with Annexin V and PI for 15 min. Stained cells were quantified with a FacsCalibur flow cytometer (BD Biosciences, Franklin Lakes, NJ, USA) using 10,000 cells per measurement.

Dual luciferase reporter assay

H1299 cells were transfected with plasmids containing luciferase reporter genes (NF-κB-pLuc and Renilla-pLuc) together with plasmids containing the vector or GαsQL by the calcium phosphate method. Luciferase activities were measured using the Dual-Luciferase Reporter Assay System (Promega Corp., Madison, WI, USA) according to the manufacturer's manual. At least four independent experiments in duplicate were performed, and promoter activities were normalized versus Renilla luciferase activity.

Animal experiment

Care, use, and treatment of animals were done in agreement with the guidelines established by the Seoul National University Institutional Animal Care and Use Committee (#SNU-110415-2). BALB/c male mice (4 week-old) were participated in our experiment. During 1 week, they

stayed in animal conditional laboratory for relieve. And then they were treated with Forskolin by I.P. and radiation exposure (10 Gy) for 30 min or 24 h. They were sacrificed by CO2 injection following the ethics of an experiment on animals.

Data analysis

At least three or more independent experiments were conducted for all the analyses, and data were presented as means ± standard errors (SE). The non-parametric Mann-Whitney U test was used to analyze mean values, and a *p* value of less than 0.05 was considered statistically significant.

Results

Gαs inhibited radiation-induced ATM activation in H1299 lung cancer cells

To investigate the effects of cAMP signaling pathway on radiation-induced DNA damage responses, a constitutively active mutant form of the α subunit of stimulatory heterotrimeric GTP binding protein (GαsQL) was transiently expressed in H1299 human lung cancer cells. Phosphorylated ATM by irradiation were showed different pattern in time-dependent manner and vector/GasQL transfected cells (Figure. 49). Following the Fig. 49. results, we knew that p-ATM was biphasic at the time courses and determined the exposer time to 30 min in this study. At this point, p-ATM decreased by GαsQL in H1299 cells. Expression of GαsQL significantly inhibited the radiation-induced phosphorylation of ATM and H2AX without changing their protein levels in H1299 cells, and it did not changed the expression of Rad50, Ku70, and 80 (Figure. 50). The densitometric analysis of the blots confirmed the decrease in phosphorylation of ATM and H2AX (Figure. 51). Subcellular fractionation analysis and confocal microscopy showed that Gαs inhibited radiation-induced ATM activation in the nucleus within 1 h after exposure to γ-ray (Figure. 52 & 53). These results show that Gαs inhibits radiation-induced ATM activation at the early phase of DNA damage responses in lung cancer cells.

Gαs activated PP2A in a PKA-dependent manner, which decreased the radiation-induced phosphorylation of ATM in H1299 lung cancer cells

To investigate the mechanism how Gαs inhibited the radiation-induced ATM phosphorylation, the effect of a PP2A inhibitor, okadaic acid, on the ATM phosphorylation was analyzed. Treatment with okadaic acid abolished the inhibitory effect of Gαs on the radiation-induced ATM phosphorylation and recovered the phosphorylation to the control level in the Gαs-transfected cells (Figure. 54). Then, to examine whether Gαs can activate PP2A, the phosphorylation of PP2A B56δ subunit at serine-566 was analyzed in GαsQL-transfected cells. Expression of GαsQL strongly increased the basal phosphorylation level of the B56δ subunit, and it maintained the increased phosphorylation level after irradiation without changing the protein level of the B56δ subunit (Figure. 55). To examine the phosphorylation of PP2A B56δ subunit is catalyzed by PKA, the effect of PKA inhibition was assessed. Inhibition of PKA with an inhibitor, H89 or dominant negative PKA decreased the phosphorylation of PP2A B56δ before and after γ-ray irradiation with a concomitant increase in ATM phosphorylation (Figure. 56). The effective inhibition of PKA by H89 and dominant negative PKA was supported by the decrease in phosphorylated CREB, which is a PKA target protein. Next, the effect of Gαs onto PP2A activity was analyzed. Expression of GαsQL increased the PP2A activity before and after γ-

radiation compared to the respective control, and the PP2A-activating effect of Gαs was completely removed by H89 and dominant negative PKA (Figure. 57). These results indicate that Gαs activates PP2A by phosphorylating PP2A B56δ subunit in a PKA-dependent manner, which decreases the radiation-induced phosphorylation of in H1299 lung cancer cells.

Gαs augmented radiation-induced apoptosis by inhibiting ATM activation in lung cancer cells and the mouse lung tissue

To investigate the effect of inhibition of radiation-induced ATM activation by Gαs, we examined the effect on radiation-induced apoptosis. Expression of GαsQL increased radiation-induced cleavage of caspase 3 and PARP (Figure. 58) and the number of cells stained with Annexin V but not with propidium iodide (Figure. 59) in H1299 cells. Treatment with an ATM inhibitor, KU55933, also increased the radiation-induced cleavage of caspase 3 and PARP and the Annexin V-stained cells (Figure. 58 & 59). To identify the relationship between p-ATM and radiation-induced apoptosis, we used p-ATM activator, Chloroquine (CQ). The cells were pre-treated CQ for 4 h and exposured γ-radiation. After 24 h, cleavage of caspase 3 and PARP decreased by CQ-cotreatment (Figure. 60). To confirm the observed effects of Gαs in other lung cancer cells, the effects of Gαs was examined in A549 human lung cancer cells. Expression of GαsQL in

A549 cells inhibited the radiation-induced phosphorylation of ATM at 30 min after irradiation, and it also increased the radiation-induced cleavage of caspase 3 and PARP and the number of Annexin V stained cells (Figure. 61 & 62). These results indicate that GαsQL augments the radiation-induced apoptosis by inhibiting ATM activation in human lung cancer cells.

Next, to verify the effect of Gαs activation in vivo, BALB/c mice were used. Before the animal experiment, the effect of forskolin, an adenylate cyclase activator like Gαs, was analyzed in B16-F10 mouse melanoma cells. Treatment with forskolin increased the radiation-induced phosphorylation of PP2A B56δ (S566) subunit and decreased the radiation-induced phosphorylation of ATM in the melanoma cells (Figure. 63). Pre-treatment of BALB/c mice with forskolin stimulated phosphorylation of PP2A B56δ, and inhibited the phosphorylation of ATM in the lung tissue following γ-ray irradiation (Figure. 64). Furthermore, forskolin treatment of BALB/c mice increased the radiation-induced apoptosis of the lung tissue evidenced by the increased cleavage of caspase-3 and PARP (Figure. 65) and by the increase in TUNEL stained spots following γ-ray irradiation (Figure. 66). These results suggest that cAMP signaling system augments radiation-induced apoptosis by inhibiting ATM activation via PP2A in mouse lung as well as in murine melanoma cells.

Gαs augmented radiation-induced apoptosis by reducing ATM-dependent activation of NF-κB

To study the mechanism how reduced ATM activation augments radiation-induced apoptosis, we examined the role of NF-κB, because NF-κB is activated by ATM to prevent apoptosis (86). Inhibition of NF-κB by treatment with PDTC, an NF-κB inhibitor, increased the radiation-induced cleavage of caspase-3 and PARP in H1299 cells (Figure. 67). Then, the effect of Gαs on radiation-induced NF-κB activation was examined. Expression of GαsQL increased the basal level of IκBα protein, and increased level in the cytosol fraction of the H1299 cells before and after γ-ray irradiation in comparison with the respective control, and it decreased the protein levels of p50 and p65 subunits of NF-κB translocation into nucleus after irradiation (Figure. 68). The IκBα protein level was also increased at 30 min after radiation exposure and at that time, NF-κB slightly regulated by radiation. In addition, IκBα did not fully recover for 24 h after radiation (Figure. 69). Furthermore, the expression of GαsQL or and inhibition of ATM by KU55933 reduced radiation-induced activation of the NF-κB promoter, (Figure. 70). These results suggest that Gαs augmented radiation-induced apoptosis by reducing ATM-dependent activation of NF-κB in H1299 cells. To investigate the correlation with CQ and NF-κB activity, CQ was used. CQ increased basal NF-κB activity and co-treatment with radiation more increased NF-κB activity (Figure. 71). To probe

how ATM regulate radiation-induced NF-κB activation, the effect of GαsQL on the p-ATM level in the cytosol, where IκBα is located. Most of phosphorylated ATM is localized in the nucleus; small amount of phosphorylated ATM was visualized by the long time exposure to the gel documentation system. γ-Ray irradiation increased p-ATM level in the cytosol, and GαsQL expression decreased the radiation-induced p-ATM level in the cytosol (Figure. 72). These Data show that NF-κB is a key of the mechanism which regulates the radiation-induced apoptosis by Gαs-p-ATM signal in H1299 lung cancer cells.

Isoproterenol and PGE2 showed the effects similar to Gαs on ATM activation and apoptosis

To confirm the effect of GαsQL expression can be induced by agonists for Gαs-coupled receptors, we analyzed the effect of prostaglandin E2 and isoproterenol. Pretreatment with prostaglandin E2 or isoproterenol increased the phosphorylation of PP2A B56δ and decreased the ATM phosphorylation following γ-ray irradiation (Figure. 73). The pretreatment with prostaglandin E2 decreased NF-κB luciferase activity from 8 h after irradiation and treatment with Isoproterenol slightly decreased NF-κB luciferase activity after irradiation (Figure. 74). Treatments with prostaglandin E2 or isoproterenol also increased the cleavage of caspase-3 and PARP, and early apoptosis in H1299 cells (Figure. 75 & 76). These results indicate that the agonists for Gαs-

coupled receptors, like the GαsQL, can activate PP2A, inhibit ATM and NF-κB, and thus augment the radiation-induced apoptosis in H1299 cells.

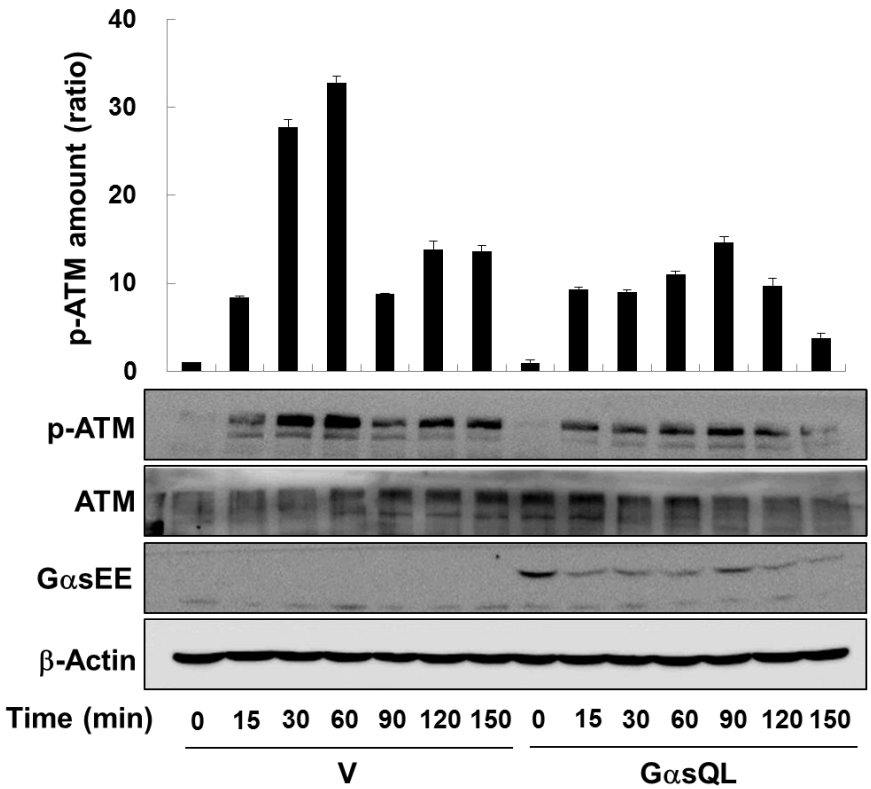

Figure 49. Effects of Gαs on the proteins involved in DNA damage response following time-dependent γ-ray irradiation

The H1299 cells were transfected with GαsQL or vector for 24 h, and irradiated with γ-rays (5 Gy) and incubated for 150 min to ATM expression. The proteins were confirmed by western blotting.

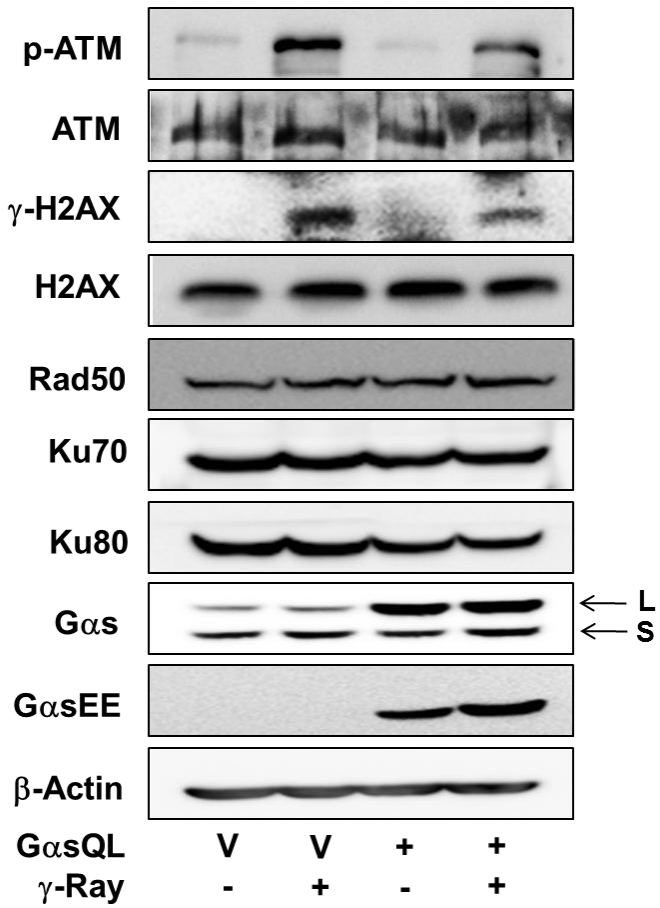

Figure 50. Effect of Gαs on the proteins involved in DNA damage response following gamma ray irradiation

L represents long forms of Gαs and S short forms of Gαs. H1299 cells were transfected with EE-tagged GαsQL or a pcDNA3 vector (V), incubated for 24 h, and irradiated with γ-rays (5 Gy). After incubation for 30 min, the expression and phosphorylation of the protein involved in DNA damage responses were analyzed by western blotting. β-Actin was used as a loading control.

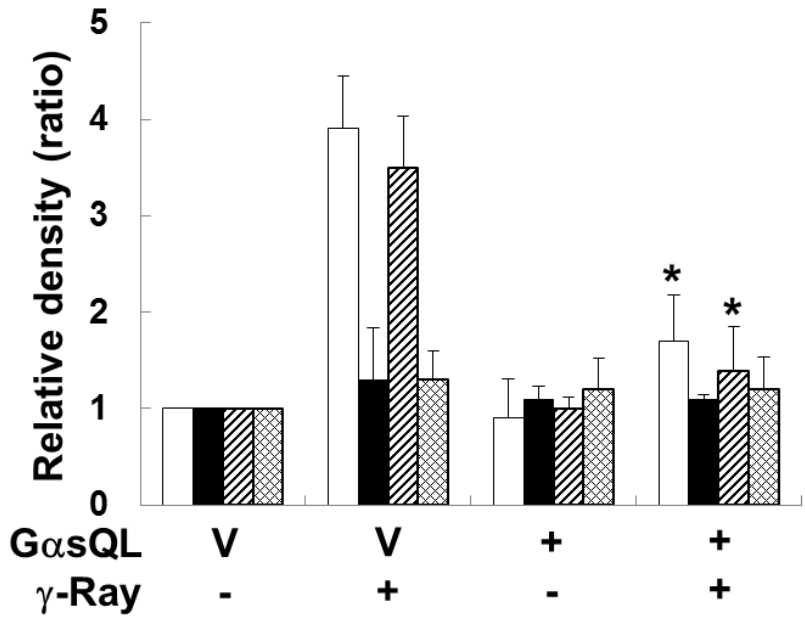

Figure 51. Densitometric analysis of ATM phosphorylation (p-ATM, ATM, gamma H2AX and H2AX)

The histograms present the means and standard errors of at least three independent experiments (empty bar: p-ATM, filled bar: ATM, striped bar: γ-H2AX, and hatched bar: H2AX), and an asterisk (*) indicates a statistically significant difference from the vector-transfected control cells ($p < 0.05$, Mann–Whitney U test).

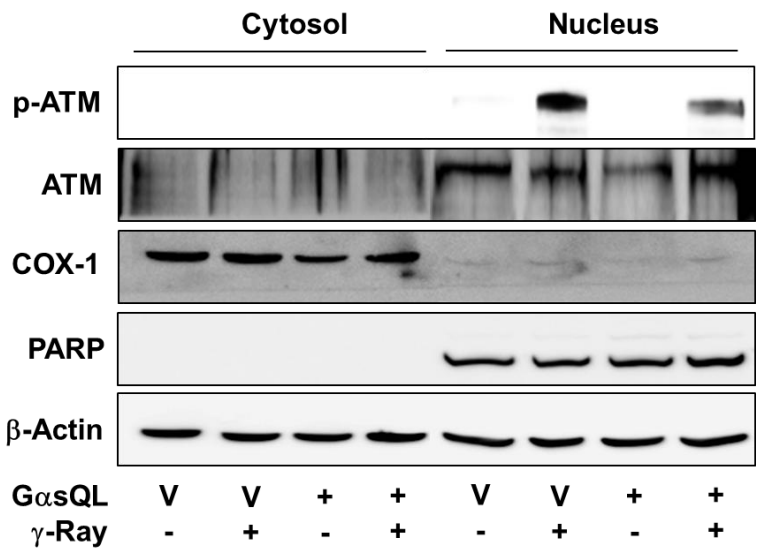

Figure 52. Subcellular fractionation analysis of ATM phosphorylation

Thirty minutes after irradiation, the cells were lysed and fractionated for western blotting. COX-1 and PARP were used as the markers for cytosol and nucleus fraction, respectively

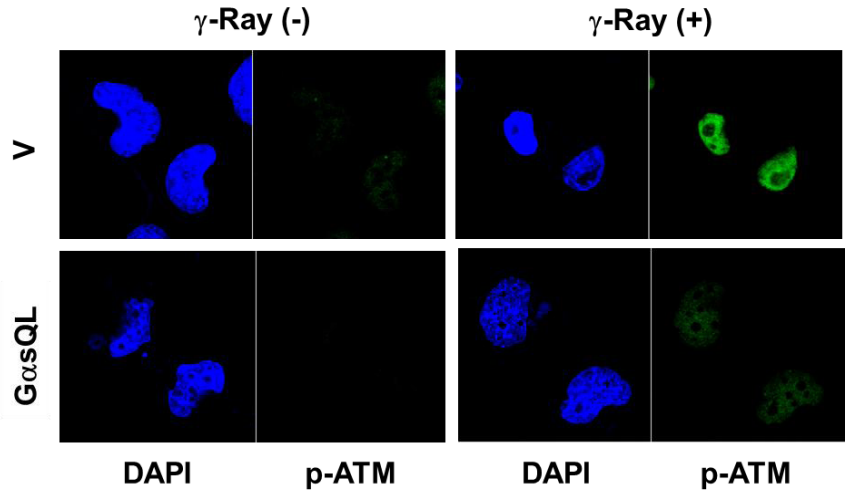

Figure 53. Confocal analysis of ATM phosphorylation

One hour after irradiation, phosphorylated ATM was assessed by staining with DAPI and p-ATM-FITC and then by confocal microscopy

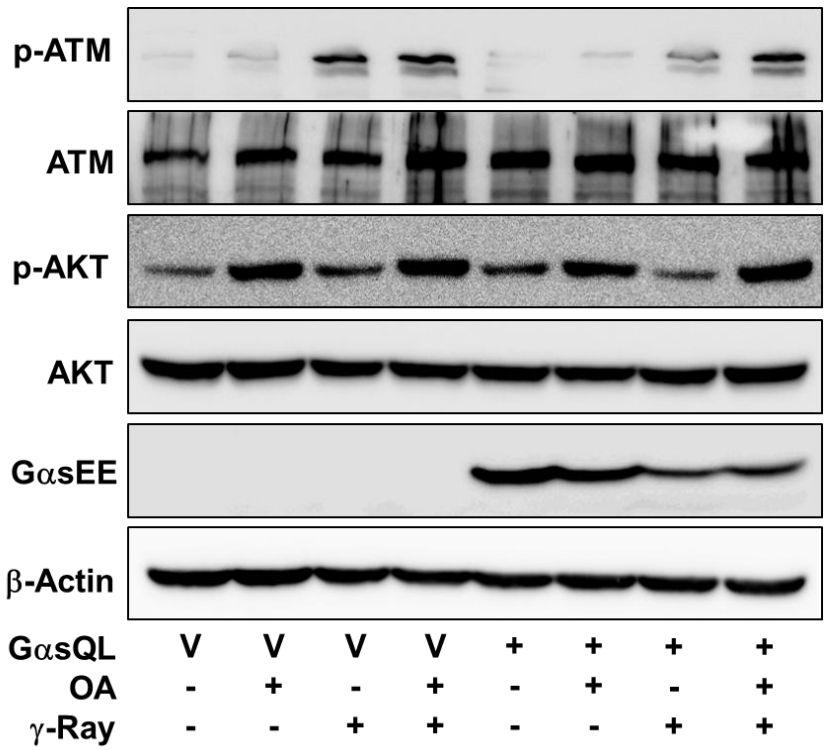

Figure 54. Effect of okadaic acid (OA) on radiation-induced ATM phosphorylation

The H1299 cells were transfected with GαsQL or vector (V) and incubated for 24 h. The cells were pre-treated with 500 nM okadaic acid or DMSO for 30 min, and then irradiated with γ-rays (5 Gy). After incubation for 30 min, the cells were harvested and analyzed by western blotting. Phosphorylated AKT (p-AKT) was analyzed as a positive control for PP2A activity.

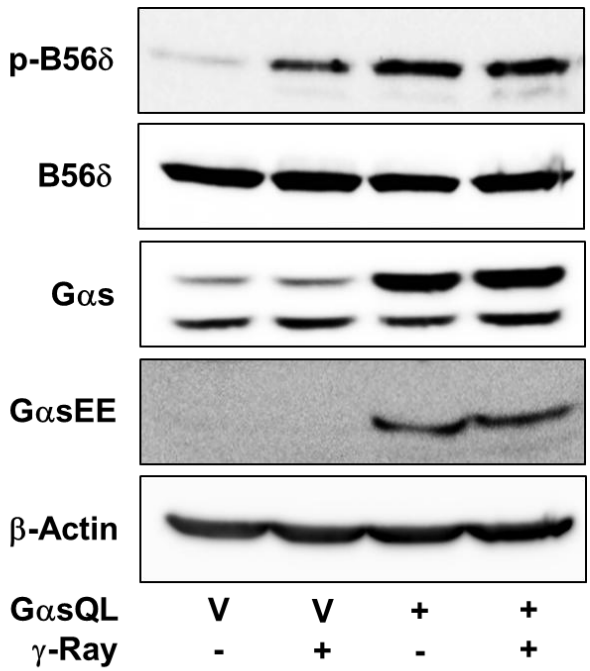

Figure 55. Effect of Gαs on the phosphorylation of PP2A B56delta

The H1299 cells were transfected with GαsQL, vector (V) and incubated for 24 h. And then cell were irradiated with γ-rays (5 Gy). After incubation for 30 min, the cells were harvested and analyzed by western blotting.

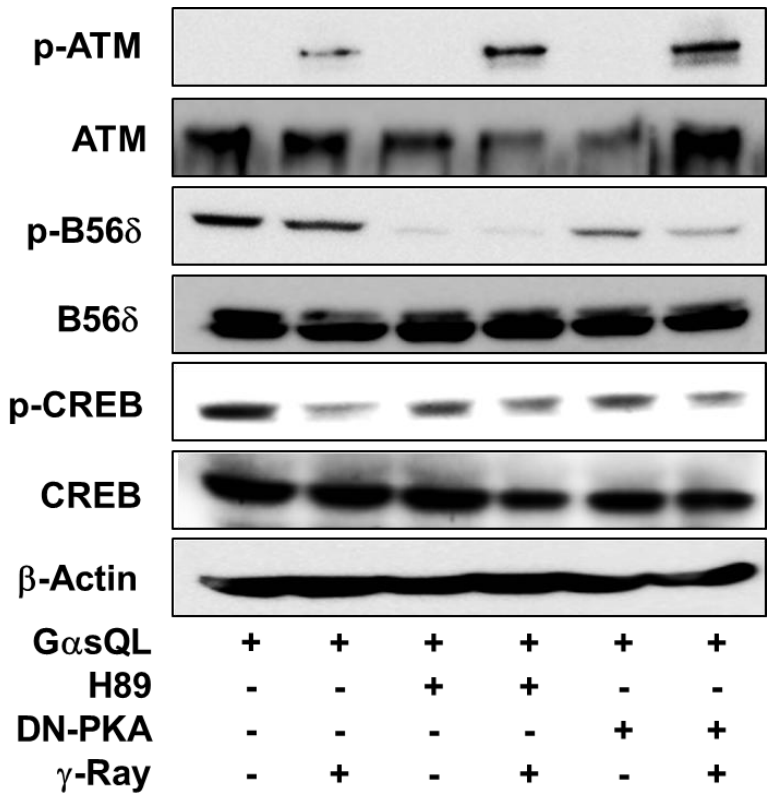

Figure 56. Effect of PKA inhibition on the phosphorylation of B56delta and ATM

The H1299 cells were transfected with GαsQL, vector (V), or dominant negative PKA (dnPKA) and incubated for 24 h. The cells were pre-treated with 10 μM H89, or DMSO for 30 min, and then irradiated with γ-rays (5 Gy). After incubation for 30 min, the cells were harvested and analyzed by western blotting.

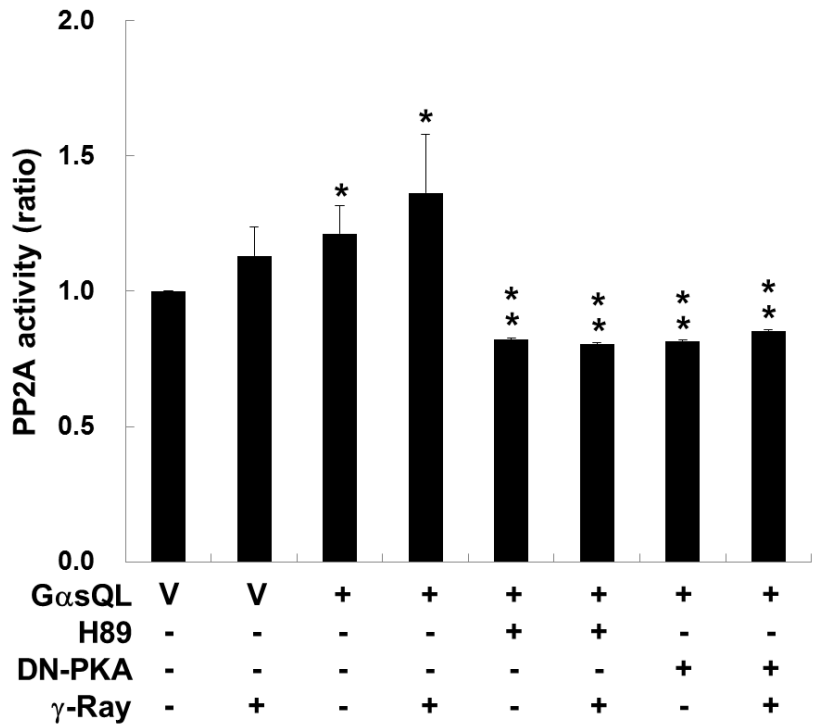

Figure 57. Effect of PKA inhibition on PP2A activity

The H1299 cells were transfected with GαsQL, vector (V), or dominant negative PKA (dnPKA) and incubated for 24 h. The cells were pre-treated with 10 μM H89, or DMSO for 30 min, and then irradiated with γ-rays (5 Gy). After incubation for 30 min, the cells were harvested and analyzed for PP2A activity. The asterisk (*) on histograms indicates a statistically significant difference from the vector-transfected control cells; the double asterisks (**) represent a statistically significant difference from the GαsQL-transfected control cells ($p < 0.05$, Mann–Whitney U test, D).

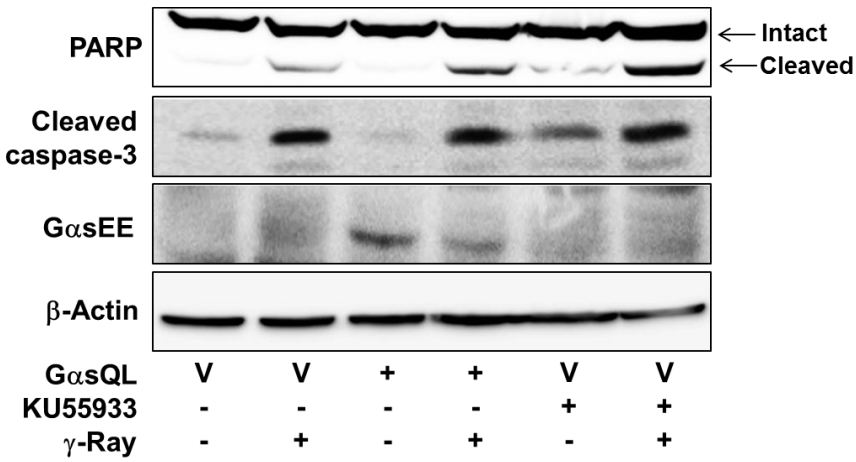

Figure 58. Effect of ATM inhibition on the gamma ray-induced cleavage of caspase-3 and PARP in H1299 cells

The cells were irradiated with γ-rays (10 Gy) and incubated for 24 h for analysis of apoptosis with/without pre-treatment with 10 μM KU55933 or DMSO for 30 min. The cells were harvested and analyzed by western blotting.

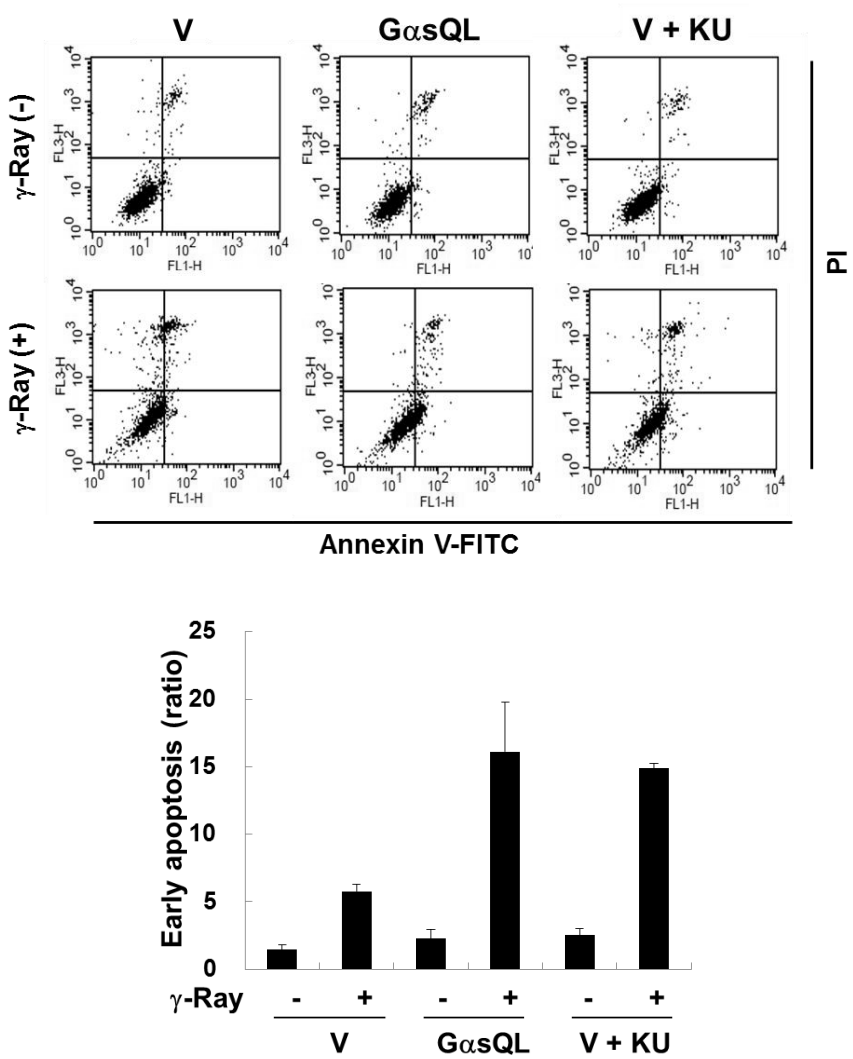

Figure 59. Effect of Gαs and ATM inhibition on radiation-induced early apoptosis in H1299 cells

The cells were irradiated with γ-rays (10 Gy) and incubated for 24 h for analysis of apoptosis. The cells were harvested and analyzed by flow cytometry after staining with Annexin V and propidium iodide (PI).

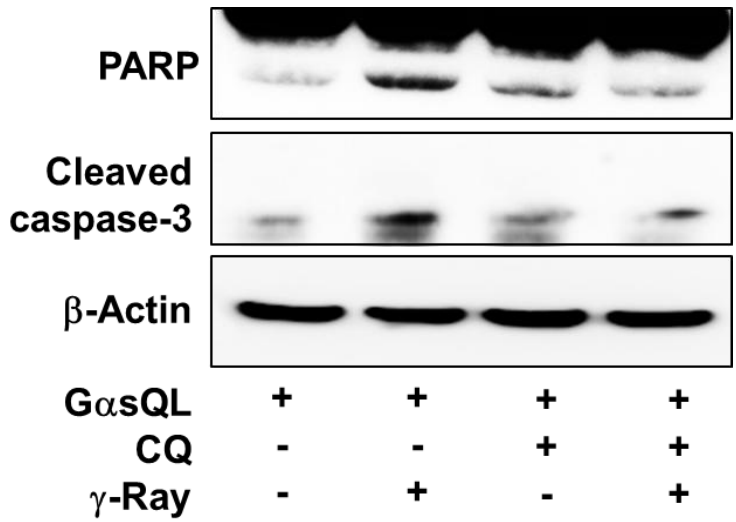

Figure 60. Effect of CQ on radiation-induced apoptosis in H1299 cells

The cells were pre-treated 20 μg/ml CQ for 4 h and exposured by irradiation. And then changed media for discard the CQ and incubated for 23 h.

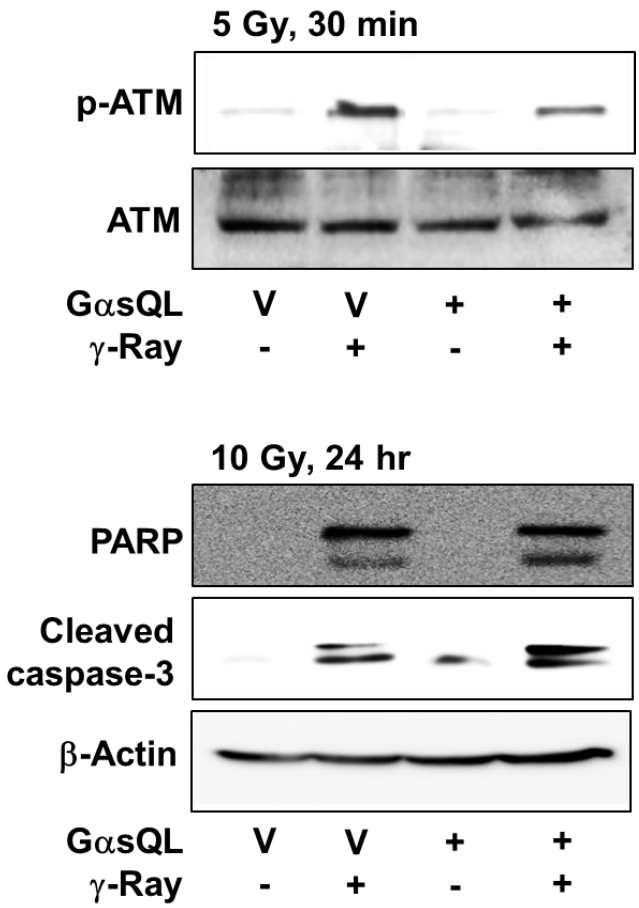

Figure 61. Effect of GαsQL on radiation-induced phosphorylation of ATM and cleavage of caspase 3 and PARP in A549 cells

The cells were irradiated with γ-rays (5 Gy) and incubated for 30 min for analysis of ATM phosphorylation; other cells were irradiated with γ-rays (10 Gy) and incubated for 24 h for analysis of apoptosis. The cells were harvested and analyzed by western blotting.

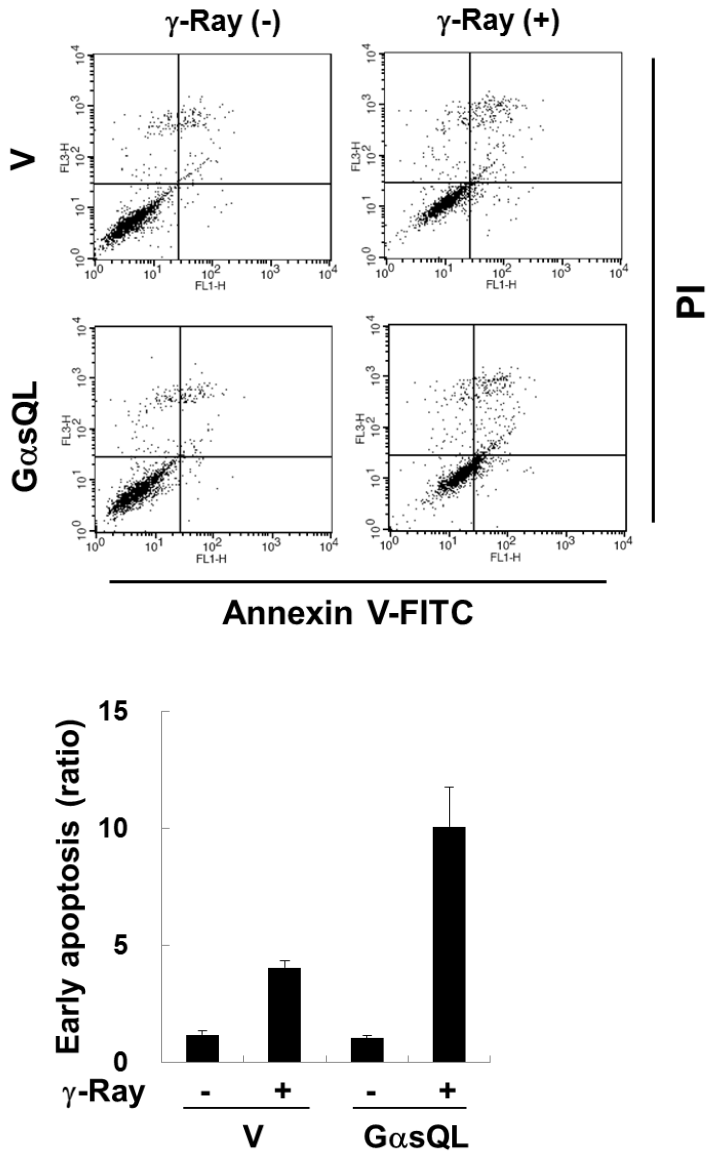

Figure 62. Effect of Gαs on radiation-induced early apoptosis in A549 cells

The H1299 cells and A549 cells were transfected with GαsQL or vector (V), and incubated for 24 h. And the cells examined by flow cytometry after staining with Annexin V and propidium iodide (PI).

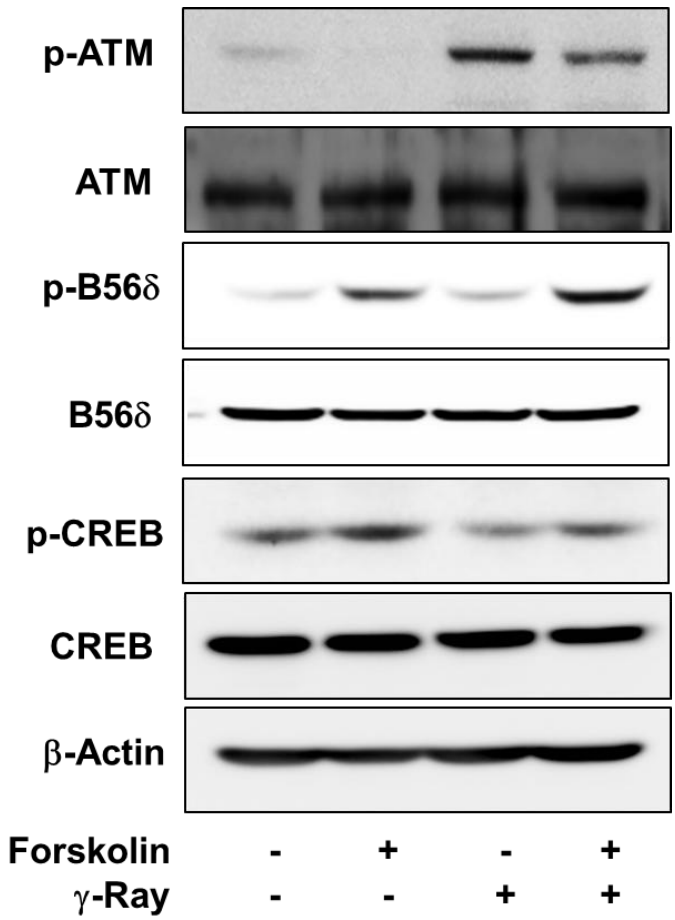

Figure 63. Effect of forskolin on the phosphorylation of PP2A B56δ and ATM in B16F10 mouse melanoma cells

The mouse melanoma cells were pre-treated with 40 μM forskolin for 30 min and irradiated with γ-rays (5 Gy). After incubation for 30 min, the phosphorylation of PP2A B56δ and ATM was analyzed by western blotting.

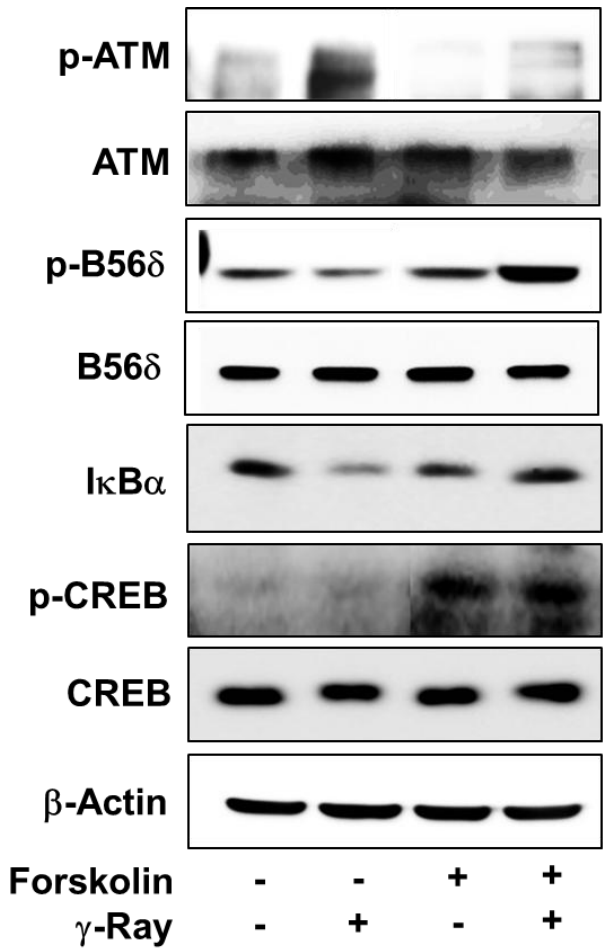

Figure 64. Effect of forskolin on the phosphorylation of PP2A B56δ and ATM in the mouse lung

The 4 week-old male BALB/c mice (20 g) were injected intraperitoneally with forskolin (20 μg/g), and after 6 h the mice were treated with a whole body γ-ray irradiation (10 Gy). After incubation for 30 min, the animals were sacrificed and lung tissues were excised and homogenized for western blot analysis.

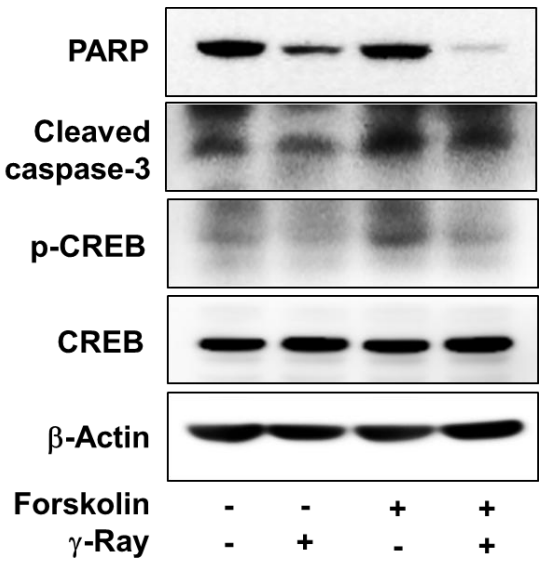

Figure 65. Effects of forskolin on apoptosis of the mouse lung

For apoptosis analysis, the animals were sacrificed after incubation for 24 h, and the lung tissues were excised. A part of the lung tissues were homogenized and analyzed for cleavage of caspase-3 and PARP by western blotting.

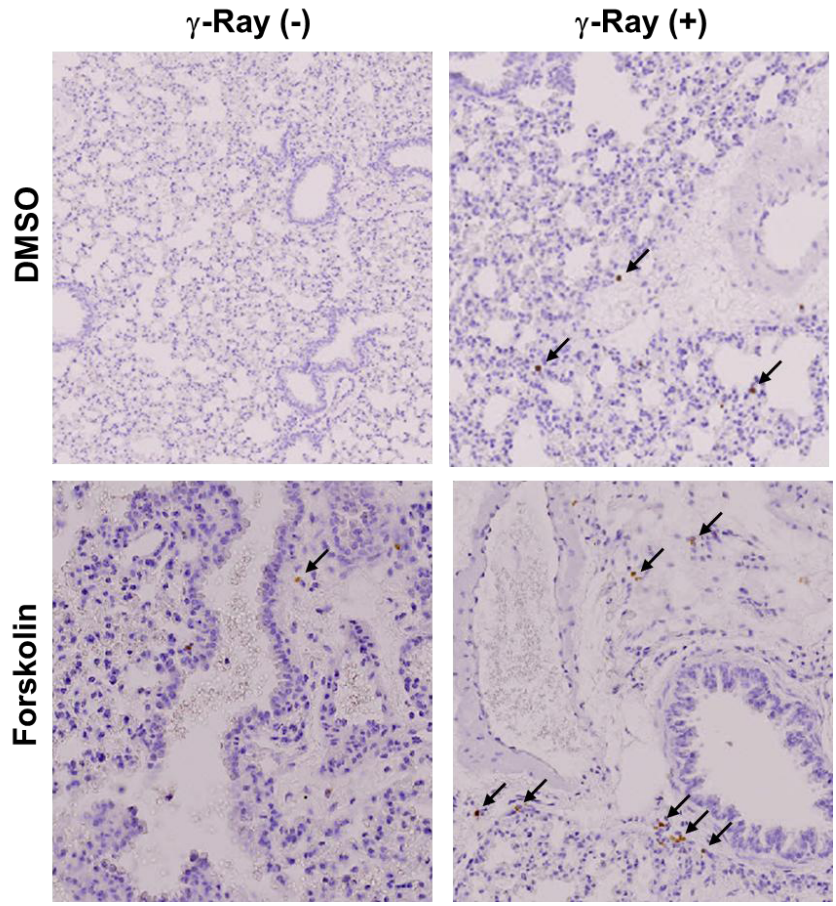

Figure 66. Effects of forskolin on apoptosis of the mouse lung analyzed by Tunel enzymatic labeling assay

For apoptosis analysis, the animals were sacrificed after incubation for 24 h, and the lung tissues were excised. A part of the lung tissues were immediately fixed with formaldehyde and were examined by TUNEL assay. The arrows indicate the stained cell undergoing apoptosis.

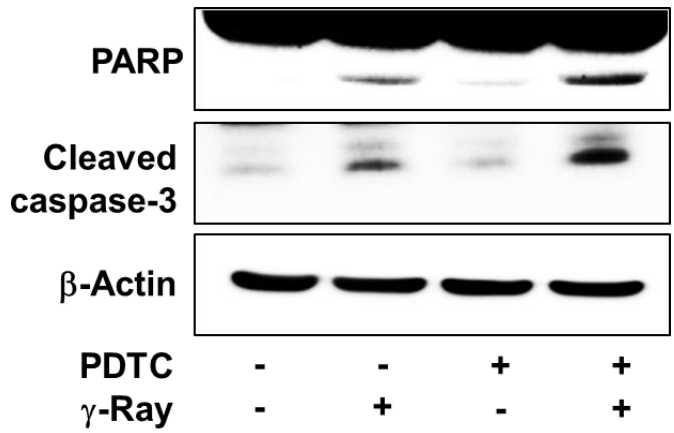

Figure 67. Effect of PDTC, an NF-κB inhibitor, on radiation-induced cleavage of Caspase 3 and PARP

H1299 cells were pretreated with DMSO or 5 μM PDTC for 30 min. Then the cells were irradiated with γ-rays (10 Gy) and incubated for 24 h.

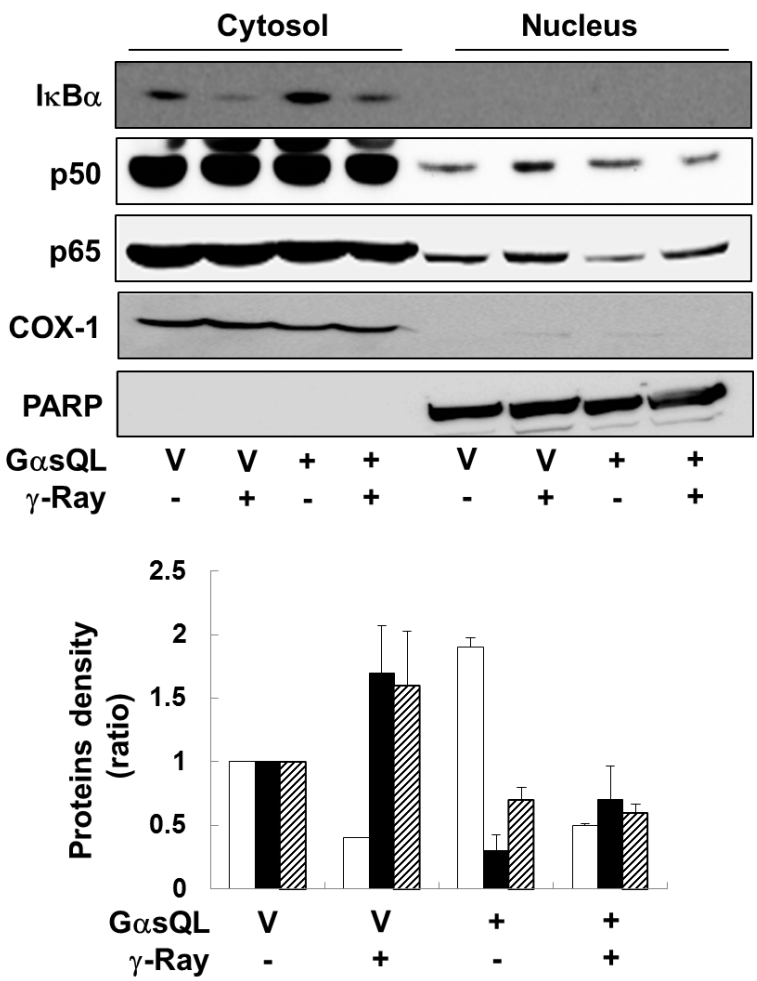

Figure 68. Effect of Gαs on the activation of NF-κB

H1299 cells were transfected with GαsQL or vector. Then the cells were irradiated with γ-rays (10 Gy) and incubated for 24 h. The IκBα and NF-κB were fractionated and analyzed by western blotting. The graph was made from the western blot band densities (white bar: cytosol IκBα, black bar: nucleus p50, and slanting bar: nucleus p65).

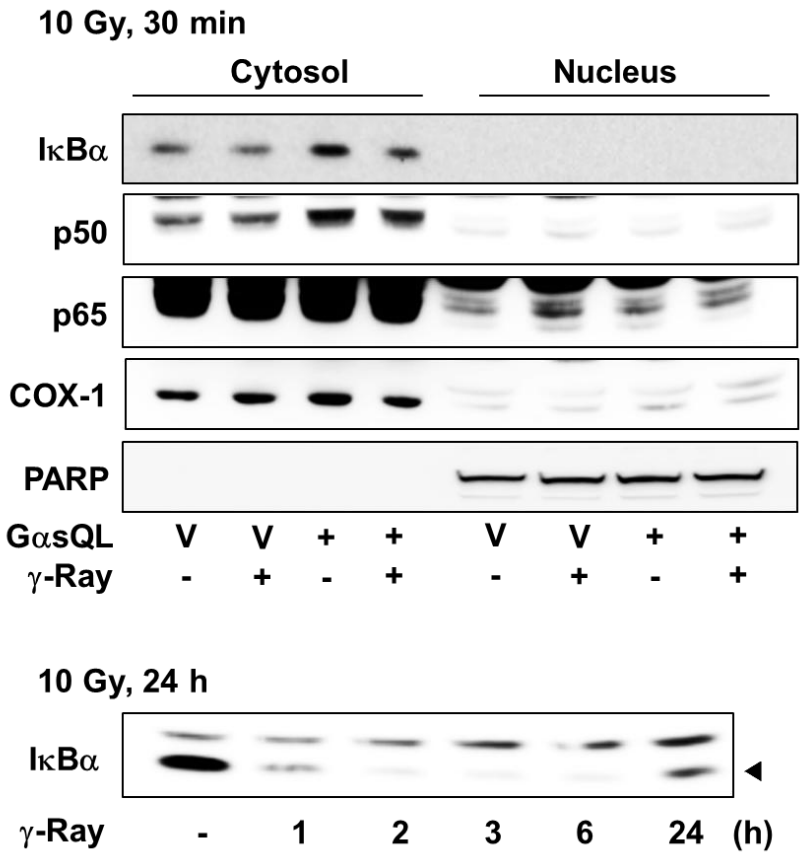

Figure 69. Expression level of IκBα and NF-κB at the 30 min radiation-exposured cells and time dependent-IκBα expression in H1299 cells

In the short time exposured cells, IkBa and NF-κB (p50 and p65) were regulated by GαsQL. IκBα decreased by radiation and could not fully recover until 24 h in H1299 cells. Arrow: IκBα band.

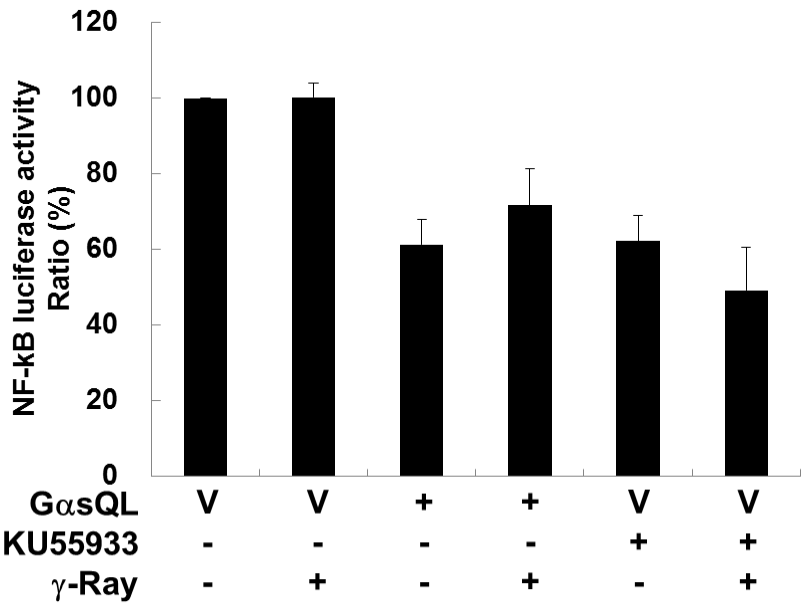

Figure 70. Effect of Gαs on the promoter activity of NF-κB

H1299 cells were pretreated with 10 μM KU55933 or DMSO 30 min with/without transfection of GαsQL or vector. Then the cells were irradiated with γ-rays (10 Gy) and incubated for 24 h. NF-κB luciferase activity was confirmed by the Dual-Luciferase Reporter Assay System by degrading IκBα in H1299 cells.

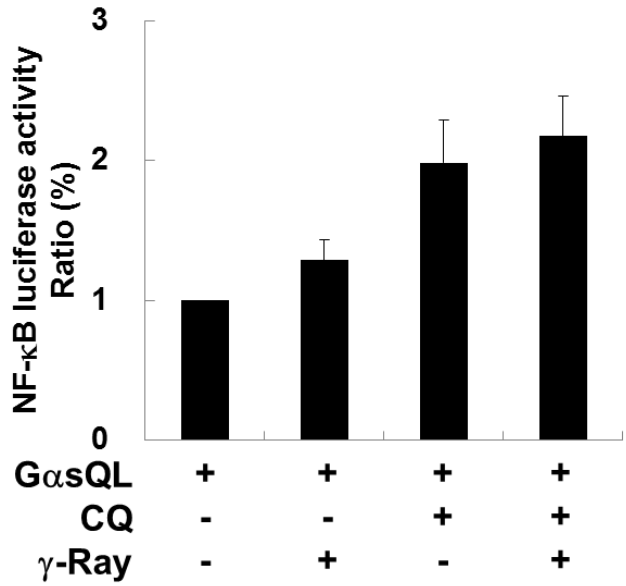

Figure 71. Effect of CQ on the NF-κB luciferase activity

H1299 cells were transfected with GαsQL and pretreated with 20 μg/ml CQ for 4 h. Then the cells were irradiated with γ-rays (10 Gy) and incubated for 1 h. After change the media, incubation for 24 h. NF-κB luciferase activity was confirmed by the Dual-Luciferase Reporter Assay System.

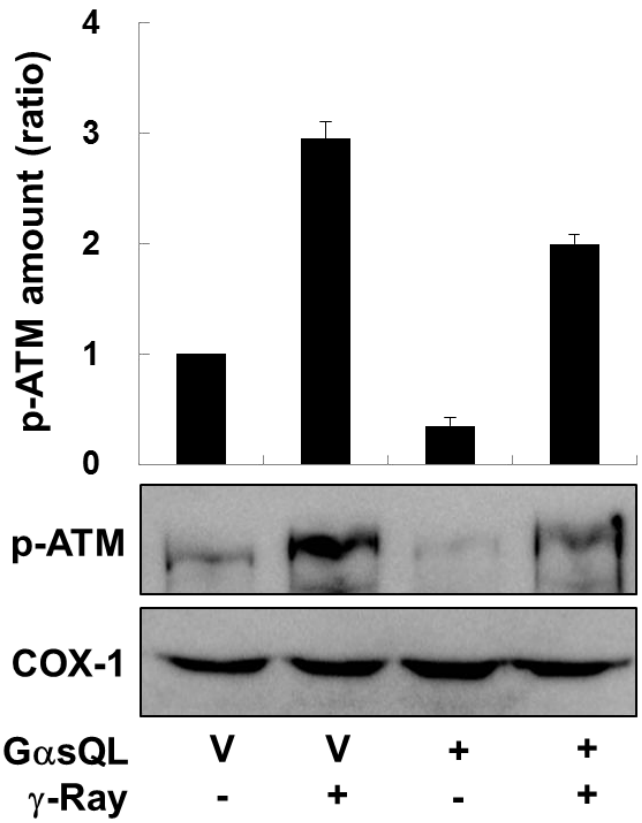

Figure 72. Gαs decreased translocation of ATM into cytosol

H1299 cells were transfected with GαsQL or vector. Then the cells were irradiated with γ-rays (10 Gy) and incubated for 24 h. Data are presented from three independent experiments.

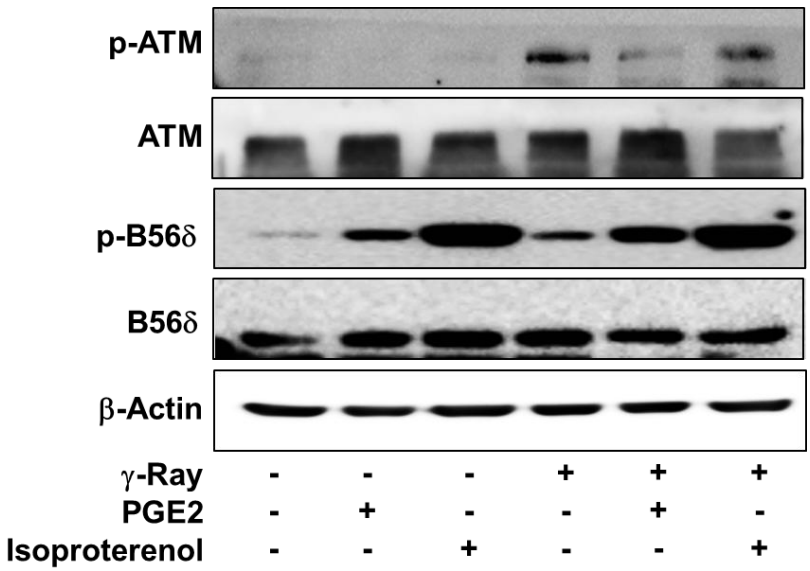

Figure 73. Effects of prostaglandin E2 (PGE2) and isoproterenol on the phosphorylation of PP2A B56δ and ATM

The H1299 cells were treated with 10 μM PGE2 or 1 μM isoproterenol for 30 min before irradiation with γ-rays (5 Gy) and incubated for 30 min for phosphorylation analysis.

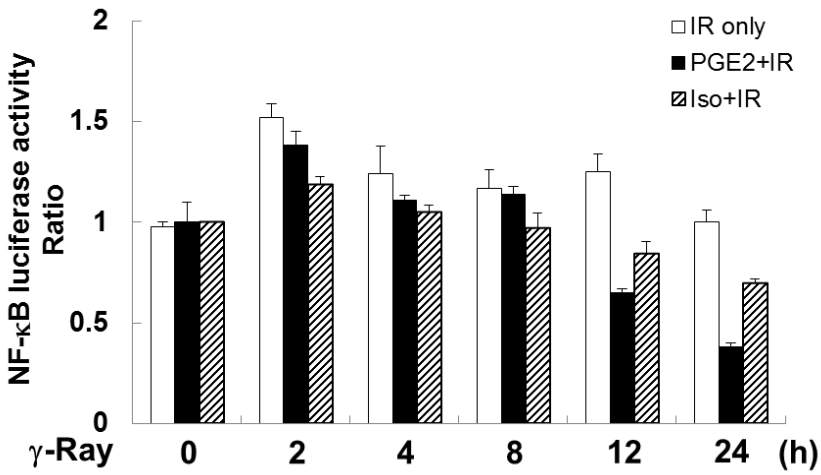

Figure 74. The time-courses of prostaglandin E2 and Isoproterenol effect on NF-κB luciferase activity

For NF-κB luciferase activity assay, the cells transfected with reporter genes were treated with PGE2 or for 30 min before irradiation (10 Gy), and luciferase activity was measures at the indicated times (empty bar: control cells, filled bar: PGE2-treated cells, striped bar: Isoproterenol-treated cells).

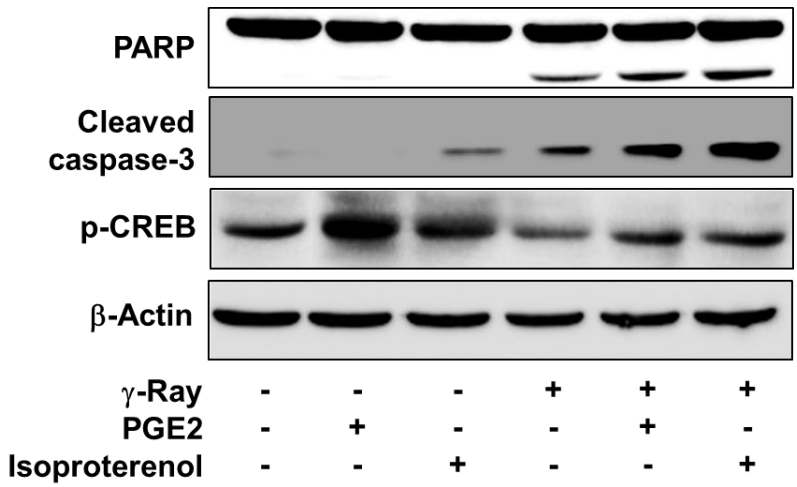

Figure 75. Effects of prostaglandin E2 and isoproterenol on the cleavage of caspase 3 and PARP

The H1299 cells were treated with 10 μM PGE2 or 1 μM isoproterenol for 30 min before irradiation with γ-rays (10 Gy) and incubated for 24 h for apoptosis analysis.

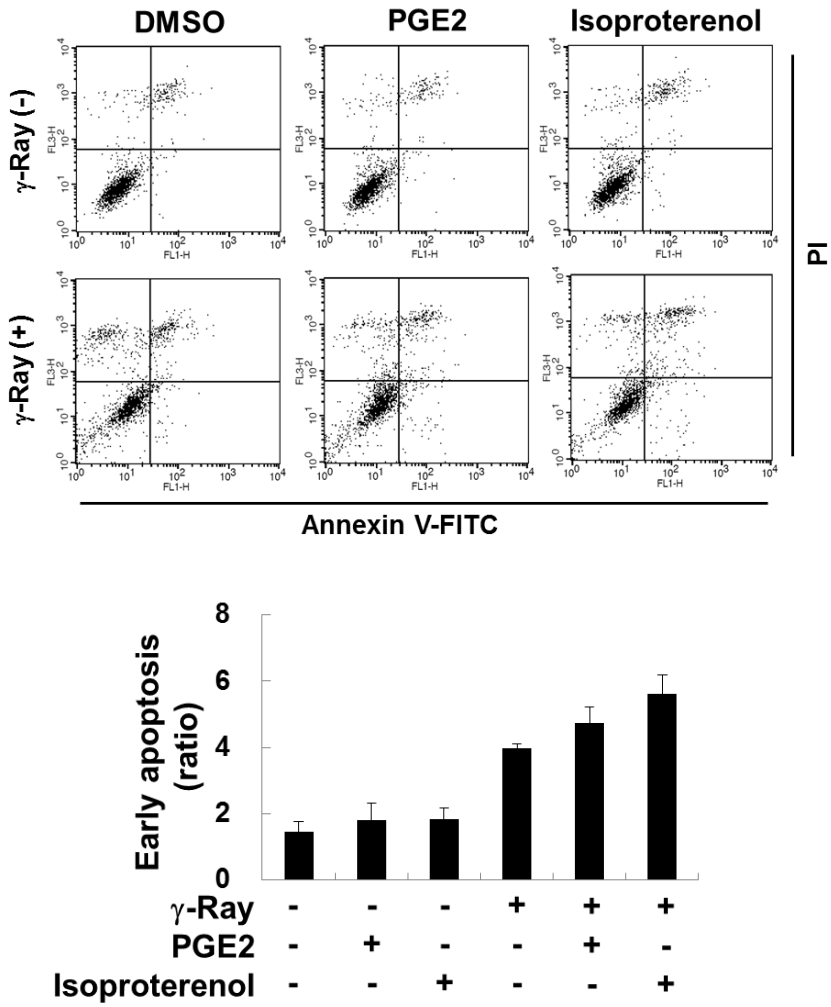

Figure 76. Effects of prostaglandin E2 and isoproterenol on the early apoptosis

The H1299 cells were treated with 10 μM PGE2 or 1 μM isoproterenol for 30 min before irradiation with γ-rays (10 Gy) and incubated for 24 h. And the cells examined by flow cytometry after staining with Annexin V and propidium iodide (PI).

Discussion

This study aimed to investigate the mechanism how cAMP signaling system might regulate the activation of ATM and apoptosis following γ-ray irradiation. We found that cAMP signaling system inhibits radiation-induced activation of ATM by PKA-dependent activation of PP2A, and that cAMP signaling system augments radiation-induced apoptosis by reducing ATM-dependent activation of NF-κB in human lung cancer cells and in the mouse lung.

Our findings that cAMP signaling system inhibits radiation-induced activation of ATM by PKA-dependent activation of PP2A is supported by the results: 1) radiation-induced phosphorylation of ATM was inhibited by expression of constitutively active Gαs and by treatment with Gαs-coupled receptor agonists or an adenylate cyclase activator, forskolin, 2) treatment with a PP2A inhibitor abolished the ATM-inhibitory effect of Gαs, 3) expression of the active Gαs increased the activating phosphorylation of PP2A B56δ subunit and PP2A activity, and inhibition of PKA abolished the PP2A activation by Gαs causing the restoration of ATM phosphorylation. Moreover, inhibition of radiation-induced ATM phosphorylation by cAMP signaling system was observed in human lung cancer cells, murine melanoma cells, and the murine lung tissue, suggesting that the inhibition occurs in many tissues.

ATM is mainly recruited to double-strand DNA breaks and activated through interactions with the MRE11–RAD50–NBS1 (MRN) complex (87). ATM protein undergoes autophosphorylation at Serine-1981 and monomerization from an inactive dimer following double-strand DNA breaks, and the ATM autophosphorylation is considered a hallmark of ATM activation (88). Recently, ATM was found to be activated independently from DNA damage through redox-dependent mechanisms and participates in a diverse signaling pathways involved in metabolic regulation and cancer (77). However, there is no previous report that cAMP signaling system regulates radiation-induced activation of ATM. Caffeine is known to inhibit ATM activation, and has been studied as a potential radioenhancer (80). Caffeine is also known to inhibit cAMP phosphodiesterase that may increase cAMP level (89), suggesting the involvement of cAMP signaling system in ATM activation. However, caffeine was reported to inhibit the enzyme activity of ATM immunoprecipitates in vitro, which was interpreted as direct inhibition of ATM by caffeine (90) regardless of cAMP signaling system. Thus, our paper, as far as we know, presents the first evidence that cAMP signaling system can regulate the radiation-induced ATM activation.

The inhibition of ATM activation by PP2A in a PKA-dependent pathway is supported by the previous reports that PKA phosphorylates serine-566 of PP2A 56δ subunit to stimulate PP2A activity (85), and that PP2A forms complexes with ATM and dephosphorylates the

autophosphorylated serine-1981 in undamaged cells to suppress the intrinsic ATM activity (13).

This study shows that cAMP signaling system augments the radiation-induced apoptosis by inhibiting ATM activation. This finding is based on the result that radiation-induced apoptosis was augmented by the activation of cAMP signaling system and by inhibition of ATM with a specific inhibitor, KU55933, in cancer cells and mouse lung and that cAMP signaling system inhibits radiation-induced activation of ATM. ATM is a master regulator of cellular responses to the DNA damage caused by ionizing radiation, and activates downstream signaling pathways to regulate various DNA damage responses including cell cycle, DNA repair, and apoptosis (91, 92). This finding suggests that cAMP signaling system can modulate radiation-induced apoptosis by regulating radiation-induced activation of ATM, and which implies that radiation-induced apoptosis can be modulated by treatment with drugs acting on cAMP signaling pathway to increase radiosensitivity of cancer cells or to protect normal cells from radiation. It is also plausible for cAMP signaling system to modulate other cellular responses to DNA damage mediated by ATM such as DNA damage repair and cell cycle arrest. The cAMP signaling system was found to regulate apoptosis cancer cells caused by γ-radiation, cisplatin, and hydrogen peroxide by modulating the expression of Bcl-2 family proteins (46, 83, 93) and X-linked inhibitor of apoptosis protein (59). Thus, cAMP signaling system seems to regulate apoptosis of cancer

cells by diverse molecular mechanisms.

The cAMP signaling system was found to augment radiation-induced apoptosis by inhibiting ATM-mediated NF-κB activation in this study. This finding is substantiated by the result that activation of cAMP signaling system or inhibition of ATM resulted in reduction of radiation-induced NF-κB activation and augmentation of apoptosis and that that inhibition of NF-κB activation by treatment with a specific inhibitor, PDTC, augmented radiation-induced apoptosis. ATM can stimulate NF-κB activation, which induces the expression of anti-apoptotic proteins to protect cells from apoptosis. Thus, inhibition of ATM may compel the cells to undergo apoptosis as observed in this study (94, 95). However, ATM can play contrast roles in DNA damage-induced apoptosis, so ATM induced apoptosis by phosphorylating the downstream target substrates such as p53, TRF1 (96) and NBS1 (97). Thus, ATM seems to shows different effects on apoptosis depending on cell types, DNA damage-inducing agents, the severity of DNA damage, and presence of functional p53 (98).

NF-κB is activated in response to various immune and inflammatory stimuli, and it is also activated by DNA damage to protect damaged cells from apoptotic cell death. The signal transduction mechanisms that link DNA damage with activation of NF-κB is relatively less known, but signaling pathways involving ATM and NF-κB essential modulator (NEMO) is reported to cooperate for direct linking

of DNA damage in nucleus to NF-κB activation in the cytosol (99). ATM is involved in the sequential post-translational modification of NEMO, and ATM translocates in a calcium-dependent manner to cytosol and membrane (100). The cytosolic ATM activates TGFβ activated kinase (TAK1), which phosphorylates IKKβ to trigger ubiquitin-proteasome dependent degradation and NF-κB activation (86). In this study, cAMP signaling system inhibits

On the ground of recent articles, NF-κB activation is regulated by ATM-TRAF6-IKK pathway (100) and via targeting of MRE11 (101).

In this study, the role of cAMP signaling system on activation of ATM, PP2A and NF-κB and on apoptosis following γ-ray irradiation was assessed by activating the signaling system by various mechanisms: expression of constitutively active Gαs, treatment with Gαs-coupled receptor agonists such as isoproterenol for β-adrenergic receptors and prostaglandin E2 for prostanoid receptors, and treatment with adenylate cyclase activator, forskolin. Furthermore, the similar effect of cAMP signaling system was observed in A549 and p53-null H1299 human lung cancer cells, murine melanoma cells, and murine lung tissue, suggesting comparable effects of cAMP signaling system in various cells and tissues. These results reinforce the role of cAMP system in inhibition of radiation-induced activation of ATM by PKA-dependent activation of PP2A and in augmentation of radiation-induced apoptosis by reduction of ATM-dependent NF-κB activation.

Decreasing ATM phosphorylation has several meaning and functions. That induced IκBα expression and reduced NF-κB relocation in nucleus after radiation. These events were observed not only long-time radiation exposure condition, but also short-time condition and after radiation, IκBα expression level did not fully recover for 24 h to compare with radiation untreated cells (Figure. 69) but Gαs and decreasing ATM phosphorylation induced IκBα basal expression and plentiful amount of IκBα remained after radiation both long- and short-time exposure cells.

It is interesting that ATM phosphorylation highly shows at the nucleus in the short-time radiation exposure but not cytosol. However, in the long-time radiation exposure cells, ATM phosphorylation strongly appears in the cytosol. It is suggested that immediately increased ATM phosphorylation in the nucleus by radiation relocates in the cytosol as time goes on and ATM may regulate NF-κB activity.

Forskolin, PGE2, and isoproterenol were used as a Gαs agonist in this study. Gαs agonists show that they decrease p-ATM and increase PP2A activation under the radiation exposure. Also, like Gαs protein, forskolin, PGE2, and isoproterenol accelerate the radiation-induced apoptosis. Particularly, PGE2 regulates p-ATM only treatment for 30 min and that happening successfully mimics KU55933 work.

Conclusion

From the results, the following conclusions were obtained.

1. Gαs inhibits cisplatin-induced apoptosis partly by increasing XIAP in cervical cancer cells. That is happened through stimulating transcription of the XIAP gene via a CRE-like element and through inhibition of degradation of the XIAP protein. These findings indicate that Gαs regulates cervical cancer cell apoptosis via cAMP-PKA-CREB-XIAP.

2. The cAMP signaling system inhibits the repair of radiation-induced DNA damage via Epac-mediated ubiquitin-proteasome dependent degradation of XRCC1 in lung cancer cells. These findings suggest that the cAMP signaling system might play important roles in regulation of DNA damage repair pathways in lung cancer cells.

3. Gs system promotes radiation-induced apoptosis and regulates the DNA damage response signals in lung cancer cells. Cyclic AMP signaling system inhibits radiation-induced activation of ATM by PKA-dependent activation of PP2A, and augments radiation-induced apoptosis by reducing ATM-dependent activation of NF-κB in

lung cancer cells and mouse lung tissue. These findings provide a novel mechanism for the Gαs-p-ATM signaling pathway to regulate radiation-induced apoptosis of lung cancer cells and suggest that the Gαs-p-ATM-apoptosis signaling pathway could be applied to enhance the therapeutic efficiency of radiation treatment of non-small cell lung cancers.

4. Taken together, these findings provide a novel mechanism for the Gαs-cAMP signaling pathway to modulate apoptosis of cervical cancer and lung cancer cells and suggest that the Gαs-cAMP signaling pathway can be utilized to enhance the therapeutic efficiency of cisplatin- or radiation- treatment of cervical cancers and lung cancers, respectively.

References

1. Oldham WM, Hamm HE. Heterotrimeric G protein activation by G-protein-coupled receptors. Nat Rev Mol Cell Biol. 2008;9(1):60-71. Epub 2007/11/29.

2. Smotrys JE, Linder ME. Palmitoylation of intracellular signaling proteins: regulation and function. Annu Rev Biochem. 2004;73:559-87. Epub 2004/06/11.

3. Pidoux G, Tasken K. Specificity and spatial dynamics of protein kinase A signaling organized by A-kinase-anchoring proteins. Journal of molecular endocrinology. 2010;44(5):271-84. Epub 2010/02/13.

4. O'Day DH. Introduction to the Human cell; the unit of life & disease2012.

5. Breckler M, Berthouze M, Laurent AC, Crozatier B, Morel E, Lezoualc'h F. Rap-linked cAMP signaling Epac proteins: compartmentation, functioning and disease implications. Cellular signalling. 2011;23(8):1257-66. Epub 2011/03/16.

6. Nikolaev VO, Bunemann M, Hein L, Hannawacker A, Lohse MJ. Novel single chain cAMP sensors for receptor-induced signal

propagation. The Journal of biological chemistry. 2004;279(36):37215-8. Epub 2004/07/03.

7. Gloerich M, Bos JL. Epac: defining a new mechanism for cAMP action. Annual review of pharmacology and toxicology. 2010;50:355-75. Epub 2010/01/09.

8. Shrivastav M, De Haro LP, Nickoloff JA. Regulation of DNA double-strand break repair pathway choice. Cell research. 2008;18(1):134-47. Epub 2007/12/25.

9. Czornak K, Chughtai S, Chrzanowska KH. Mystery of DNA repair: the role of the MRN complex and ATM kinase in DNA damage repair. Journal of applied genetics. 2008;49(4):383-96. Epub 2008/11/26.

10. Zhou BB, Bartek J. Targeting the checkpoint kinases: chemosensitization versus chemoprotection. Nature reviews Cancer. 2004;4(3):216-25. Epub 2004/03/03.

11. Schneider J, Classen V, Helmig S. XRCC1 polymorphism and lung cancer risk. Expert review of molecular diagnostics. 2008;8(6):761-80. Epub 2008/11/13.

12. Lavin MF. Ataxia-telangiectasia: from a rare disorder to a paradigm for cell signalling and cancer. Nat Rev Mol Cell Biol. 2008;9(10):759-69. Epub 2008/09/25.

13. Goodarzi AA, Jonnalagadda JC, Douglas P, Young D, Ye R, Moorhead GB, et al. Autophosphorylation of ataxia-telangiectasia mutated is regulated by protein phosphatase 2A. EMBO J. 2004;23(22):4451-61. Epub 2004/10/29.

14. Shivapurkar N, Reddy J, Chaudhary PM, Gazdar AF. Apoptosis and lung cancer: a review. Journal of cellular biochemistry. 2003;88(5):885-98. Epub 2003/03/05.

15. Gewies A. Introduction to Apoptosis. 2003.

16. Taylor RC, Cullen SP, Martin SJ. Apoptosis: controlled demolition at the cellular level. Nat Rev Mol Cell Biol. 2008;9(3):231-41. Epub 2007/12/13.

17. LaCasse EC, Baird S, Korneluk RG, MacKenzie AE. The inhibitors of apoptosis (IAPs) and their emerging role in cancer. Oncogene. 1998;17(25):3247-59. Epub 1999/01/23.

18. Altieri DC. The molecular basis and potential role of survivin in cancer diagnosis and therapy. Trends in molecular medicine. 2001;7(12):542-7. Epub 2001/12/06.

19. Riedl SJ, Shi Y. Molecular mechanisms of caspase regulation during apoptosis. Nat Rev Mol Cell Biol. 2004;5(11):897-907. Epub 2004/11/03.

20. Kostova I. Platinum complexes as anticancer agents. Recent Pat Anticancer Drug Discov. 2006;1(1):1-22. Epub 2008/01/29.

21. Sato S, Kigawa J, Minagawa Y, Okada M, Shimada M, Takahashi M, et al. Chemosensitivity and p53-dependent apoptosis in epithelial ovarian carcinoma. Cancer. 1999;86(7):1307-13. Epub 1999/10/03.

22. Mansouri A, Ridgway LD, Korapati AL, Zhang QX, Tian L, Wang YB, et al. Sustained activation of JNK/p38 MAPK pathways in response to cisplatin leads to Fas ligand induction and cell death in ovarian carcinoma cells. Journal of Biological Chemistry. 2003;278(21):19245-56.

23. Tamm I, Schriever F, Dorken B. Apoptosis: implications of basic research for clinical oncology. Lancet Oncol. 2001;2(1):33-42. Epub 2002/03/22.

24. Jiang X, Wang X. Cytochrome C-mediated apoptosis. Annu Rev Biochem. 2004;73:87-106. Epub 2004/06/11.

25. Hamm HE. The many faces of G protein signaling. The Journal of biological chemistry. 1998;273(2):669-72. Epub 1998/02/14.

26. Cabrera-Vera TM, Vanhauwe J, Thomas TO, Medkova M, Preininger A, Mazzoni MR, et al. Insights into G protein structure, function, and regulation. Endocrine Reviews. 2003;24(6):765-81.

27. Neer EJ. Heterotrimeric G proteins: organizers of transmembrane signals. Cell. 1995;80(2):249-57. Epub 1995/01/27.

28. Burchett SA. Regulators of G protein signaling: A bestiary of modular protein binding domains. Journal of Neurochemistry. 2000;75(4):1335-51.

29. Lennon G, Auffray C, Polymeropoulos M, Soares MB. The IMAGE consortium: An integrated molecular analysis of genomes and their expression. Genomics. 1996;33(1):151-2.

30. Lee TJ, Jung EM, Lee JT, Kim S, Park JW, Choi KS, et al. Mithramycin A sensitizes cancer cells to TRAIL-mediated apoptosis by down-regulation of XIAP gene promoter through Sp1 sites. Mol Cancer Ther. 2006;5(11):2737-46. Epub 2006/11/24.

31. Kim SY, Seo M, Kim Y, Lee YI, Oh JM, Cho EA, et al. Stimulatory heterotrimeric GTP-binding protein inhibits hydrogen peroxide-induced apoptosis by repressing BAK induction in SH-SY5Y human neuroblastoma cells. The Journal of biological chemistry. 2008;283(3):1350-61. Epub 2007/11/10.

32. Wilson SP, Liu F, Wilson RE, Housley PR. Optimization of calcium phosphate transfection for bovine chromaffin cells: relationship to calcium phosphate precipitate formation. Anal Biochem. 1995;226(2):212-20. Epub 1995/04/10.

33. Ahn YH, Koh JY, Hong SH. Protein synthesis-dependent but Bcl-2-independent cytochrome C release in zinc depletion-induced neuronal apoptosis. Journal of neuroscience research. 2000;61(5):508-14. Epub 2000/08/24.

34. Zhang X, Odom DT, Koo SH, Conkright MD, Canettieri G, Best J, et al. Genome-wide analysis of cAMP-response element binding protein occupancy, phosphorylation, and target gene activation in human tissues. Proc Natl Acad Sci U S A. 2005;102(12):4459-64. Epub 2005/03/09.

35. Eckelman BP, Salvesen GS. The human anti-apoptotic proteins cIAP1 and cIAP2 bind but do not inhibit caspases. The Journal of biological chemistry. 2006;281(6):3254-60. Epub 2005/12/13.

36. Salvesen GS, Duckett CS. IAP proteins: blocking the road to death's door. Nat Rev Mol Cell Biol. 2002;3(6):401-10. Epub 2002/06/04.

37. Zhang Y, Wang Y, Gao W, Zhang R, Han X, Jia M, et al. Transfer of siRNA against XIAP induces apoptosis and reduces tumor cells growth potential in human breast cancer in vitro and in vivo. Breast Cancer Res Treat. 2006;96(3):267-77.

38. Checinska A, Hoogeland BS, Rodriguez JA, Giaccone G, Kruyt FA. Role of XIAP in inhibiting cisplatin-induced caspase activation in non-small cell lung cancer cells: a small molecule Smac mimic sensitizes for chemotherapy-induced apoptosis by enhancing caspase-3 activation. Exp Cell Res. 2007;313(6):1215-24.

39. Ikuyama S, Shimura H, Hoeffler JP, Kohn LD. Role of the cyclic adenosine 3',5'-monophosphate response element in efficient expression of the rat thyrotropin receptor promoter. Mol Endocrinol. 1992;6(10):1701-15.

40. Berhane K, Boggaram V. Identification of a novel DNA regulatory element in the rabbit surfactant protein B (SP-B) promoter that is a target for ATF/CREB and AP-1 transcription factors. Gene. 2001;268(1-2):141-51.

41. Giono LE, Varone CL, Canepa ET. 5-Aminolaevulinate synthase gene promoter contains two cAMP-response element (CRE)-like sites that confer positive and negative responsiveness to CRE-binding protein (CREB). Biochem J. 2001;353(Pt 2):307-16.

42. Matsumiya T, Imaizumi T, Yoshida H, Kimura H, Satoh K. Cisplatin inhibits the expression of X-chromosome-linked inhibitor of apoptosis protein in an oral carcinoma cell line. Oral Oncol. 2001;37(3):296-300. Epub 2001/04/05.

43. Nomura T, Mimata H, Yamasaki M, Nomura Y. Cisplatin inhibits the expression of X-linked inhibitor of apoptosis protein in human LNCaP cells. Urol Oncol. 2004;22(6):453-60. Epub 2004/12/22.

44. Liou JY, Matijevic-Aleksic N, Lee S, Wu KK. Prostacyclin inhibits endothelial cell XIAP ubiquitination and degradation. J Cell Physiol. 2007;212(3):840-8.

45. Kim SY, Seo M, Oh JM, Cho EA, Juhnn YS. Inhibition of gamma ray-induced apoptosis by stimulatory heterotrimeric GTP binding protein involves Bcl-xL down-regulation in SH-SY5Y human neuroblastoma cells. Exp Mol Med. 2007;39(5):583-93.

46. Choi YJ, Oh JM, Kim SY, Seo M, Juhnn YS. Stimulatory heterotrimeric GTP-binding protein augments cisplatin-induced apoptosis by upregulating Bak expression in human lung cancer cells. Cancer Sci. 2009;100(6):1069-74. Epub 2009/03/27.

47. Ruchaud S, Seite P, Foulkes NS, Sassone-Corsi P, Lanotte M. The transcriptional repressor ICER and cAMP-induced programmed cell death. Oncogene. 1997;15(7):827-36.

48. Schloffer D, Horky M, Kotala V, Wesierska-Gadek J. Induction of cell cycle arrest and apoptosis in human cervix carcinoma cells during therapy by cisplatin. Cancer Detect Prev. 2003;27(6):481-93.

49. Kastan MB. DNA damage responses: mechanisms and roles in human disease: 2007 G.H.A. Clowes Memorial Award Lecture. Molecular cancer research : MCR. 2008;6(4):517-24. Epub 2008/04/12.

50. Branzei D, Foiani M. Regulation of DNA repair throughout the cell cycle. Nat Rev Mol Cell Biol. 2008;9(4):297-308. Epub 2008/02/21.

51. Thompson LH, Brookman KW, Jones NJ, Allen SA, Carrano AV. Molecular cloning of the human XRCC1 gene, which corrects defective DNA strand break repair and sister chromatid exchange. Molecular and cellular biology. 1990;10(12):6160-71. Epub 1990/12/01.

52. Thompson LH, West MG. XRCC1 keeps DNA from getting stranded. Mutation research. 2000;459(1):1-18. Epub 2000/03/14.

53. Caldecott KW. Cell signaling. The BRCT domain: signaling with friends? Science. 2003;302(5645):579-80. Epub 2003/10/25.

54. Ginsberg G, Angle K, Guyton K, Sonawane B. Polymorphism in the DNA repair enzyme XRCC1: utility of current database and implications for human health risk assessment. Mutation research. 2011;727(1-2):1-15. Epub 2011/03/01.

55. Ang MK, Patel MR, Yin XY, Sundaram S, Fritchie K, Zhao N, et al. High XRCC1 protein expression is associated with poorer survival in patients with head and neck squamous cell carcinoma. Clinical cancer research : an official journal of the American

Association for Cancer Research. 2011;17(20):6542-52. Epub 2011/09/13.

56. Wettschureck N, Offermanns S. Mammalian G proteins and their cell type specific functions. Physiological reviews. 2005;85(4):1159-204. Epub 2005/09/27.

57. Sands WA, Palmer TM. Regulating gene transcription in response to cyclic AMP elevation. Cellular signalling. 2008;20(3):460-6. Epub 2007/11/13.

58. Entschladen F, Zanker KS, Powe DG. Heterotrimeric G protein signaling in cancer cells with regard to metastasis formation. Cell Cycle. 2011;10(7):1086-91. Epub 2011/03/25.

59. Cho EA, Oh JM, Kim SY, Kim Y, Juhnn YS. Heterotrimeric stimulatory GTP-binding proteins inhibit cisplatin-induced apoptosis by increasing X-linked inhibitor of apoptosis protein expression in cervical cancer cells. Cancer Sci. 2011;102(4):837-44. Epub 2011/01/25.

60. Levis MJ, Bourne HR. Activation of the alpha subunit of Gs in intact cells alters its abundance, rate of degradation, and membrane avidity. The Journal of cell biology. 1992;119(5):1297-307. Epub 1992/12/01.

61. Parsons JL, Tait PS, Finch D, Dianova, II, Allinson SL, Dianov GL. CHIP-mediated degradation and DNA damage-dependent

stabilization regulate base excision repair proteins. Molecular cell. 2008;29(4):477-87. Epub 2008/03/04.

62. Cvijic ME, Yang WL, Chin KV. Cisplatin resistance in cyclic AMP-dependent protein kinase mutants. Pharmacology & therapeutics. 1998;78(2):115-28. Epub 1998/06/12.

63. Wang Y, Mallya SM, Sikpi MO. Calmodulin antagonists and cAMP inhibit ionizing-radiation-enhancement of double-strand-break repair in human cells. Mutation research. 2000;460(1):29-39. Epub 2000/06/17.

64. Zhou ZQ, Walter CA. Cloning and characterization of the promoter of baboon XRCC1, a gene involved in DNA strand-break repair. Somatic cell and molecular genetics. 1998;24(1):23-39. Epub 1998/10/20.

65. Liu F, Li B, Wei Y, Yan L, Wen T, Zhao J, et al. XRCC1 genetic polymorphism Arg399Gln and hepatocellular carcinoma risk: a meta-analysis. Liver international : official journal of the International Association for the Study of the Liver. 2011;31(6):802-9. Epub 2011/06/08.

66. Yoon SM, Hong YC, Park HJ, Lee JE, Kim SY, Kim JH, et al. The polymorphism and haplotypes of XRCC1 and survival of non-small-cell lung cancer after radiotherapy. International journal of

radiation oncology, biology, physics. 2005;63(3):885-91. Epub 2005/10/04.

67. Jaremko M, Justenhoven C, Schroth W, Abraham BK, Fritz P, Vollmert C, et al. Polymorphism of the DNA repair enzyme XRCC1 is associated with treatment prediction in anthracycline and cyclophosphamide/methotrexate/5-fluorouracil-based chemotherapy of patients with primary invasive breast cancer. Pharmacogenetics and genomics. 2007;17(7):529-38. Epub 2007/06/15.

68. Holz GG, Chepurny OG, Schwede F. Epac-selective cAMP analogs: new tools with which to evaluate the signal transduction properties of cAMP-regulated guanine nucleotide exchange factors. Cellular signalling. 2008;20(1):10-20. Epub 2007/08/25.

69. Loizou JI, El-Khamisy SF, Zlatanou A, Moore DJ, Chan DW, Qin J, et al. The protein kinase CK2 facilitates repair of chromosomal DNA single-strand breaks. Cell. 2004;117(1):17-28. Epub 2004/04/07.

70. Parsons JL, Dianova, II, Finch D, Tait PS, Strom CE, Helleday T, et al. XRCC1 phosphorylation by CK2 is required for its stability and efficient DNA repair. DNA repair. 2010;9(7):835-41. Epub 2010/05/18.

71. Kang HC, Lee YI, Shin JH, Andrabi SA, Chi Z, Gagne JP, et al. Iduna is a poly(ADP-ribose) (PAR)-dependent E3 ubiquitin ligase that

regulates DNA damage. Proc Natl Acad Sci U S A. 2011;108(34):14103-8. Epub 2011/08/10.

72. Bos JL. Epac proteins: multi-purpose cAMP targets. Trends in biochemical sciences. 2006;31(12):680-6. Epub 2006/11/07.

73. Begg AC, Stewart FA, Vens C. Strategies to improve radiotherapy with targeted drugs. Nature reviews Cancer. 2011;11(4):239-53. Epub 2011/03/25.

74. Bartek J, Bartkova J, Lukas J. DNA damage signalling guards against activated oncogenes and tumour progression. Oncogene. 2007;26(56):7773-9. Epub 2007/12/11.

75. Savitsky K, Bar-Shira A, Gilad S, Rotman G, Ziv Y, Vanagaite L, et al. A single ataxia telangiectasia gene with a product similar to PI-3 kinase. Science. 1995;268(5218):1749-53. Epub 1995/06/23.

76. Canman CE, Lim DS, Cimprich KA, Taya Y, Tamai K, Sakaguchi K, et al. Activation of the ATM kinase by ionizing radiation and phosphorylation of p53. Science. 1998;281(5383):1677-9. Epub 1998/09/11.

77. Ditch S, Paull TT. The ATM protein kinase and cellular redox signaling: beyond the DNA damage response. Trends in biochemical sciences. 2012;37(1):15-22. Epub 2011/11/15.

78. Lempiainen H, Halazonetis TD. Emerging common themes in regulation of PIKKs and PI3Ks. EMBO J. 2009;28(20):3067-73. Epub 2009/09/26.

79. Kurz EU, Lees-Miller SP. DNA damage-induced activation of ATM and ATM-dependent signaling pathways. DNA repair. 2004;3(8-9):889-900. Epub 2004/07/29.

80. Sarkaria JN, Eshleman JS. ATM as a target for novel radiosensitizers. Seminars in radiation oncology. 2001;11(4):316-27. Epub 2001/10/26.

81. Golding SE, Rosenberg E, Adams BR, Wignarajah S, Beckta JM, O'Connor MJ, et al. Dynamic inhibition of ATM kinase provides a strategy for glioblastoma multiforme radiosensitization and growth control. Cell Cycle. 2012;11(6):1167-73. Epub 2012/03/01.

82. Kopperud R, Krakstad C, Selheim F, Doskeland SO. cAMP effector mechanisms. Novel twists for an 'old' signaling system. FEBS letters. 2003;546(1):121-6. Epub 2003/06/28.

83. Seo M, Nam HJ, Kim SY, Juhnn YS. Inhibitory heterotrimeric GTP-binding proteins inhibit hydrogen peroxide-induced apoptosis by up-regulation of Bcl-2 via NF-kappaB in H1299 human lung cancer cells. Biochem Biophys Res Commun. 2009;381(2):153-8. Epub 2009/02/24.

84. Cho EA, Juhnn YS. The cAMP signaling system inhibits the repair of gamma-ray-induced DNA damage by promoting Epac1-mediated proteasomal degradation of XRCC1 protein in human lung cancer cells. Biochem Biophys Res Commun. 2012;422(2):256-62. Epub 2012/05/12.

85. Ahn JH, McAvoy T, Rakhilin SV, Nishi A, Greengard P, Nairn AC. Protein kinase A activates protein phosphatase 2A by phosphorylation of the B56delta subunit. Proc Natl Acad Sci U S A. 2007;104(8):2979-84. Epub 2007/02/16.

86. Miyamoto S. Nuclear initiated NF-kappaB signaling: NEMO and ATM take center stage. Cell research. 2011;21(1):116-30. Epub 2010/12/29.

87. Lee JH, Paull TT. Activation and regulation of ATM kinase activity in response to DNA double-strand breaks. Oncogene. 2007;26(56):7741-8. Epub 2007/12/11.

88. Bakkenist CJ, Kastan MB. DNA damage activates ATM through intermolecular autophosphorylation and dimer dissociation. Nature. 2003;421(6922):499-506. Epub 2003/01/31.

89. Berthet J, Sutherland EW, Rall TW. The assay of glucagon and epinephrine with use of liver homogenates. The Journal of biological chemistry. 1957;229(1):351-61. Epub 1957/11/01.

90. Sarkaria JN, Busby EC, Tibbetts RS, Roos P, Taya Y, Karnitz LM, et al. Inhibition of ATM and ATR kinase activities by the radiosensitizing agent, caffeine. Cancer research. 1999;59(17):4375-82. Epub 1999/09/15.

91. Lee Y, McKinnon PJ. ATM dependent apoptosis in the nervous system. Apoptosis : an international journal on programmed cell death. 2000;5(6):523-9. Epub 2001/04/17.

92. Derheimer FA, Kastan MB. Multiple roles of ATM in monitoring and maintaining DNA integrity. FEBS letters. 2010;584(17):3675-81. Epub 2010/06/29.

93. Choi YJ, Kim SY, Oh JM, Juhnn YS. Stimulatory heterotrimeric G protein augments gamma ray-induced apoptosis by up-regulation of Bak expression via CREB and AP-1 in H1299 human lung cancer cells. Exp Mol Med. 2009;41(8):592-600. Epub 2009/04/22.

94. Rashi-Elkeles S, Elkon R, Weizman N, Linhart C, Amariglio N, Sternberg G, et al. Parallel induction of ATM-dependent pro- and antiapoptotic signals in response to ionizing radiation in murine lymphoid tissue. Oncogene. 2006;25(10):1584-92. Epub 2005/11/30.

95. Wang Y, Liu Q, Liu Z, Li B, Sun Z, Zhou H, et al. Berberine, a genotoxic alkaloid, induces ATM-Chk1 mediated G2 arrest in prostate cancer cells. Mutation research. 2012;734(1-2):20-9. Epub 2012/05/09.

96. Kishi S, Zhou XZ, Ziv Y, Khoo C, Hill DE, Shiloh Y, et al. Telomeric protein Pin2/TRF1 as an important ATM target in response to double strand DNA breaks. The Journal of biological chemistry. 2001;276(31):29282-91. Epub 2001/05/29.

97. Stracker TH, Morales M, Couto SS, Hussein H, Petrini JH. The carboxy terminus of NBS1 is required for induction of apoptosis by the MRE11 complex. Nature. 2007;447(7141):218-21. Epub 2007/04/13.

98. Jiang H, Reinhardt HC, Bartkova J, Tommiska J, Blomqvist C, Nevanlinna H, et al. The combined status of ATM and p53 link tumor development with therapeutic response. Genes & development. 2009;23(16):1895-909. Epub 2009/07/18.

99. McCool KW, Miyamoto S. DNA damage-dependent NF-kappaB activation: NEMO turns nuclear signaling inside out. Immunological reviews. 2012;246(1):311-26. Epub 2012/03/23.

100. Hinz M, Stilmann M, Arslan SC, Khanna KK, Dittmar G, Scheidereit C. A cytoplasmic ATM-TRAF6-cIAP1 module links nuclear DNA damage signaling to ubiquitin-mediated NF-kappaB activation. Molecular cell. 2010;40(1):63-74. Epub 2010/10/12.

101. Zhang J, Xin X, Chen Q, Xie Z, Gui M, Chen Y, et al. Oligomannurarate sulfate sensitizes cancer cells to doxorubicin by inhibiting atypical activation of NF-kappaB via targeting of Mre11.

International journal of cancer Journal international du cancer. 2012;130(2):467-77. Epub 2011/03/10.

국문 초록

촉진성 신호전달 G 단백질 (Gαs)은 cAMP 신호전달계를 활성화함으로써 세포의 성장, 증식, 분열, 그리고 세포사멸을 조절하는 데에 중요한 역할을 수행한다. 그러나 Gαs 단백질이 DNA 손상 반응의 조절에 관여하는지에 대하여 알려진 바가 거의 없다. Gαs 단백질이 DNA 복구나 세포사멸 등 DNA 손상반응에 미치는 영향과 그 분자 기전을 밝히고자 연구를 시행하였다.

이 논문의 첫째 부분에서는 Gαs 단백질이 세포사멸을 조절하는 기전을 밝히기 위하여 자궁경부암 세포주에서 Gαs 단백질이 시스플라틴에 의한 세포사멸을 조절하는 기전을 연구하였다. 항시활성형인 GαsQL 단백질이 계속해서 안정적으로 발현되는 HeLa 세포주를 확립하였다. GαsQL 은 HeLa 세포주에 시스플라틴 30 μM 를 처리시, 미토콘드리아로부터 세포질로 분비되는 시토크롬 C 와 분해된 caspase-3 와 PARP 를 감소시켰다. 이는 Gαs 가 시스플라틴에 의해 유도되는 세포사멸을 억제시킴을 말해준다. 또한 포스콜린을 자궁경부암 세포주 C33A 와 CaSKi 에 처리시 세포사멸이 억제되었다. GαsQL 의 발현은 XIAP 의 발현을 증가시켰고 시스플라틴을 처리한 후에도 GαsQL 의 남아있는 발현양을 증가시켰다. GαsQL 를 siRNA 로 넉다운 시 세포사멸이 촉진되었다. Gαs 발현은 GαsQL mRNA 를 증가시켰다. 이러한

증가는 PKA 억제제와 CRE-decoy 에 의하여 억제되었다. XIAP 프로모터에 있는 CRE 와 유사한 요소의 1369 bp 는 Gαs 에 의하여 XIAP 가 유도되는 것을 매개함을 찾았다. 더욱이, GαsQL 의 발현은 XIAP 단백질의 유비퀴틴/프로테아좀-의존성 감성을 막는 것을 확인하였다. 이러한 연구는 자궁경부암 세포주 HeLa 에서 Gαs 가 XIAP 의 전사를 증가시키고 XIAP 단백질의 감성을 감소시킴으로써 시스플라틴에 의해 유도된 세포사멸을 억제함을 보여준다.

둘째 부분에서는, Gαs/아데닐 고리화 효소 신호전달계가 DNA 복구활성에 미치는 영향과 분자기전을 구명하기 위하여, H1299 폐암세포주에서 Gαs 신호전달계가방사선에 의해 초래된 DNA 손상의 복구에 미치는 영향을 분석하였다. 항시 발현하는 돌연변이 G 단백질 (GαsQL)를 발현시키거나 아데닐 고리화 효소 활성제인 포스콜린을 처리하면, H1299 폐암세포주가 방사선에 의한 DNA 손상을 더 많이 받고 손상 회복을 저해 받았다 GαsQL 의 발현이나 포스콜린 또는 이소프로테레놀을 처리는 방사선에 의하여 발현되는 XRCC1 단백질을 저해시켰다. 그리고 외부에서 넣어 XRCC1 발현을 증대시키면 포스콜린에 의하여 DNA 복구가 저해되던 것이 없어졌다. 포스콜린 처리는 XRCC1 단백질의 유비퀴틴/프로테오좀-의존성 감성을 증대시켰고, 그 결과, 방사선 조사 후 단백질 하프라이프가 현저하게 줄어들었다. XRCC1 발현에 있어서 포스콜린의 영향은 PKA 억제제에 의하여 저해되지 않았다.

그러나, Epac 아고니스트인 8-pCPT-2'-O-Me-cAMP 은 XRCC1 단백질 유비퀴틴화를 증가시켰고 XRCC1 발현은 감소시켰다. Epac1 을 넉다운하면 8-pCPT-2'-O-Me-cAMP 의 효과는 사라지고 방사선 조사 후 XRCC1 단백질의 레벨이 회복되었다. 이러한 결과들로부터 우리는 아데닐 고리화 효소 신호체계가 폐암세포주들에서 방사선 조사에 의한 DNA 손상을 회복하는데 저해한다고 말할 수 있으며, 이는 Epac 에 의존적인 신호에 의하여 XRCC1 의 유비퀴틴/프로테오좀-의존성 감성을 조절함으로써 DNA 손상 회복이 저해된다고 결론을 지을 수 있다.

셋째 부분에서는, Gαs/아데닐 고리화 효소 신호전달계가 DNA 손상반응에서 중심역할을 수행하는 ATM 분자의 활성에 미치는 영향과 기전을 연구하였다. 항시활성형 GαsQL 을 H1299 사람 폐암세포에 발현시키면 방사선에 의하여 유도되는 ATM 인산화를 억제시켰다. 오카데익 산을 처리하면 방사선에 의하여 유도된 ATM 인산화에 있어서 영향을 미쳤던 Gαs 의 역할이 사라진다. GαsQL 은 PP2A B56δ subunit 의 인산화와 PP2A 활성을 증대시켰고, 이러한 Gαs 에 의한 PP2A 의 활성은 H89 에 의하여 없어졌다. GαsQL 의 발현은 방사선을 세포에 주었을 때, caspase-3 와 PARP 의 분해를 증대시켰고, 초기 세포사멸 수를 증가시켰으며, KU55933 을 처리하였을 때에도 세포사멸이 증가되었다. B16-F10 마우스 세포에 포스콜린을 처리하면, 방사선에

의하여 B56δ 인산화가 증가되었다. 그러나 마우스 폐 조직에서 방사선에 의한 ATM 인산화는 감소하였다. GαsQL 의 발현은 IκBα 단백질을 증가시켰고, 방사선 처리 후 핵 내에 NF-κB 인 p50 과 p65 의 발현 레벨을 감소시켰다. 그리고 PDTC 는 방사선에 의한 세포사멸을 증가시켰다. 프로스타글란딘 E2 또는 이소프로테레놀을 전 처리하면 B56δ 인산화가 증가되었고 방사선에 의한 ATM 인산화는 감소하였으며 세포사멸은 증대되었다.

이러한 연구결과로부터 Gαs-cAMP 신호전달계는 DNA 손상복구와 세포사멸과 같은 DNA 손상반응을 다양한 분자기전을 통하여 조절한다는 결론을 얻었다. 이는 Gαs-cAMP 신호전달계의 활성을 조절함으로써 암에 대한 치료효과를 증진시킬 수 있는 가능성을 제시하였다.

주요 단어들: G 단백질 (Gαs), 시스플라틴, XIAP; cAMP 신호체계, DNA 회복, XRCC1, Epac; ATM, 방사선, 세포사멸, 그리고 자궁경부암과 폐암

학 번: 2006-30571